Tu-Pos233

MECHANICAL EFFICIENCY OF RAT ANOCOCCYGEUS AT 27 °C ((**J.S. Walker**, and R.A. Murphy)) Department of Molecular Physiology & Biological Physics, University of Virginia, Charlottesville, VA 22908

The aim of this study was to evaluate the mechanical efficiency (the ratio of work to total energy expended) of the rat anococcygeus muscle, a fast, tonic, visceral smooth muscle, at 27 °C. Direct electrical stimulation (3s, 10 Hz, 7–10 V, 0.1–0.5 ms) produced a phasic contraction with a myosin regulatory light chain phosphorylation of about 95%. Total heat production, including recovery heat, was measured using a thermopile during afterloaded isotonic contractions. Total heat represents the sum of work and enthalpy. Work was calculated as Δlength × load (*P*). Enthalpy was calculated by subtracting twice the work from the total heat. The mean total isometric energy expenditure in a 3s contraction was about 45 mJ/g. Similar results to those shown were obtained in 12 preparations. The slope of the mean total heat vs load was not significantly different from zero. Peak efficiency under these conditions was about 11.5% under loads of 0.3–0.4 P_o. This estimate is likely conservative, since with increasing contraction duration, more heat is evolved that is unrelated to work production. Shorter duration contractions may be more efficient. *Supported by NIH 5PO1 HL19242 & AHA VA-95-F-6.*

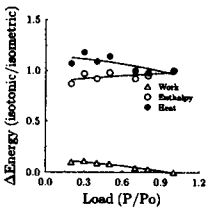

Tu-Pos234

THE IDENTIFICATION OF SPECIFIC PKC ISOFORMS IN PDBU-INDUCED CA^{2+}-SENSITIZATION OF SMOOTH MUSCLE. ((P.E. Jensen, **L.A. Walker**, M.C. Gong, P. Gailly, J. Sando, A.V. Somlyo, and A.P. Somlyo)) Univ. of VA, Dept. of Mol. Phys. & Biol. Physics, Charlottesville, VA 22908 (Spon. by J.M. Gillis)

The multiplicity of Protein Kinase Cs (PKCs) leaves considerable uncertainty about the identity of the isoforms involved in Ca^{2+}-sensitization of smooth muscle by phorbol esters, although recent evidence shows that this pathway plays at most, a very minor role in physiological, G-protein-coupled Ca^{2+}-sensitization (1,2). The purpose of this study was to identify specific PKC isoforms mediating this minor pathway of phorbol ester-induced Ca^{2+}-sensitization. PKC isoforms α, β1, β2, ε, θ and ζ were detected in rabbit portal vein (PV), femoral artery (FA) and ileum smooth muscle. PKC-η was only detected in PV. Contrary to an earlier report, PKC-ε was also present in ferret PV, and γ, and δ were not detected. A ζ antibody also recognized a yet to be identified ~88 kDa band. Treatment (24-96 hrs) with phorbol ester or bryostatin abolished PDBu-induced Ca^{2+}-sensitization and downregulated PKCs α, β1, β2, ε, θ and the ~88 kDa band detected with the ζ antibody, but not η or ζ. Downregulation with PDBu was reversible within 24 hrs: Ca^{2+}-sensitization and the unidentified ~88 kDa ζ-reactive band returned and PKCs β1 and β2 were also present; PKCs α and θ were absent, and ε was unchanged. Treatment of FA with PDBu (16 hr) under Ca^{2+}-free conditions downregulated "conventional" (α and β1) as well as novel (ε and θ) PKCs. We conclude that PKCs α, η, θ and ε are not required for, and PKCε plays no special role in, PDBu-induced Ca^{2+}-sensitization of smooth muscle. Supported by the Danish Nat. Sci. Res.Council and NIH Grants HL19242 and HL07284.

1.Jensen, P. E. et al. (1996) **In press**
2.Hori, Y. (1992) *Kobe J. Med. Sci.* **38,** 79-92

Tu-Pos235

INTERACTION OF MYOSIN PHOSPHATASE WITH PHOSPHOLIPIDS ((F. Jianhua[1], **J. Tanaka**[1], M. Ito[1], K. Ichikawa[1], B. Yamamori[1], M. Inagaki[2], and T. Nakano[1])) [1]Dept. of Int. Med., Mie Univ. School of Med., Tsu 514, Japan, and [2]Lab. Biochem., Aichi Cancer Res. Inst., Nagoya 464, Japan. (Spon. by D.E. Goll)

Contractile activity in smooth muscle is regulated by phosphorylation of myosin. Recently the myosin phosphatase (MP) was purified from several smooth muscles and found to be a heterotrimer of a 38 kD catalytic subunit (PP1cδ) and two regulatory subunits of 130 kD (M130) and 20 kD (M20). The cellular localization of the holoenzyme and/or the component subunits is not known. The M130 was detected in the cytosol, the cytoskeletal fraction and unexpectedly from the membrane fraction in T24 cells using immunoblotting. This study was undertaken to investigate the possible MP/lipid interaction. Interaction between MP and phospholipid vesicles was examined using a sedimentation assay. It was found that MP binds to acidic phospholipids, namely phosphatidylserine (PS), phosphatidylinositol and phosphatidic acid, but not to neutral phospholipids. The amount of MP bound to PS decreased on increasing Mg^{2+} concentration and at 2 mM Mg^{2+} only 20% of MP was bound to PS. The MP/acidic phospholipid interaction inhibited the activity of myosin phosphatase. It was shown, using limited α-chymotryptic digestion and various truncation mutants that phospholipid binding was associated with M20 and with the C-terminal third of M130. M130 and M20 were phosphorylated by protein kinase A (PKA) to 3 mol P/mol and 1 mol P/mol, respectively. Phosphorylation by PKA caused a dissociation of MP from phospholipids and resulted in the recovery of phosphatase activity toward myosin. These results suggest that MP may associate with phospholipids and that this interaction is regulated by phosphorylation by PKA. This mechanism may play an important role in the regulation of myosin phosphatase and its cellular localization.

Tu-Pos236

RHO-ASSOCIATE KINASE (RHO-KINASE), INDUCES MYOSIN LIGHT CHAIN PHOSPHORYLATION AND CA^{2+}-SENSITIZATION OF THE TRITON X-100-PERMEABILIZED RABBIT PORTAL VEIN.

((**Y. Kureishi**[1], S. Kobayashi[2], M. Ito[1], M. Amano[4], K. Kimura[4], M. Fujioka[1], H. Kanaide[3], K. Kaibuchi[4] and T. Nakano[1]))[1]Dept. of Int. Med., Mie Univ. School of Med., Tsu 514, Japan, [2]1st Dept. of Physiol., Yamaguchi Univ. School of Med., Ube 775, Japan, [3]Mol. Cardiol., Faculty of Med., Kyushu Univ., Fukuoka, 812 Japan, and [4]Div. of Signal Transduction, NAIST, Ikoma 630-01, Japan.

Members of the Rho family of guanosine nucleotide-binding proteins (G proteins) are involved in the regulation of the myosin light chain (MLC) phosphorylation and contraction of the smooth muscle. RhoA, in particular, has been shown to be an upstream messenger of Ca^{2+}-sensitization of the contractile apparatus of the smooth muscle. However, the possible cofactor(s) in the 'downstream' of the pathway modulating the Rho-mediated Ca^{2+} sensitization has yet to be identified. Using the membrane permeabilization with Triton X-100, we introduced the recombinant catalytic subunit of Rho-associate kinase (RK), a nobel serine/threonine-protein kinase which is activated by the GTP-bound, active form of RhoA, into the cytosol of smooth muscle of rabbit portal vein (RPV). Cytosolic RK induced a contraction and a concomitant increase in the monophosphorylation of MLC in the Triton X-100-permeabilized RPV at a nominally zero cytosolic Ca^{2+} (buffered with 10mM EGTA) in the absence of calmodulin. The both effects of RK on the force and the MLC monophosphorylation were insensitive to wortmannin (WM), a MLCK blocker. Our results suggest that RK directly induces the Ca^{2+} sensitization of the contractile apparatus of the smooth muscle through the mechanism which is dependent on the levels of the MLC phosphorylation but independent of a Ca^{2+}-calmodulin-MLCK pathway.

MYOSIN

Tu-Pos237

REGULATION OF MYOSIN Iβ ACTIVITY: BINDING OF Ca^{2+} TO CALMODULIN.

((**T. Zhu**, K. Beckingham* and M. Ikebe)) Department of Physiology, University of Massachusetts Medical Center, Worcester, MA 01655, *Department of Biochemistry and Cell Biology, Rice University, Houston, TX 77005

Previously, we have functionally expressed a mammalian myosin Iß with its light chain, calmodulin, in a baculovirus expression system [Biochemistry, 1996, 35:513]. The purified myosin Iß is composed of one heavy chain and three molecules of calmodulin as light chains. One of the three molecules of calmodulin is dissociated from the heavy chain when the calcium concentration is above 1 μM, while Mg^{2+}-ATPase activity of myosin Iß is increased above pCa 6. To further characterize this calcium dependent regulation, we have coexpressed myosin Iß heavy chain with a calmodulin mutant in which the Glu at position 12 in all four of the calcium binding loops is mutated to Gln. We found that the calcium dependent dissociation of calmodulin was abolished in myosin Iß containing this mutated calmodulin. Furthermore, the regulation of Mg^{2+}-ATPase activity by calcium was also lost. These results suggest that the effects of calcium on ATPase activity as well as the binding of calmodulin to myosin Iß heavy chain are due to the binding of calcium to calmodulin. (supported by NIH).

Tu-Pos238

POLARIZATION MEASUREMENTS OF SINGLE FLUOROPHORES ATTACHED TO MOTOR PROTEIN IN AQUEOUS SOLUTION. ((**K. Saito**[1], M. Tokunaga[1], A. Iwane[2], T. Yanagida[1,2,3])) [1]Yanagida Biomotron Project, ERATO, JST, Mino, Osaka, Japan & [2]Department of Biophysical Engineering, [3]Department of Physiology, Medical School, Osaka University, Japan. (Spon. by K. Namba)

In order to measure the orientation and conformation of proteins directly at the single molecular level, we have refined total internal reflection microscopy (*Nature*, **374**, 555-,'95) in order to detect the polarization of a single fluorophore attached to a protein. Two polarized evanescent fields, whose wave vectors were both parallel to the glass surface and intersected, were produced by totally reflecting two s-polarized laser beams passing through an objective lens in a glass-water interface. The polarization direction of the evanescent field was changed with a rate of 10/s by switching the two laser beams in a flip-flop manner. The fluorescence intensities from a single fluorophore that were excited by two polarized evanescent fields were measured with a photon counter (avalanche photodiode). And the orientation of a fluorophore that was bound to a protein was obtained by calculating the polarization and defining as $Q=(I_1 - I_2)/(I_1 + I_2)$.

We measured Q for single myosin subfragment-1s(S-1) bound to the glass surface, which were labeled with TRIA at SH1 or at RLC. These results show that the orientation of TRIA that was bound to RLC was almost random but that bound to SH1 was relatively order. This is consistent with the results obtained from muscle fibers. Our system can therefore resolve the orientation and conformation of protein molecules directly at the single molecular level.

Tu-Pos239

DESIGN PRINCIPLES OF INSTRUMENTS FOR KINETIC STUDIES WITH SINGLE FLUORESCENT MOLECULES ((**M. Anson**[1] and K. Oiwa[2])) [1]Natl. Inst. Med. Res., London NW7 1AA, U.K., [2]Kansai Adv. Res. Center, Kobe 651-24, Japan.

Biological processes are now being probed by video microscopy at the level of single molecules through the application of analogs of effector molecules that are conjugated to intense fluorophores, e.g. the dyes Cy-3 and Cy-5 (Funatsu *et al.* (1995), *Nature*, **374,** 555 , Eccleston *et al.*, Oiwa *et al.* (1996), *Biophys. J.* **70,** A159). To facilitate optimization of such instruments we have developed design principles based on the physics involved. Fluorescent photon emission rate depends upon dye extinction coefficient, quantum yield and evanescent-wave power density which also determine photobleaching rates. Detection efficiency and spatial resolution are limited by objective lens NA, magnification, photocathode quantum efficiency of the image intensifier, its gain, MTF and CCD pixel size. Signal-to-noise ratio, determined by the number of photoelectrons detected by each CCD pixel in each time-bin, is normally limited by dark noise; this may be improved by cooling, permitting detection and recording of individual photoelectrons. The optimal magnification for measurements with isolated single molecules images the bright central lobe of the Airy disk, containing 84% of the total light, over 3 x 3 pixels, whereas discrimination between fluorescent molecules close to the Rayleigh limit requires at least 4 x 4 pixels. Post-detection averaging, digitization and digital image processing are employed to extract as much information from the data as practicable from both time and spatial domains. We describe our instrument designed using these principles for kinetic studies *in vitro* of myosin interacting with single molecules of Cy3(Cy5)-EDA-ATP(ADP) (Oiwa *et al. Biophys. J.* **72,** *Abstract this meeting*).

Tu-Pos240

MICROSCOPIC KINETIC MEASUREMENTS OF SINGLE Cy3-EDA-ADP MOLECULES INTERACTING WITH MYOSIN FILAMENTS *IN VITRO*.
((**K. Oiwa**[1], M. Anson[2], J.F. Eccleston[2], A. Yamada[1], H. Nakayama[1] & D.R. Trentham[2])) [1]Kansai Adv. Res. Center, Kobe 651-24, Japan, [2]Nat. Inst. Med. Res., London NW7 1AA, U.K.

Using evanescent-wave laser excitation and fluorescence video microscopy, single molecules of fluorescent nucleotide analogs have been visualized, recorded and their life-times bound to myosin measured. We have used Cy3-EDA-ADP, the conjugate of Cy3.29.OH with 2'(3')-*O*-(N-2-aminoethyl)carbamoyl-adenosine 5'-diphosphate to determine the kinetics of association and dissociation of individual molecules from rabbit fast-twitch skeletal myosin *in vitro*. Synthetic filaments on a quartz surface appeared as uniformly-bright fluorescent images with 300 nM Cy3-EDA-ADP. At 3 nM Cy3-EDA-ADP discrete bright spots were visible on the filaments. These appeared suddenly, remained at the same position and brightness for a while and then abruptly disappeared. The spot dwell times fitted a single exponential of rate 0.43 s^{-1} for Cy3-EDA-ADP at 10 °C; close to the dissociation rate-constant, 0.67 s^{-1}, of Cy3-EDA-ADP from myosin S1 measured at 10 °C by stopped-flow. The corresponding association rate-constants were estimated as 2 × 10^5 $M^{-1}s^{-1}$ and 2.8 × 10^5 $M^{-1}s^{-1}$. These results together with earlier single-molecule studies using Cy3-EDA-ATP (Eccleston *et al.* (1996), Oiwa *et al.* (1996), *Biophys. J.* **70,** A159) show that single-molecule events can be used to determine the kinetics of myosin-nucleotide interactions. These studies with Cy3-EDA-ADP serve as a model for ligand-receptor binding at the level of single molecules.

Tu-Pos241

TWO-DIMENSIONAL ARRANGEMENT OF A FUNCTIONAL PROTEIN BY CYSTEINE-GOLD INTERACTION: ENZYME ACTIVITY AND CHARACTERIZATION OF A PROTEIN MONOLAYER ON GOLD SUBSTRATE.

((**Yuji C. Sasaki**,[1] Kenji Yasuda,[1] Yoshio Suzuki,[1] Tadashi Ishibashi,[1] Isamu Satoh,[2] Yasutake Fujiki,[3] and Shin'ichi Ishiwata[3, 4]))

[1]Advanced Research Laboratory, Hitachi Ltd.,Japan. [2]Institute for Materials Research, Tohoku University,Japan. [3]Department of Physics, School of Science and Engineering, [4]Advanced Research Institute for Science and Engineering, Waseda University, Japan.

We have characterized the functional protein, myosin subfragment 1(S1), attached to a gold substrate by the sulfhydryl groups of cysteine in proteins. The amino groups of the regulatory light chain (RLC) isolated from myosin were labeled with a radioisotope (^{125}I), and the labeled RLC was incorporated into S1 from which the RLC had been removed. The radiation from ^{125}I showed that S1 molecules had attached to the gold and, through the interference effect of the monochromatic radiation from ^{125}I, provided information about the position of labeled RLC sites in the S1 monolayer. The interference fringes showed that the RLC was located close to the gold surface and that all the adsorbed S1 molecules had the same orientation. We confirmed that the motor function of S1 on the gold surface is maintained by observing sliding movement at low ionic strength and by observing the detachment at high ionic strength of fluorescent actin filaments in the presence of ATP. We also found that the adsorbed S1 molecules were not removed from the Au surface by a reducing agent. Thus, the Au-S bond is more stable than the S-S bond.

Tu-Pos242

CONTRACTILE AND BIOCHEMICAL PROPERTIES OF SINGLE SKELETAL MUSCLE FIBERS AND MYOSIN HEAVY CHAIN COMPOSITION FROM ADVANCED AGED RATS. ((**L.V. THOMPSON**, R.E. NELSON, AND J.A. SHOEMAN)) University of Minnesota, Minneapolis, MN 55455

The maximum velocity of unloaded shortening (Vo), lactate dehydrogenase activity and the myosin heavy chain composition (MHC) were determined in 116 single fibers of the deep region of the lateral head of the gastrocnemius muscles (RG) from advanced aged (30 months) male rats. Single permeabilized fiber techniques were used to examine Vo (slack test at 15°C) and single freeze-dried skeletal fiber biochemical assays were used to quantitate LDH activity. Single fiber MHC profile was determined by SDS-PAGE and quantified by densitometry. In the RG, Vo was significantly faster in type IIa MHC fibers (3.55 ± 0.41 fl/s) than type I MHC fibers (1.05 ± 0.15 fl/s). Individual fibers co-expressing both MHCI and MHCIIa isoforms had a mean Vo of 2.22 fl/s, with a Vo range of 0.62 - 5.02 fl/s. Densitometric analysis demonstrated a significant correlation between Vo and the percentage of MHCIIa isoform in fibers co-expressing both MHCI and MHCIIa isoforms. In this fiber type, fibers with greater than 50% MHCIIa content had faster Vo (mean = 3.45 fl/s), in contrast to fibers with less than 50% MHCIIa content (Vo, mean = 1.86 fl/s). LDH activity (expressed in nmoles/ug dry wt/hour) was 32.6 ± 7.7, 56.3 ± 4.2 and 45.9 ± 5.7 for type I MHC fibers, type IIa MHC fibers, and fibers co-expressing both MHCI and MHCIIa isoforms, respectively. In conclusion, this study demonstrates fiber-type specific Vo which is influenced by the MHC isoform profile and fiber-type specific LDH activity in advanced aged rats. Supported by AHA-Minn. Affiliate, Univ. of Minn. Center on Aging.

Tu-Pos243

MOTILITY OF STRIATED AND CATCH MOLLUSCAN MYOSINS AND PHOSPHORYLATION OF A CATCH-SPECIFIC RLC. ((**C.L. Perreault**, K.M. Trybus,*M.A. Geeves, *S. Kurzawa, A.G. Szent-Györgyi)) Brandeis University, Waltham, MA 02254,*Max Planck Institute, Dortmund, Germany.

The actin activated ATPase turnover rates of *Placopecten* striated muscle myosins are higher than catch muscle myosins (1.5 vs. 0.6 μmol/min/mg). The respective S1s also differ (V_{max} = 20 vs. 7 s^{-1}). These differences are not due to light chains, but to small heavy chain sequence variations in the surface loop near the nucleotide binding pocket (Perreault-Micale *et al., J. Muscle Res. Cell. Motil.*, 1996). *In vitro* motility parallels the enzymatic activity. The velocity of movement was 3.8±0.94 μm/s for *Placopecten* striated myosin and 0.85±0.09 μm/s for *Placopecten* catch. We are measuring the individual steps in the ATPase cycle to identify the steps that are different between these muscle-specific isoforms.

We have cloned a catch-specific regulatory light chain (RLC) isoform that encodes a putative consensus sequence for phosphorylation. This RLC can be phosphorylated with myosin light chain kinases from both *Physarum* and chicken gizzard. We constructed RLC hybrids with the phosphorylated and unphosphorylated RLC. ATPase activities of the hybrids was independent of RLC phosphorylation. We are currently testing if phosphorylation of this RLC can regulate vertebrate smooth muscle. Thus, phosphorylation of a catch-specific RLC can occur, but it is not a regulatory switch for molluscan muscle contraction, nor is it capable of modulating enzymatic activity. (Supported by NIH Grants AR15963, AR41808, and MDA grants.)

Tu-Pos244

CENTRAL HELIX OF REGULATORY LIGHT CHAIN IS CRITICAL FOR THE REGULATION OF SMOOTH MUSCLE MYOSIN.

((**T. Kambara**, R. Ikebe, M. Sata, E. Katayama and M. Ikebe)) Department of Physiology, University of Massachusetts Medical Center, Worcester MA 01655

Motor function of smooth muscle myosin is activated by phosphorylation of the regulatory light chain (RLC) at Ser^{19} and/or Thr^{18}. However, the molecular mechanism by which the phosphorylation activates the motor function of myosin is not yet understood. It has been suggested that some communication between the N-terminal domain of RLC containing the phosphorylation sites and the C-terminal domain containing the heavy chain binding site is operating and is critical for phosphorylation mediated regulation. In the present study, we focused our attention on the role of central helix of RLC for regulation. The flexible region at the middle of the central helix (Gly^{95}-Pro^{98}) was deleted to various extent and the effects of the deletion on the regulation of the motor activity were examined. Deletion of Gly^{95}-Asp^{97}, Gly^{95}-Thr^{96}, or Thr^{96}-Asp^{97} decreased the actin translocating activity of myosin a little but the regulation was not disrupted. In contrast, deletion of Gly^{95}-Pro^{98} of RLC completely abolished the acin translocating activity of phosphorylated myosin. However, the unregulated S1 containing this RLC mutant retained the motor activity. These results suggest that the deletion of these residues at the central helix of RLC disrupts the phosphorylation mediated activation mechanism. On the other hand, the eliminatioin of Pro^{98} resulted in the activation of actin translocating activity of dephosphorylated myosin, while it did not affect the motor activity of phosphorylated myosin. Together, these results clearly indicate the importance of the hinge at the central helix of RLC on the phosphorylation mediated regulation of smooth muscle myosin. (supported by NIH)

Tu-Pos245

CRYO ATOMIC FORCE MICROSCOPY OF SMOOTH MUSCLE MYOSIN.
((Yiyi Zhang, Zhifeng Shao, Andrew P. Somlyo and Avril V. Somlyo))* Department of Molecular Physiology and Biological Physics, University of Virginia, Charlottesville, Virginia, 22908

The physiologically relevant extended (6S) form of smooth muscle gizzard myosin was imaged with the newly developed cryo atomic force microscope (cryo-AFM)[1,2] at 80-85 K under ambient pressure. The motor and regulatory domains of the head and the 14 nm pitch of the α-helical coiled-coil of the tail were resolved and the effects of thiophosphorylation of the regulatory light chain were examined. The tail was 4 nm shorter in thiophosphorylated than in nonphosphorylated myosin. The first major bend was invariant, at ~51 nm from the head-tail junction (H-T), coincident with low probability in the paircoil score (Berger et al., 1995). The second major bend was 100 nm from the H-T junction in nonphosphorylated and closer to a skip residue than the bend (at 95 nm) in thiophosphorylated molecules. The shorter tail and distance between the two major bends induced by thiophosphorylation is interpreted to result from melting of the coiled-coil. An additional bend not previously reported occurred, with a lower frequency, approximately 24 nm from the H-T. The range of separation between the two heads was greater in thiophosphorylated molecules. Occasional high-resolution images showed slight unwinding of the coiled-coil of the base of the heads. We suggest that phosphorylation of MLC_{20} can affect the structure of extended, 6S myosin.

References: [1]Han et al., *Biochemistry* 34:8215 (1995). [2]Zhang et al., *Biophys. J.* 71:2168 (1996).
*Supported by NIH grants RO1-RR07720 and PO1-HL48807.

Tu-Pos246

CONFORMATIONAL CHANGE AT THE SH1 AND SH2 REGIONS OF MYOSIN ACCOMPANIED BY FORMATION OF MYOSIN - ATP ANALOGUES COMPLEXES WHICH MIMIC THE DIFFERENT TRANSIENT STATE INTERMEDIATES ALONG THE ATPASE CYCLE
((**Kazuaki Homma** and Shinsaku Maruta)) Department of Bioengineering, Soka University, Hachioji, Tokyo 192 JAPAN. (Spon. by T. Mitsui)

It is well known that the flexible region of reactive cystein residues, SH1 and SH2 changes its conformation dramatically along the ATPase cycle. The conformational change at the SH1-SH2 region induced by forming complexes of myosin:8-N_3(Br)-ATP or myosin:ADP:Phosphate analogues (BeFn, Vi, AlF_4^- and ScFn) which may mimic different transient state along the ATPase cycle were studied using environmentally sensitive fluorescent dye. SH1 of skeletal muscle myosin S-1 was specifically labeled with 4-Fluoro-7-sulfamoylbenzofurazan (ABDF) according to the methods of Hiratsuka[Hiratsuka (1993) J. Biol. Chem. 268,24742-24750]. SH2 was specifically labeled with 2-(4'-maleimidylanilino) naphthalene-6-sulfonic acid (MIANS) [Hiratsuka (1992) J. Biol. Chem. 267, 14941-14948]. Complex formation of ABD-S-1 with ADP and phosphate analogues of BeFn, AlF_4^- or ScFn resulted in a significant increase of 110% in the fluorescence intensity as well as in the presence of ATP. On the contrary, when 8-N_3(Br)-ATP was added to ABD-S-1, the fluorescence intensity increased by only 60% which is about half as much as that of ATP. These results may suggest that SH1 of the myosin-ADP-Pi ternary complexes move toward a more hydrophobic enviroment due to formation of transient state intermediate which is close to the transition state. When ADP:BeFn and ADP:Vi were added to MIANS-S-1, the fluorescence intensity decreased by 40%. Interestingly, although the ternary complexes of S-1:ADP:AlF_4^- and ScFn were actually formed, the fluorescence intensity decreased by 30% which is identical to that induced by ADP. These results may suggest that the conformational change at SH2 is not accompanied by the formation of the transition state and that MIANS detect the conformational differences among these ternary complexes more sensitively.

Tu-Pos247

ANALYSIS OF STABLE ANALOGUES OF TRANSIENT INTERMEDIATES OF MYOSIN USING PHOTOAFFINITY-LABELLING.
((**Shinsaku Maruta**, Takashi Ohki, Taketoshi Kanbara* and Mitsuo Ikebe*)) Department of Bioengineering, Soka University, Hachioji, Tokyo 192 JAPAN. * Department of Physiology, University of Massachusetts Medical School Worcester, MA 01655-0127.

Myosin forms stable ternary complexes with ADP and phosphate analogues of fluoroaluminate (AlF_4^-), fluoroberyllate (BeFn) or orthovanadate (Vi) which mimic the transient intermediates of myosin ATPase cycle. Previously, we demonstrated that these complexes may mimic the different myosin ATPase reaction intermediates corresponding to each step of cross-bridge cycle [Maruta et al. (1993) J. Biol. Chem. 268, 7093-7100]. In the present study, photoaffinity labelling ADP analogue, 3'-O-(N-methylanthraniloyl)-2-azido-ADP (Mant-2-N_3-ADP) were employed as probe to study the conformational differences of the ATPase site of these complexes. Mant-2-N_3-ADP was trapped into skeletal muscle myosin active site in the presence of these phosphate analogues. The trapped Mant-2-N_3-ADP was covalently incorporated into the 25kDa N-terminal fragment of S-1 in myosin/Mant-2-N_3-ADP/AlF_4^- and BeFn complexes, presumably at Trp 130. However, although the amount of the trapped nucleotide was the same for both in the presence of AlF_4^- and BeFn, the efficiency of the photolabelling of the trapped Mant-2-N_3-ADP into S-1 was approximately two times higher for the BeFn complex than for the AlF_4^- complex. These results are consistent with our previous results, the ^{19}F-NMR spectra of the bound ^{19}F-labelled ADP analogue, TFNDP in the ternary complexes formed in the presence of AlF_4^- or BeFn showed small differences from each other [Maruta et al. (1993) Biophys. J. 64, a141]. Together, these results suggest that there are some differences in the conformation of the adenine binding site of these three ternary complexes.

Tu-Pos248

OPENING OF THE MYOSIN "PHOSPHATE TUBE" DURING THE HYDROLYSIS CYCLE.
((**E. Pate**, N. Naber, T. Pham, M. Matuska, K. Franks-Skiba, and R. Cooke)) Dept. Biochem. and Biophys., UCSF, Dept. Math., WSU.

We show that a series of ATP analogs, in which moieties of various sizes have been added to the γ-phosphorous of ATP, bind to the active site of myosin and to the actomyosin complex in chemically skinned, rabbit psoas fibers. The added moieties are (1) -CH_3 (ATP-CH_3),(2) a benzyl pyrroline nitroxide spin label (ATP-SL), and (3) 3',5'-dimethyl benzyl moiety (ATP-DMB). The affinity of the analogs for the active site shows only a slight dependence on the size of the added moiety. Addition of even our smallest group (CH_3) reduced the binding affinity of ATP-CH_3 to S1 by a factor of 10^5 from than observed for ATP. Computer molecular docking of ATP-CH_3 into the myosin-ADP•BeF_x crystal structure indicates no steric interference to prevent binding of ATP-CH_3. This suggests that the maintenance of charge at the γ-phosphate is crucial for tight nucleotide binding. Addition of the larger groups reduced the binding affinity by approximately a factor of 10 over that of ATP-CH_3. In the crystal structure of S1 complexed with nucleotides, the phosphates are buried within the protein in a tightly closed structure called the "phosphate tube". Due to the bulk of the modifying group, the binding of ADP-SL, and ATP-DMB appears incompatible with threading of the phosphates down the "phosphate tube". Thus the above results suggests that the tightly closed domain surrounding the triphosphates in the crystal structure must open during the ATPase cycle. Similar domain movements have been found in other proteins including members of the G-protein super-family, a famiIty that has structural homologies to myosin.

Tu-Pos249

THE COUPLING BETWEEN NUCLEOTIDE AND ACTIN BINDING TO S1 IS DIFFERENT BETWEEN SMOOTH AND SKELETAL MUSCLE PROTEINS.
((**Christine Cremo** & Michael Geeves.)) Department of Biochem. & Biophys. Washington State University, Pullman Washington 99164-4660. MPI for Molecular Physiology, 44137 Dortmund, Germany.

Previous studies have shown that release of ADP from smooth actomyosin S1(acto.sm-S1) produces a rotation of the neck region (Witttaker et. al. Nature, 378, 748 (1995); Gollub et. al. Nature Struct. Biol. 3, 796 (1996); Poole et al 1997 in press). Skeletal myosin S1 (sk-S1) in contrast shows little change on ADP release. We have used transient kinetic methods to study the interaction between actin, ADP and sm-S1. The K_d of actin for sm-S1 was 20 nM similar to that of sk-S1. The K_d of actin for sm-S1 was increased only 3 fold by saturation of the complex with ADP compared to a 30-100 fold increase for the skeletal system. The K_d of ADP for sm-S1 was 1 μM and was increased to 3.5 μM in the presence of saturating actin (similar to the K_d's measured in the above studies). In contrast the K_d of ADP for sk-S1 was increased from 1 μM to 100 μM by actin. Thus the coupling between ADP binding and actin binding is weaker for sm-S1. One explanation of the differences could be in the fractional occupancy of the A- and R-states of the acto.S1 complex (Geeves Biochem.J. 274 1, (1991)). However fluorescence studies with pyrene-actin and mant.ADP demonstrate little (<5%) occupancy of the A-state in the presence or absence of ADP, similar to sk-S1. The implications for the ADP induced structural change in acto.sm-S1 will be discussed.

Tu-Pos250

MEAN-VARIANCE ANALYSIS OF FORCES AND DISPLACEMENTS GENERATED BY MYOSIN IN THE LASER TRAP
(William H. Guilford, Joseph B. Patlak and David M. Warshaw) Department of Molecular Physiology and Biophysics, University of Vermont, Burlington, VT 05405

In recent years the laser trap has been used to measure single steps in force and displacement generated by myosin (Finer *et al.*, 1994; Molloy *et al.*, 1995). To date, however, steps were hand-selected. Hand selection could significantly bias the data, and it is a difficult practice to defend statistically (Block and Svoboda, 1995). To derive an unprejudiced estimate of force and displacement from our laser trap data, we applied the technique of "mean-variance" (MV) analysis (Patlak, 1993), originally developed for the statistical analysis of single ion-channel current data. Like ion-channel recordings, single time records of displacement or force events produced by myosin appear as "steps" in the data record, and are thus amenable to this style of analysis which emphasizes intervals of constant amplitude within the data. MV analysis begins with a model-independent transformation of the time record, thus giving an alternative view of the data (a MV histogram). Generation of the MV histogram requires no assumptions about, nor interpretation of the underlying data. Quantitative descriptions of the data are subsequently derived from curve fits to the histogram. Thus, MV analysis is less prone to the biases introduced by manual scoring methods, and may be used to estimate the size, distribution, number and duration of events in the data. One may also test, in an unbiased fashion, models describing the distribution of event sizes. We will give examples of this technique's application to both actual and modelled data.

Tu-Pos251

THE REGULATORY LIGHT CHAIN OF FILAMENTOUS SMOOTH MUSCLE MYOSIN INTERACTS WITH THE HEAVY CHAIN OF A SECOND MYOSIN MOLECULE ((**Jennifer J. Olney*** and Christine R. Cremo*)) *Dept. of Biochem. and Biophys., Washington State Univ., Pullman, WA 99164.

Smooth muscle myosin was labeled with a photoreactive crosslinker on Cys-108 in the C-terminal domain of the regulatory light chain (RLC). The RLC crosslinked to the heavy chain (HC) during irradiation of myosin filaments but not the extended 6S monomer. Filaments composed of two populations of myosin were used to detect inter-myosin crosslink formation. Fifty percent of the myosin was specifically tritiated on Ser-180 of the heavy chain while the other 50% contained the photoreactive crosslinker on the RLC. Detection of tritium in the isolated HC-LC crosslink indicates the RLC of one myosin interacts with the HC of a second myosin molecule in filaments. Preliminary data suggests the crosslink occurs between the C-terminal of the RLC and the subfragment 1 region of the HC of the second myosin molecule. These results indicate head-head interaction occurs between separate myosin molecules in filaments. Studies are underway to determine the site of the crosslink within the HC and to determine the effect of phosphorylation upon crosslink formation.

Tu-Pos252

SYNTHESIS AND CHARACTERIZATION OF A SPIN LABELED NON-NUCLEOSIDE ATP PHOTOAFFINITY LABEL; REACTION WITH MYOSIN AND MUSCLE FIBERS **((X. Chen‡, J. C. Grammer‡, E. Pate*, R. Cooke+ and R. G. Yount‡)) ‡Depts. of Biochemistry and Biophysics and *Mathematics, Washington State University, Pullman, WA 99164, +Dept. Biochem/Biophys & CVRI, UCSF, San Francisco, CA 94143**

Previous studies have shown that a photoreactive non-nucleoside ATP analog, 2-[(4-azido-2-nitrophenyl)amino] ethyl triphosphate (NANTP) behaves remarkably like ATP in its interaction with myosin and muscle fibers. Its diphosphate product (NANDP) is trapped at the active site by cross-linking SH_1 and SH_2 or by use of phosphate analogs, such as vanadate or AlF_4. Upon irradiation it specifically photolabels Trp-130 in rabbit skeletal myosin in high yields. Here we have synthesized a new derivative of NANTP (see Fig. 1) in which a spin label is attached via an aminomethyl side chain to NANTP. This derivative, called SLam-NANTP, is a substrate for myosin and is stably trapped by addition of vanadate and Co^{2+}. Upon brief irradiation above 300 nm SLam-NANDP photoincorporates >50% in both subfragment 1 and in myosin in skinned muscle fibers. The epr spectra of labeled fibers indicates it has two components, one highly mobile and a second more restricted spectrum consistent with motion of the probe in a core of 85° to 90°. Photolabeled fibers contract normally upon activation with Ca^{2+} and MgATP. These studies show it is possible to attach a spin probe covalently in high yield specifically near the active site (presumably to be Trp-130) without affecting the normal function of the fibers. Supported by MDA (R.G.Y. and R.C.) and NIH; DK 05195 (R. G. Y.), AR 39643 (E. P.) HL 32145 (R. C.)

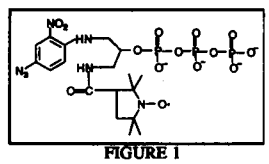

FIGURE 1

Tu-Pos253

CONFORMATIONAL CHANGES IN THE ALKALI LIGHT CHAINS OF MYOSIN INDUCED BY TRIFLUOPERAZINE AND DETECTED USING ELECTRON PARAMAGNETIC RESONANCE AND CIRCULAR DICHROISM SPECTROSCOPY. ((W Huang, GJ Wilson#, H Lam & B Hambly)) Pathology Dept., University of Sydney, NSW 2006 & #CRC for Cardiac Technology, Royal North Shore Hospital, NSW 2065 Australia.

We studied the interaction of isolated alkali light chains (ALCs) of myosin with the calmodulin antagonist phenothiazine drug, trifluoperazine (TFP), using two spectroscopic techniques. Paramagnetic spin probes covalently bound to the ALCs (LC1 and LC3) were used to detect conformational changes occurring in LC1 and LC3 upon binding of TFP. The rotational correlation time of a spin probe attached to either of the two ALCs is progressively slowed in the [TFP] range of 0.01-1.2 mM. The half-maximal effect was observed at 0.3 mM and a Hill plot did not detect cooperative binding. Circular dichroic (CD) spectroscopy was used to study the effect of TFP on the helical content of the ALCs. Addition of TFP increased the helical content of the ALCs over the 10 fold increase from 5-600 μM. The half-maximal effect was observed at ~30 μM, an order of magnitude lower than that observed using ESR spectroscopy, and a Hill plot showed co-operative binding. These differences can be explained by the different effects detected by the different spectrosopic techniques. CD spectroscopy is more sensitive for detecting changes in conformation at binding sites of higher affinity. Above the range of CD spectroscopy, the further binding of TFP to other lower affinity sites slows mobility of the spin probe on the C-terminal domain of the ALCs. Comparative sequence analysis between Ca^{2+}-binding superfamily proteins shows significant conservation between the hydrophobic parts expected to bind TFP in calmodulin and Troponin C. Supported by NH&MRC and ARC of Australia.

Tu-Pos254

RECOMBINANT ESSENTIAL LIGHT CHAIN 3 OF SKELETAL MUSCLE MYOSIN SUBFRAGMENT 1 ((**Z. Gong¶**, W-J. Dong‡ and H. C. Cheung‡)) ¶Biophysical Sciences Program and ‡Dept. Biochemistry & Molecular Genetics, Univ. of Alabama at Birmingham, Birmingham, AL 35294. (Spon. By R. Krishna)

We have expressed the essential light chain 3 (LC3) of rabbit fast skeletal muscle in *E. coli*. The expressed protein was secreted from the bacteria with unblocked amino terminus and was exchangeable with endogenous LC3 in myosin S-1 in a high salt concentration. The α-amino group was converted into a sulfhydryl group, using Traut's reagent. This procedure yielded a recombinant LC3 which contains two sulhydryl groups, one at the N-terminus and the other at residue 136 (Cys136). These two -SH groups were individually labelled with the fluorescent probe IAEDANS. The fluorescence properties (intensity and lifetime) of the label at the N-terminus of LC3 were strongly quenched upon exchange into S-1, whereas the fluorescence of the label attached to Cys136 was insensitive to exchange. The intersite distance between the N-terminus and Cys136 was investigated using IAEDANS attached to Cys136 as the energy donor and the probe DAB attached to the N-terminus as energy acceptor. The energy transfer data were analyzed in terms of a distribution of the distances. Similar results were obtained when the donor and acceptor sites were interchanged. Preliminary results indicated an increase in energy transfer between the two sites of LC3 after the light chain was exchanged into S-1. This preparation of chemically modified recombinant LC3 is potentially useful for studies of the conformation of the essential light chain in myosin under different biochemical state.

Tu-Pos255

TENSION-MODULATION OF SMOOTH MUSCLE ADP AFFINITY ((**J. Gollub** and R. Cooke)) Dept. of Biochemistry, & Biophysics, Cardiovascular Research Institute, University of California, San Francisco, CA 94143.

The regulatory domain of smooth muscle myosin rotates ~20° upon release of ADP from the catalytic site. Cryo-electron microscopy studies reveal that this rotation is in the appropriate direction to generate force in a working muscle cell. It is therefore possible that this conformational change is related to force generation and could be reversed by external tension on the cell; i.e., the regulatory domain could be driven from the rigor state to the ADP-bound state, effectively increasing the protein's affinity for ADP. We have developed a technique to measure a muscle cell's affinity for ADP under conditions of external tension. A known tension is applied to a small section of skinned smooth muscle tissue. Mant•ADP, a fluorescent nucleotide analog, is titrated into the preparation in the presence of 400 mM acrylamide, a solution quenching agent. Mant•ADP bound to myosin is shielded from solution quenchers, allowing measurement of a binding curve from the increase in fluorescence over background. Rabbit taenia coli under no external stress has been ascertained to have an ADP affinity of approximately $2x10^5$ M^{-1}. Further results will be discussed at the meeting. Supported by, AR42895

Tu-Pos256

EXPRESSION OF SMOOTH MUSCLE SPECIFIC MYOSIN BY URINARY BLADDER SMOOTH MUSCLE CELLS *IN VITRO* ((**G.S. Kim**, Z. Wang, and S. Chacko)) Department of Pathobiology and Division of Urology, University of Pennsylvania, Philadelphia, PA 19104.

Experiments were carried out to determine the stability of the differentiated phenotype *in vitro* by smooth muscle cells isolated from bladder walls. Cells from neonatal rabbit bladder smooth muscle layers were isolated by collagenase (1 mg/ml) treatment, and the dissociated cells were cultured in nutrient medium (M199 supplemented with 10% fetal calf serum and 1% antibiotic-antimycotic) in collagen-coated tissue culture dishes. Upon reaching confluency, cells were dissociated with trypsin-EDTA (0.05%) and subcultured. The expression of smooth muscle myosin heavy chain (MHC) isoforms encoded by MHC mRNA alternatively spliced at the 3'end (SM1 and SM2), and the isoforms encoded by MHC mRNA alternatively spliced at the 5' end (inserted and noninserted) were investigated using RT-PCR, QC-PCR, and Southern blotting. The level of expression of SM1 and SM2 at the mRNA level in the cultured cells was the same as in the adult intact bladder. However, electrophoresis of the proteins from these cells on highly porous SDS-polyacrylamide gel and western blot analysis revealed only the SM2 isoform. The RT-PCR analysis of the mRNA also showed that the MHC mRNA transcript expressed by these cells has a 21-nucleotide insert at the 5'end, thus capable of translating the myosin which has a 7-amino acid insert at the ATP-binding region in the myosin head. The data indicate that cells cultured from rabbit urinary bladder smooth muscle layer express smooth muscle specific myosin even after two subcultures; hence, capable of expressing differentiated phenotypes *in vitro*. Supported by NIH Grants. DK39740 & DK47514.

Tu-Pos257

EXPRESSION OF THE "INTESTINAL" MYOSIN HEAVY CHAIN IN RAT BLOOD VESSELS. ((U. Wetzel, **H. Haase**, G. Lutsch, I. Morano)) Max Delbrück Center for Molecular Medicine, 13122 Berlin, Germany.

Myosin heavy chain (MHC) isoforms of smooth muscle (SM) arise from alternative splicing at both the 3' end (SM1, SM2) and the 5' end (SM1A, SM2A, SM1B, SM2B). The SM-MHC type B contains an inserted sequence of seven amino acids (QGPSFAY) near the ATP binding region. In the hypertrophied SM cells of rat myometrium (Haase & Morano, 1996) and of mouse megacolon (Siegmann et al, 1997) a down-regulation of the SM-MHC type B expression was reported while the maximal shortening velocity of the SM fibers increased. We used a polyclonal antibody directed against the inserted sequence to identify SM-MHC type B expression in adult rat heart by immunofluorescence microscopy. Specific immunostaining was clearly obtained in small blood vessels (wall thickness about 5 μm). Large vessels (wall thickness about 20 μm) as well as aortic SM cells were not stained by the antibody. Parallel immunostaining of SM actin was performed to evaluate size and wall thickness of the vessels. Our results indicate that the SM-MHC type B isoforms hitherto considered as intestinal forms are also expressed in SM cells of resistance vessels. The heterogeneity in the expressed SM isoforms may contribute to differential responsiveness and contractility within the vascular tree.

Haase H, Morano I (1996) J Cell Biochem 60: 521-528
Siegman MJ et al. (1997) J Gastrointestinal and Liver Physiol: submitted.

Tu-Pos258

CARBONIC ANHYDRASE EXPRESSION INCREASES EARLY DURING STIMULATION-INDUCED SKELETAL MUSCLE TRANSFORMATION. ((**William O. Kline**[1,3] and Peter J. Reiser[1,2,3])) [1]Exercise Science, [2]Oral Biology & [3]Biophysics Program, The Ohio State University, Columbus, OH 43210.

The level of expression of carbonic anhydrase (CA), an enzyme involved in buffering intracellular [H^+] and [CO_2], is positively correlated with the level of slow-type myosin in adult skeletal muscles. Chronic electrical stimulation of skeletal muscle results in fast-to-slow phenotype transformation and a correlation between increased levels of CA and of slow-type myosin heavy chain (MHC-s) following stimulation has been reported. In general, increases in MHC-s in normally fast-twitch muscle occur following several weeks of experimentally-induced altered motor activity. An increase in the level of CA would be expected to be beneficial at much earlier times following the onset of continuous stimulation. We, therefore, examined simultaneously the time courses of changes in CA and MHC-s levels, as well as those of MHC fast-types IIA and IID, in continuously stimulated (10 Hz) rabbit tibialis anterior (normally fast-twitch) muscle. A significant increase in the relative amount of MHC-s does not occur until the third week of stimulation. The level of MHC-IIA increases by ~50% and becomes the predominant isoform after two weeks of stimulation whereas the level of the normally-predominant MHC-IID isoform decreases by ~35% during the same period. A marked 6-fold increase in the level of CA is observed as early as the second week of stimulation. These results indicate that the level of CA increases earlier than previously reported during stimulation-induced phenotype transformation and suggest that CA increases in transforming fast fibers and not only in established slow fibers. An increased level of CA is, therefore, likely to have an important role in buffering intracellular pH and CO_2 during early, as well as late, stages of fast-to-slow muscle transformation. Supported by NIH Grant AR39652.

Tu-Pos259

DISPLACEMENT AND FORCE FROM NATIVE THICK FILAMENTS MEASURED WITH AN OPTICAL TRAP.
((**A. Trombetta**, J. Sleep and R.M. Simmons)) MRC Muscle and Cell Motility Unit, The Randall Institute, King's College London, UK. (Spon. by M. Chew)

A single bead optical trap technique was used to measure the interaction between an actin filament and a native myosin filament from the slow adductor of the oyster *O. edulis*. Filaments were used so that the orientation of the myosin molecules could be determined. Aliphatic amine latex beads were activated with EDC and coated with NEM labelled myosin and actin filaments were then bound. To reduce interactions between bound actin filament and the densely populated myosin surface of a thick filament, short lengths of sonicated actin were used (average length 0.2 μm) and the beads were labelled sparsely with actin, as low as one filament per bead. Further, the proportion of active myosin molecules was kept small by using a low calcium concentration (pCa 6.5). The vector of force and displacement in single interactions was closely aligned with the axis of the myosin filament. Mean amplitudes were: isometric 3.7 pN; low load 10 nm (Finer method), 6 nm (Molloy method).
Supported by Medical Research Council, Human Frontier Science Program.

Tu-Pos260

THERMAL ACTIVATION OF ACTOMYOSIN MOTORS WITH TEMPERATURE-PULSE MICROSCOPY. ((H. Kato[1], T. Nishizaka[1], T. Iga[1], K. Kinosita,Jr.[2], **S. Ishiwata**[1,3])) Department of Physics, School of Science and Engineering, Waseda University, 3-4-1 Okubo, Shinjuku-ku, Tokyo 169, Japan[1]; Department of Physics, Faculty of Science and Technology, Keio University, 3-14-1 Hiyoshi, Kohoku-ku, Yokohama 223, Japan[2]; Advanced Research Institute for Science and Engineering, Waseda University, Japan[3].

Microscopic real-time imaging of temperature on sliding actin filaments in an in vitro motility assay system (heavy meromyosin (HMM) was used as motor proteins) has been achieved by monitoring the fluorescence intensity of rhodamine phalloidin attached to actin filaments. Temperature pulse could be locally and reversibly introduced by illuminating metal particles with an infrared laser light (λ = 1.053 μm) by splitting the laser beam used for the optical tweezers. Combining these techniques (temperature-pulse microscopy: TPM), reversible increase and decrease of an order of magnitude of sliding velocity and tension generation were observed with repetitive temperature modulation between about 20 ℃ and 45 ℃. An abrupt displacement of sliding actin filaments as large as 2 to 0.2 μm occurred following temperature pulse (from 18 to 45 ℃ on average) in a duration as short as 1/16 to 1/128 s, respectively, which corresponds to the sliding velocity of 26 to 32 μ m/s. Judging from the fact that Q_{10} of ATPase per head of HMM is larger than 2, several to only a few ATPase cycles (even a fraction of cycle) appear to occur during these short pulses. This may imply that the displacement is proportional to the number of ATPase cycles even to a fraction of cycle. The TPM should be applicable to the studies on spatio-temporal response of supramolecules, organelles and living cells over a wide range of thermal modulation.

SMOOTH MUSCLE BIOCHEMISTRY AND PHYSIOLOGY

Tu-Pos261

KINETICS OF $[Ca^{2+}]_i$ DURING THE PHOTOMECHANICAL RESPONSE OF ALBINO RAT SPHINCTER PUPILLAE.
((**A.P. Krivoshik** & L. Barr)) Molec. & Integ. Physiol., Univ. of Illinois at Urbana-Champaign, Urbana, IL 61801. (NIDA NRSA F30 DA05574)

Absorption of light by the rhodopsin of albino rat sphincter pupillae myocytes evokes contraction by triggering the release of calcium ions from the sarcoplasmic reticulum. Isolated sphincter preparations were pre-loaded with the calcium sensitive fluorescent probe, indo-1. Subsequently, force and intracellular calcium, $[Ca^{2+}]_i$, were measured concurrently following stimulations by light flashes of varying duration and intensity. During the responses to flashes, $[Ca^{2+}]_i$ and force rise to half maximal values in about 0.5 seconds and 2.0 seconds, respectively. The time courses of $[Ca^{2+}]_i$ contain both fast and slow components. The former has a latency in the neighborhood of 100 milliseconds. The time courses of $[Ca^{2+}]_i$ and force compare well with the predictions of our hypothetical Ca^{2+}-calmodulin-MLCK signal transduction model. We conclude that the largest fraction of the force latency is downstream from the release of calcium from the sarcoplasmic reticulum.

Tu-Pos262

HETEROGENEITY OF SUBCELLULAR CALCIUM SIGNALLING IN SINGLE SMOOTH MUSCLE CELLS. ((**D.V. Gordienko**, M.B. Cannell and T.B. Bolton)) Department of Pharmacology & Clinical Pharmacology, St. George's Hospital Medical School, London SW17 0RE, U.K.

Calcium is a major regulator of a variety of cell functions and in smooth muscle cells there is increasing evidence for spatial non-uniformities in calcium signal transduction. Single myocyes were obtained by enzymatic dissociation of the longitudinal muscle layer of guinea-pig ileum. Cells were exposed to 10 μM fluo-3 AM for 15 min followed by a 30-min wash in physiological salt solution (to allow time for de-esterification). Cells were used within 5 hours of isolation. The fluo-3 fluorescence was imaged with a laser scanning confocal microscope and, as illustrated in Fig. 1, microscopic increases in fluorescence could be clearly resolved. These events were similar to calcium "sparks" reported in other preparations. Other patterns of spontaneous calcium release such as regular and irregular calcium waves and synchronous calcium mobilisation throughout the cell were also observed. The extent to which the various patterns of subcellular calcium signalling reflect summation of calcium spark-like events is being investigated. Supported by the BHF, MRC and Wellcome Trust.

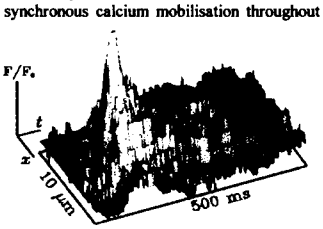

Fig. 1. Line scan data illustrating one type of spatio-temporal pattern of spontaneous Ca^{2+} -release.

Tu-Pos263

EFFECTS OF HYDRALAZINE UPON β-ESCIN SKINNED RABBIT AORTA.
((**D.C.Ellershaw** and A.M.Gurney)) Deptartment of Physiology & Pharmacology, Strathclyde University, Glasgow, G1 1XW and Deptartment of Pharmacology, UMDS, St Thomas's Hospital, London, SE1 7EH.

Hydralazine has been proposed to produce vasodilation by interfering with Ca^{2+} release from the smooth muscle SR (Gurney AM & Allam M, 1995, *Br J Pharmac*, **114**, 238-244). This hypothesis was tested by investigating the inhibitory effects of hydralazine upon contractions of rabbit aorta, either to phenylephrine (PE; 1-10μM) in intact preparations or to Ca^{2+}, IP_3 (100μM) and caffeine (20mM) in β-escin permeabilised preparations. Isometric tension was measured from aortic strips bathed in physiological solution (mM): NaCl 112, KCl 5, NaH_2PO_4 0.5, KH_2PO_4 0.5, $NaHCO_3$ 15, $MgCl_2$ 1, glucose 11, $CaCl_2$ 2 (pH 7.4). In PE precontracted aorta, hydralazine produced relaxation with an EC_{50} of 19μM and maximum of 90% at 100μM. Transient contractions to PE were more potently suppressed, with EC_{50} of 6μM and maximum inhibition of 74% at 100μM. In β-escin permeabilised aorta, hydralazine did not significantly alter the $[Ca^{2+}]$-tension relationship, although at low $[Ca^{2+}]$ contractions appeared to be slowed. At 100μM hydralazine reduced contractions to IP_3 by 52 ± 3% (n=5) and contractions to caffeine by 32 ± 5% (n=5). In conclusion, hydralazine reduced transient contractions to PE more effectively than sustained contractions. The mechanism appears to involve reduced cytoslic $[Ca^{2+}]$ rather than inhibition of Ca^{2+} action. This can be explained in part by inhibition of IP_3-induced Ca^{2+} release, with some additional action on the caffeine sensitive $[Ca^{2+}]$ stores.

Tu-Pos264

PURIFICATION AND RECONSTITUTION OF A Ca^{2+}-INSENSITIVE SARCOLEMMAL Cl^- CHANNEL FROM AIRWAY SMOOTH MUSCLE.
((**D. Salvail**, M. Dumoulin, and E. Rousseau)) Dept. of Physiology & Biophysics, University of Sherbrooke, Sherbrooke, Qc, Canada.

Much attention has been given to the characteristics and roles of trans-sarcolemmal Cl^- movements in smooth muscle. Yet, aside from the abundance of information gathered on Ca^{2+}-activated Cl^- conductances, few observations have been reported on other types of Cl^- channels, especially in airway smooth muscle (ASM). We have used the lipid bilayer reconstitution technique to functionally characterize a novel sarcolemmal Cl^- channel (Salvail *et al.* Am. J. Physiol., 1996) which displays an ohmic unitary conductance of 77 pS when studied in the presence of a 50 / 250 CsCl gradient. The reconstituted channel is characterized by a high open probability that is independent of both membrane potential and variations of cytoplasmic $[Ca^{2+}]$. The selectivity of the channel for the tested small mono- and divalent anions is as follows: $Cl^- > I^- > Br^- > F^- >> HCO_3^- \approx SO_4^{2-}$. Although the channel's activity is unaltered by phosphorylation cocktails containing PKG and PKA, DIDS (EC_{50} = 30 mM) and NPPB (EC_{50} = 130 mM) successfully inhibit the unitary currents as well as the tonic tension induced by exposing ASM tissue strips to carbamylcholine. Digitonin was used to solubilize the channel-protein from bovine tracheae. The channel was then partially purified by chromatography, followed by sequential membrane reconstitution to ascertain the functionality of the purified membrane protein. Reconstitution of the purified channels should provide insights as to what mechanisms may be involved in the regulation of the activity of this channel and, indirectly, in the control of the membrane potential of ASM cells.

Tu-Pos265

PROMINENT ROLE OF SARCOPLASMIC RETICULUM CA^{2+} STORES IN CANINE HYPOXIC PULMONARY VASOCONSTRICTION.
((**R.I. Jabr** and J.R. Hume)) Department of Physiology and Cell Biology, Univ. of Nevada School of Medicine, Reno, NV, 89557.

The possible role of sarcoplasmic reticulum (SR) Ca^{2+} stores in hypoxic pulmonary vasoconstriction (HPV) is not well understood. We examined the effects of (1) ryanodine (RYN, 10μM) depletion of Ca^{2+} stores and/or (2) pretreatment with cyclopiazonic acid (CPA, 10μM) on HPV. Isometric tension was measured from canine pulmonary artery rings suspended in Krebs-Henseliet solution (K-H) bubbled with 95%O_2/5%CO_2. Hypoxia was induced by bubbling phenylephrine (PE, 1μM) precontracted rings with 95%N_2/5%CO_2. HPV was observed in both intact and denuded arteries and expressed as a percent of maximal KCl contraction ($\%T_{Kmax}$)= 21.3±3.2%; n=13 and 21.7±4%; n=4, respectively. When SR caffeine (CAF) sensitive Ca^{2+} stores were depleted by pretreatment with RYN and frequent CAF (15mM) incubation, the hypoxic response was significantly smaller ($\%T_{Kmax}$= 3.4±2.4; n=6; p<0.001). On the other hand, in normoxic rings pretreated with CPA, the PE response was significantly smaller ($\%T_{Kmax}$= 9.2±5% compared to 52.3±9.6%; n=6; p<0.001) with no significant effect on CAF induced contractions suggesting that CPA preferentially depletes the IP_3 Ca^{2+} store, without affecting the CAF sensitive Ca^{2+} store. When hypoxia was induced in presence of CPA, developed tension was significantly larger than without CPA ($\%T_{Kmax}$= 78.2±15%; n=6; p<0.05) and was only partially blocked by nisoldipine (NISOL, 10μM) and RYN ($\%T_{Kmax}$= 20.3±3.7%; n=6). These data suggest that: (1) CAF Ca^{2+} stores contribute significantly to HPV under control conditions and in CPA and (2) in CPA, an additional NISOL- and RYN-insensitive Ca^{2+} pathway is evoked by hypoxia. (supported by NIH HL 49254)

Tu-Pos266

TOXIN B (TOXB) FROM *C. DIFFICILE* AS A PROBE FOR THE PARTICIPATION OF RHO PROTEINS IN CA^{2+}-SENSITIZATION IN *INTACT* SMOOTH MUSCLE.
((**G. Pfitzer**[1], C. Lucius[1], M. Seehafer[1], F. Hofmann[2], K. Aktories[2], A. Arner[3])) [1]Humboldt University of Berlin, [2]University of Freiburg, Germany, and [3]University of Lund, Sweden

ToxB monoglucosylates small GTPases of the Rho subfamiliy thereby inhibiting them. We used it to probe participation of Rho proteins in agonist-induced contractions in *intact* smooth muscle. In longitudinal intestinal guinea pig smooth muscle strips, carbachol induced a biphasic contraction: an initial rapid rise in force (peak 1) followed by a partial relaxation and a second delayed increase in force (peak 2). In strips incubated with ToxB for 12 h, peak 2 was inhibited by 80% while the effect on peak 1 was variable (about 40% inhibition (n=3) to no inhibition (n=3)). The rise in cytosolic Ca^{2+} ($[Ca^{2+}]_{cyt}$), which was measured in the same strips with fura2, preceded peak 1 and then declined to a suprabasal steady state level. Peak 2 was not associated with a corresponding increase in $Ca^{2+}{}_{cyt}$. Unlike force, the Ca^{2+}-transient (n=6) was not affected by ToxB. Inhibition of force by ToxB was associated with a significant decrease in myosin light chain phosphorylation (MLC-P) from 54 to 24% (peak 1) and 28 to 16% (peak 2). Basal MLC-P was not affected by ToxB. ToxB did not inhibit norepinephrine (NE, 30 μM) and endothelin induced contractions in *intact* rabbit femoral arteries while the NE-induced increase in Ca^{2+}-sensitivity in ß-escin *permeabilized* femoral arteries was signifcantly inhibited by C3. In conclusion, in smooth muscles susceptible to ToxB, it inhibits sustained force most likely by inhibiting a small GTPase mediated process involved in the agonist induced Ca^{2+}-sensitization of MLC-P.

Tu-Pos267

GROWTH STIMULATION *IN VITRO* OF INTESTINAL SMOOTH MUSCLE REDUCES CALCIUM CURRENT DENSITY AND INTRACELLULAR CALCIUM.
((**M. Gomez**, K.H. Swärd and P. Hellstrand)) Dept. of Physiology and Neuroscience. S-223 62 Lund, Sweden.

Guinea pig ileum strips were isometrically mounted and cultured for five days in the absence (control) and presence of 10 % fetal calf serum (FCS) as growth stimulator. After culture, strips were mounted for force and intracellular calcium ($[Ca^{2+}]_i$) measurements with Fura-2. Whole-cell voltage clamp experiments were carried out to investigate the effects of growth stimulation on voltage-activated calcium channels. The relationship between extracellular calcium and force during depolarization with 60 mM K^+ solution was investigated. Growth stimulation shifted this relationship threefold to the right. In addition, the slope of the relationship between extracellular Ca^{2+} and $[Ca^{2+}]_i$ was reduced. Whole-cell inward currents were elicited by depolarizing pulses from -80 mV to +10 mV in a solution containing 10 mM Ba^{2+}. Maximum currents, normalized using cell capacitance as an index of cell surface area, was 8.8±1.7 pA/pF (n=5) in growth stimulated cells and 56.5±0.5 pA/pF in control cells (n=2). Current in cells isolated from fresh tissue was 44.5±3.9 pA/pF (n=11). We suggest that the decreased calcium current density contributes to the reduced intracellular calcium and to the rightward shift of the relationship between extracellular calcium and force observed after growth stimulation.

Tu-Pos268

PKC INHIBITOR Ro 31-8220 DOSE-DEPENDENTLY BLOCKS INWARD Ba^{2+} CURRENT IN VASCULAR SMOOTH MUSCLE MYOCYTES.
((**A.L. Miller** & P.D. Langton)) Dept. Physiology, University of Bristol, Bristol, England BS8 1TD.

The bisindolymaleimide, Ro 31-8220, is thought to be a specific inhibitor of protein kinase C (PKC).

Inhibition by Ro 31-8220 of both first phase hypoxia-induced, Ca^{2+}-dependent contraction of prostaglandin F(2α) or KCl precontracted intrapulmonary arteries could be inhibited by Ro 31-8220 suggests a link between PKC and intracellular Ca^{2+} handling.

Whether inhibition of PKC influences release Ca^{2+} internal stores, or activation of plasmalemmal voltage-sensitive Ca^{2+} channels has not being established. We investigated the latter possibility by examining the effect of Ro 31-8220 on L-type (dihydropyridine-sensitive) Ca^{2+} channels under normoxic conditions at room temperature. Rat cerebral artery smooth muscle myocytes were superfused using a rapid change-over micro superfusion system. By minimising outward current with CsCl in the internal solution, inward Ba^{2+} current was recorded using conventional whole-cell patch in the absence and presence of Ro 31-8220. Test steps from -80 mV to a range of more positive potentials in the absence and presence of increasing concentrations of Ro 31-8220 (0.3, 1.0, 3.0, 10.0 μM) resulted in a concentration dependent reversible inhibition of inward current with an IC_{50} of 3.94 ± 0.79 μM, slope of 0.9 ± 0.1 at +10 mV (n = 4 cells). The effect of 2 other inhibitors of PKC on inward current were also investigated. Both calphostin C and staurosporine failed to influence inward current.

Ro 31-8220 also reduced K^+-induced isometric tension measured from artery segments mounted on a wire myograph. Unlike its influence on inward current, Ro 31-8220 irreversibly inhibited developed tension. This prevents determination of an IC_{50}.

Due to the difference in reversibility between patch and wire experiments, it is likely that Ro 31-8220 has more than one effect in this tissue, one of which is the inhibition or blockade of DHP-sensitive Ca^{2+} channels.

The authors would like to thank Hoffman La Roche, Welwyn Garden City, Herts, England for their kind donation of Ro 31-8220. This work supported by the BHF, grant PG94/101.

Tu-Pos269

CALCIUM SPARKS IN PORCINE TRACHEAL SMOOTH MUSCLE CELLS ((**Y.S. Prakash**, M.S. Kannan and G.C. Sieck)) Depts. of Anesthesiology and Physiology & Biophysics, Mayo Foundation, Rochester, MN 55905; Dept. of Veterinary PathoBiology, University of Minnesota, St. Paul, MN 55108. (Spon. D.O. Warner).

Spontaneous, localized $[Ca^{2+}]_i$ transients (Ca^{2+} sparks) have been reported in skeletal, cardiac and smooth muscle cells. Both spontaneous and agonist-induced propagating $[Ca^{2+}]_i$ oscillations have also been observed in various cell types. We used real-time confocal imaging to examine the spatial and temporal relationships between Ca^{2+} sparks and propagating $[Ca^{2+}]_i$ oscillations in porcine tracheal smooth muscle (TSM) cells. Individual Ca^{2+} sparks displayed relatively constant rise times and amplitudes, but these attributes varied across different foci within a TSM cell. Ca^{2+} sparks often occurred in "bursts" that were coupled across adjacent regions. Fusion of individual Ca^{2+} sparks produced larger local elevations in $[Ca^{2+}]_i$ that triggered a single spontaneous propagating $[Ca^{2+}]_i$ wave. The incidence of Ca^{2+} sparks increased by exposing TSM cells to either ryanodine (100 nM) or caffeine (50 μM), but was unaffected by removal of extracellular Ca^{2+}. These results suggest that Ca^{2+} sparks represent unitary SR Ca^{2+} release through ryanodine receptor (RyR) channels. Exposure of TSM cells to acetylcholine (ACh) triggered repetitive, propagating $[Ca^{2+}]_i$ oscillations that always originated from foci with high spark incidence. ACh-induced $[Ca^{2+}]_i$ oscillations were blocked by ruthenium red and modulated by cyclic ADP ribose, suggesting that they also represent SR Ca^{2+} release through RyR channels. Supported by NIH grant HL51736 and the Mayo Foundation. YSP is a recipient of an Abbott Fellowship.

Tu-Pos270

Relationship of Mitochondrial Ca^{2+} Homeostasis to $[Ca^{2+}]$ in the Cytosol and Sarcoplasmic Reticulum in Smooth Muscle Cells. ((R.M. Drummond, D.S. Bowman, R.A. Tuft and F.S. Fay)) Dept. Physiology and Biomedical Imaging Group, Univ. of Massachusestts Medical Center, Worcester, MA 01605.

We have recently shown that inhibition of mitochondrial Ca^{2+} uptake has a significant effect on Ca^{2+} removal from the cytosol of smooth muscle cells (*Pflagers Arch.*(1996) 431:473-482). To further investigate the role of mitochondria in Ca^{2+} homeostasis, we have developed techniques which allow us to monitor the changes in $[Ca^{2+}]$ within individual mitochondria, that occur during stimulation. Freshly isolated smooth muscle cells from the stomach of *Bufo marinus* were exposed to the permeant cation Rhod-2AM. This probe preferentially accumulates within mitochondria and becomes trapped there following hydrolysis to the Ca^{2+} sensitive indicator Rhod-2. Using an ultrafast digital imaging microscope, cells were imaged in 9 focal planes at 15 msec intervals, for each time point, and the resultant images were processed using a constrained iterative deconvolution algorithm. Following a 5 sec train of depolarizations (-110 to +10 mV; 2 pulses sec^{-1}) mitochondrial fluorescence increased rapidly, returning slowly towards baseline over the next several minutes. The increase in mitochondrial fluorescence following depolarization was largely attenuated following pre-treatment of the cells with FCCP. In response to stimulation with caffeine, which releases Ca^{2+} from the sarcoplasmic reticulum, mitochondrial fluorescence also increased rapidly, returning to baseline values within the next 2 minutes. The faster decline in mitochondrial fluorescence seen after depletion of Ca^{2+} from the sarcoplasmic reticulum may indicate a preferential efflux mechanism from the mitochondria to the sarcoplasmic reticulum. Using a high speed multi-wavelength microfluorimeter, we have recently been able to simultaneously monitor cytosolic and mitochondrial $[Ca^{2+}]$. These studies reveal that in response to a 5 sec train of depolarizations, the change in mitochondrial fluorescence is slower and considerably more prolonged than that observed in the cytosol. (Supported by an AHA Fellowship (RMD) and NIH HL 14523 (FSF).

Tu-Pos271

INTRACELLULAR MECHANISMS OF HALOTHANE ACTION IN SKINNED RABBIT PULMONARY ARTERIAL STRIPS. ((J.Y. Su and L. J. Tang)) Dept. of Anesthesiology, Box 356540, Univ. of Washington, Seattle, WA 98195

In vascular smooth muscle, halothane has been shown to increase cytosolic Ca^{2+} associated with contraction and to induce Ca^{2+} independent relaxation. There is, however, no direct evidence of the sources of increased Ca^{2+} or decreased sensitivity of the contractile proteins in response to halothane. Accordingly, we examined halothane effects on SR Ca^{2+} release and the contractile proteins in saponin-permealized (skinned) strips from rabbit pulmonary arteries. SR Ca^{2+} stores were examined by immersing the skinned strips sequentially in solutions to load Ca^{2+} into and to release Ca^{2+} from the SR, monitored with tension and a Ca^{2+} fluorescent dye, fura-2. The contractile proteins were assessed by activating the strips with pCa 6.0, measured with tension and myosin light chain phosphorylation (MLC-p). Halothane (0.5%–2%) dose-dependently induced Ca^{2+} release from the SR as shown by increased fura-2 fluorescence ratios of 340 nm to 380 nm excitation wavelength and tension transients. This halothane-induced Ca^{2+} release was reduced in skinned strips pre-treated with caffeine or IP_3. In skinned strips activated by clamped Ca^{2+}, halothane also caused a transient increase in tension, Ca^{2+}, and MLC-p, followed by a decrease in tension but not MLC-p below baseline. We conclude that in skinned strips of rabbit pulmonary arteries (i) the mechanism of halothane-induced tension transient is by increased MLC-p due to Ca^{2+} released from caffeine- and IP_3-releasable SR Ca^{2+} stores, and (ii) the halothane-induced delayed relaxation is not regulated by MLC in the Ca^{2+} clamped condition. Supported by NIH-GM48243.

Tu-Pos272

Luminal Ca^{2+} determines spontaneous transient outward currents in stomach smooth muscle cells from *Bufo marinus*. ((R. ZhuGe and F. S. Fay)) Dept. Physiology and Biomedical Imaging Group, Univ. of Massachusetts Medical Center, Worcester, MA 01605. (Spon. by Yu Li Wang).

Spontaneous transient outward currents (STOCs) have been suggested to be triggered by Ca^{2+} sparks resulting from Ca^{2+} release from intracellular stores upon activation of ryanodine receptors in smooth muscle cells. The underlying mechanisms by which Ca^{2+} sparks and STOCs are induced, however, are not yet clear. Here, we have simultaneously monitored STOCs with whole-cell patch clamp technique and free Ca^{2+} concentration in intracellular stores ($[Ca^{2+}]_{ics}$) with the Ca^{2+}-sensitive fluorescent indicator mag-fura-2, with the purpose of defining the role of luminal Ca^{2+} in generation of STOC, in single stomach smooth muscle from *Bufo marinus*. The steady state $[Ca^{2+}]_{ics}$ in cells with STOCs was 151±9 μM, which was not significantly different from 157±10 μM in STOC-free cells. Activation of ryanodine receptors by caffeine elicited a rapid decrease in $[Ca^{2+}]_{ics}$ in association with a fusion of STOCs, followed by a gradual recovery of $[Ca^{2+}]_{ics}$ and STOCs. During the recovery process, activities of STOC, i.e., the frequency, amplitude and duration, were highly correlated with refilling of intracellular stores, which was fitted by two exponential functions. Many STOCs appeared before the stores were fully restored. Sodium nitroprusside increased steady state $[Ca^{2+}]_{ics}$, and enhanced STOC activity and the rate of refilling of the stores in response to caffeine. These results suggest that Ca^{2+} in the intracellular stores can modulate the activities of ryanodine receptors and may function as an important determinant of STOC generation in smooth muscle cells. (Supported by NIH HL 47530).

Tu-Pos273

REGULATION OF ARTERIAL SMOOTH MUSCLE $[Ca^{2+}]$ IN INTACT CEREBRAL ARTERIES BY MEMBRANE POTENTIAL & THE SARCOPLASMIC RETICULUM. ((Harm J. Knot, [a]Nicholas B. Standen, and Mark T. Nelson)) University of Vermont, Dept. of Pharmacology, CMRF, 55A South Park Drive, Colchester VT 05446-2500. [a]University of Leicester, Dept of Cell Physiology & Pharmacology, PO Box 138, Leicester LE1 9HN, U.K.

Intravascular pressure depolarizes and constricts cerebral resistance arteries from rat, and thus contributes to the regulation of cerebral blood flow. Using digital fluorescence imaging of intact small pressurized cerebral arteries (< 200 μm) loaded with FURA-2, we tested the hypotheses; (1) that pressure depolarizes myogenic cerebral arteries, activating voltage-dependent Ca^{2+}-channels, leading to increased "global" cytosolic Ca^{2+} $[Ca^{2+}]_c$, resulting in vasoconstriction measured as reduction of arterial diameter, (2) that inhibition of localized Ca^{2+} release (Ca^{2+} sparks, see Nelson et al., *Science* (270) 633-637 1995) through ryanodine-sensitive release channels in the sarcoplasmic reticulum (SR) decreases the activity of Ca^{2+} sensitive K^+ (K_{Ca}) channels which leads to membrane potential depolarization, increased $[Ca^{2+}]_c$, and vasoconstriction. The following observations are consistent with these hypotheses: (1) Increasing pressure from 0 to 60 mmHg depolarizes and increases $[Ca^{2+}]_c$. The calcium channel blocker nisoldipine (10 nM) fully dilated these arteries to 194 ± 13 μm without changing membrane potential while $[Ca^{2+}]_c$ fell to 76 ± 17 nM. At 60 mm Hg, arterial V_m was -45 ± 1.4 mV, $[Ca^{2+}]_c$ was 199 ± 20 nM and the arteries had constricted from 194 ± 6 to 121 ± 9 μm. Under these conditions, depolarization (to about -22 mV) increased $[Ca^{2+}]_c$ to 349 ± 12 nM and the arteries constricted further to 40 ± 3 μm. Hyperpolarization (to about -58 mV), decreased $[Ca^{2+}]_c$ to 126 ± 7 nM and the arteries dilated to 190 ± 7 μm; (2) Ryanodine (10 μM) depolarized the arteries by 7 ± 1 mV, increased $[Ca^{2+}]_c$ by 46 ± 17 nM and constricted the arteries by 44 ± 8 μm . Similarly, 100 nM iberiotoxin (a K_{Ca} channel blocker) depolarized these arteries by 8 ± 2 mV, raised $[Ca^{2+}]_c$ by 51 ± 21 nM and constricted the arteries by 37 ± 2 μm. The effects of Ryanodine and Iberiotoxin were not additive, and nisoldipine fully dilated these arteries in the presence of either compound. We propose that pressure constricts myogenic cerebral arteries through membrane depolarization activating voltage-dependent Ca^{2+} channels, thus elevating $[Ca^{2+}]_c$. Further, we propose that the ryanodine-sensitive Ca^{2+} release channel in the SR modulates arterial tone through changes in membrane potential by activating K_{Ca} channels via Ca^{2+} sparks. Supported by NSF and NIH.

Tu-Pos274

FLUORESCENCE SIGNALS OF THE Mg^{2+} INDICATOR FURAPTRA (MAG-FURA-2) CALIBRATED IN GUINEA PIG TAENIA CAECI ((M. Tashiro, M. Konishi, and S. Kurihara)) Dept. of Physiol., The Jikei Univ. Sch. of Med., Tokyo 105, Japan

The properties of fluorescent indicators, including the dissociation constant (K_D), are generally altered in the cell interior, due to the indicator binding to cytoplasmic constituents. We studied the relation between fluorescence signals of furaptra and the intracellular free Mg^{2+} concentration ($[Mg^{2+}]_i$) in smooth muscle cells. Thin strips of guinea pig taenia caeci were incubated with furaptra-AM, and the ratio of furaptra fluorescence excited at 382 nm and 350 nm (R) was analyzed at 25°C. The ionophores (20 μM Br-A23187 plus Monensin and Nigericin) were used to equilibrate $[Mg^{2+}]_i$ with extracellular $[Mg^{2+}]$ ($[Mg^{2+}]_o$). Shortly after the application of the ionophores, a slight increase in R (ΔR_{jump}) was observed, independent of $[Mg^{2+}]_o$, and this was followed by a slow change in R which reached a steady level in 3 - 5 hours. The steady levels of R at 0 - 49 mM $[Mg^{2+}]_o$ (18 data points from 10 preparations) were well fitted with a theoretical 1:1 binding curve with a K_D value of 5.1 mM, which was 40% higher than that obtained in solutions. With the *in vivo* calibration curve and correction for the ΔR_{jump} (thought unrelated to $[Mg^{2+}]_i$ change), the basal $[Mg^{2+}]_i$ in taenia caeci (1.2 mM $[Mg^{2+}]_o$) was estimated to be 0.97±0.05 mM (mean±s.e.m, n=12). When the same calibration was applied to A7r5 cells and rat ventricular myocytes, the basal $[Mg^{2+}]_i$ of these cells was calculated to be 0.74±0.02 mM (n=33) and 1.11±0.06 mM (n=9), respectively.

Tu-Pos275

Na^+ GRADIENT-DEPENDENT Mg^{2+} TRANSPORT IN TAENIA CAECI OF GUINEA PIG

((M. Tashiro, M. Konishi, and S. Kurihara)) Dept. of Physiol., The Jikei Univ. Sch. of Med., Tokyo 105, Japan (spon. by Y. Umazume)

To study the mechanism of cellular Mg^{2+} extrusion, we measured the intracellular Mg^{2+} concentration ($[Mg^{2+}]_i$) in guinea pig taenia caeci, using the Mg^{2+} indicator furaptra with intracellular calibration (25℃). Lowering the extracellular Na^+ concentration ($[Na^+]_o$) in Ca^{2+}-free condition caused a slow and reversible increase in $[Mg^{2+}]_i$, probably due to the inhibition of Na^+ gradient-dependent extrusion of cellular Mg^{2+} (Na^+/Mg^{2+} exchange). The relation between $[Na^+]_o$ and the initial rate of rise of $[Mg^{2+}]_i$ yielded a curve with a Hill coefficient of ~3, $[Na^+]_o$ at half maximal rate of rise ~30 mM and the maximum rate 0.16 ±0.01 μM/s (mean±s.e.m, n=6). Assuming cytoplasmic Mg^{2+} buffering power of 3, the maximal rate of Mg^{2+} extrusion was calculated to be ~0.2 pmol/cm²/s. This rate is an order of magnitude smaller than the Ca^{2+} transport rate by Na^+/Ca^{2+} exchanger reported in guinea pig cardiac myocytes under comparable conditions. Depolarization with high K^+ (56 mM) slightly shifted the curve towards higher $[Na^+]_o$, suggesting that the Na^+/Mg^{2+} exchange was slightly inhibited by depolarization. Ouabain (2 μM) increased the intracellular Na^+ concentration, as assessed by SBFI (a Na^+ indicator) fluorescence, and also elevated $[Mg^{2+}]_i$. Na^+-free perfusion of the ouabain-treated preparations caused a rapid increase in $[Mg^{2+}]_i$ (~1.0 μM/s), which could be attributed to Mg^{2+} influx by Na^+/Mg^{2+} exchanger occuring in the reverse direction.

Tu-Pos276

GENISTEIN, INHIBITOR OF TYROSINE KINASE, SUPPRESS CA^{2+} INFLUX STIMULATED BY HIGH K^+ AND NOREPINEPHRINE IN RAT AORTA

((Hee-Yul Ahn, Jin-Young Jung, Young-Hak Chang, Sun-Hee Kim, Hun-Sik Kim and Ki-Churl Chang*)) Department of Pharmacology, College of Medicine, Chungbuk National University, Cheongju, Chungbuk 361-763, S. Korea and *Department of Pharmacology, College of Medicine, Gyeongsang National University, Chinju S. Korea

We observed the effect of genistein, inhibitor of tyrosine kinase, on high K^+ and norepinephrine (NE)-induced contractions in rat aorta. Genistein (10^{-6}-10^{-4} M) inhibited the high K^+ and NE-induced contractions in a concentration-dependent manner. High K^+ and NE increased $^{45}Ca^{2+}$ uptake from resting values, respectively. 10^{-4} M genistein inhibited the high K^+ and NE-increased $^{45}Ca^{2+}$ uptake. From these results, genistein may act as non-specific Ca^{2+} channel blocker in rat aorta. The possibility that Ca^{2+} influx through voltage-dependent Ca^{2+} channel and receptor-operated Ca^{2+} channel may be regulated by tyrosine kinase cannot be excluded in rat aorta.

Tu-Pos277

DELAYED RECTIFIER K^+ CURRENT ($K_{(v)}$) OF RAT RENAL RESISTANCE VESSELS: ALTERATIONS IN HYPERTENSION.

((Jeffrey R. Martens and Craig H. Gelband)) Department of Physiology, University of Florida, Gainesville, FL 32610.

Delayed rectifier K^+ current ($K_{(v)}$) has been implicated in the control of resting membrane potential of small resistance blood vessels (Knot and Nelson, 1995; Martens & Gelband, 1996). $K_{(v)}$ current was identified using voltage-step and ramp depolarizations in smooth muscle cells enzymatically dissociated from rat interlobar/arcuate artery (diameter < 200 μm). $K_{(v)}$ current was pharmacologically isolated using extracellular charybdotoxin (100 nM, n = 3) or TEA (K_i = 683 μM, n = 4) both of which significantly inhibited Ca^{2+}- activated K^+ current ($K_{(Ca)}$) without affecting $K_{(v)}$ current. The charge carrier of the $K_{(v)}$ current was identified as K^+ by measuring tail-current reversal potential (-76 ± 2.4 mV in 5.0 mM $[K^+]_o$/140 $[K^+]_i$). $K_{(v)}$ current activated near -30 mV with $V_{1/2}$ of 21.9 mV (n = 9) and was sensitive to bath application of 4-aminopyridine (4-AP, K_i = 421 μM at 0 mV, n = 5). $K_{(v)}$ current displayed both steady-state inactivation ($V_{1/2}$ = -32.0 mV, n = 5) as well as inactivation during a voltage step. At + 20 mV, inactivation could be fit by a single exponential (τ = 2.7 ± 0.4 sec., n = 6). Preliminary experiments in renal vascular smooth muscle cells from spontaneous hypertensive resistance rats (SHR), indicate there may exist alterations in the biophysical properties of the $K_{(v)}$ current when compared to control. This suggests that the decreased $K_{(v)}$ current and subsequent membrane depolarization observed in hypertensive renal vasculature smooth muscle cells (Martens and Gelband, 1996) may be due to alterations in $K_{(v)}$ channel gating. (Supported by NIH HL-52189 and a AHA Predoctoral Fellowship, FL Affiliate)

Tu-Pos278

ESOPHAGEAL MOTOR ACTIVITY OF SYMPTOMATIC PATIENTS IS ALTERED BY REFLUX.

((Yatian Zhang, M.D.,Ph.D. and Hulya Levendoglu, M.D.)) Dept. of Medicine, Brookdale University Hospital Medical Center and SNUY Health Science Center at Brooklyn, Brooklyn, N.Y.

The aim of this study was to investigate the relationship between reflux and esophageal contractions in symptomatic patients. Twenty four hour pH and esophageal motility recordings were obtained from 57 patients who had symptoms suggestive of esophageal diseases. A solid state portable digital recorder (MicroDigitrapper, Synactics) with a motility/pH probe was used, the esophageal pH sensor was located at the tip of the probe and the sensors of motility were positined at 5, 10, 15 and 20 cm above the manometrically determined upper border of the lower esophageal sphincter (LES). Patients with reflux (R) were distinguished from non-reflux patients (NR) according to DeMeester scores calculated for the six parameters, namely, total number of episodes, longer than 5.0 minutes, duration of longest, percent time below 4.0 for total, upright and supine periods. The R group consisted of 23 female and 7 male subjects, aged 21-80 years (mean 53 years); 10 complained of heartburn and 13 had chest pain. The NR group had 20 females and 7 males, aged 27-77 years (mean 49 years); 4 had heartburn and 13 had chest pain. Contractions were uniformly distributed throughout the whole esophagus in R, but in the NR group they were concentrated in the middle and distal esophagus compared to the proximal esophagus. Peristaltic waves occurred with equal frequency throughout the esophagus in the R group, but were more frequent in the proximal esophagus in the NR group. Repetitive wave activity was more frequent in R than NR, and the median amplitude of the waves were greater in R than NR; however the amplitude in the proximal esophagus was higher in R, while the distal esophagus amplitude was higher in NR. Repetitive waves were uniformly distribued in R, but were concentrated in the middle and distal esophagus in NR. There was a greater incidence of both complete and dropped peristalsis in R, while interrupted peristalsis occurred more often in NR. These findings demonstrate that reflux is associated with an altered pattern of esophageal wave and motility activity in symptomatic patients. The effect of reflux appears to extend to the entire esophagus, while in symptomatic patients without reflux, esophageal disorder is confined to the middle and distal esophagus. Chest pain, which occurs equally in the two groups, may be associated with a motility disorder of the middle or distal esophagus.

Tu-Pos279

AZIDODANTROLENE: A PHOTOACTIVE CONGENER OF DANTROLENE

((B. Bin[1], S.S. Palnitkar[2], L.S. Jimenez[1] and **J. Parness**[2,3])) [1]Dept. of Chemistry, Rutgers University, Piscataway, NJ 08855; Depts. Anesthesia[2], Pharmacology[3], & Pediatrics[3], UMDNJ-R W Johnson Medical School, New Brunswick, N.J. 08901

Dantrolene inhibits skeletal muscle Ca^{2+} release from sarcoplasmic reticulum (SR), suggesting a regulatory site of action. We have demonstrated specific dantrolene binding sites in SR that are pharmacologically and molecularly distinct from ryanodine binding sites. Early structure-activity studies on the muscle relaxant activity of dantrolene congeners revealed that the strongly electron withdrawing nitro group on the phenyl ring was essential for activity. We reasoned that replacement of this group with the more weakly electron withdrawing azido group would result in a photoactivatable derivative that still exhibited reasonable binding affinity, while maintaining binding specificity. We report the successful synthesis of azidodantrolene using the following general scheme: an aryldiazonium salt was coupled to 2-furaldehyde, and the resulting azidophenylfuraldehyde then condensed with aminohydantoin hydrochloride. The resultant acid form of azidodantrolene was reacted with sodium methoxide to give the corresponding sodium salt (yield: ~20%). This compound is pure by HPLC, NMR, mass spectral and elemental analysis, and is degraded by UV light in less than five seconds. Inhibition of [^{3}H]dantrolene binding to pig skeletal muscle SR by azidodantrolene reveals a specific, monophasic inhibition curve with an apparent K_i of 1.5 μM. Thus, we have synthesized a potential probe for the molecular identification of the dantrolene receptor. (Support: FAER/AYI award to JP, and ACS and NSF awards to LSJ)

Tu-Pos280

ACTIVATION AND SORTING OF WHITE BLOOD CELLS IN A LATTICE. ((**Robert H. Carlson**, Christopher V. Gabel, Shirley S. Chan and Robert H. Austin)), Department of Physics, Princeton University, Princeton, NJ 08544.

Cells respond to their environments in a variety of ways. For the human leukocyte, this complex environment consists of the human circulatory system, the study of which is most often physiological in nature. Here we demonstrate, using physiological flow conditions and a microfabricated array of channels with length scales similar to those of human capillaries, a novel interaction of leukocytes with their physical environment. Using vital chromosome stains and cell specific, flourochrome labled antibodies, we observe that the eventual adhesion of the leucocytes to the silicon array does not occur in a manner consistent with a random process. Futher, the distribution of cells in the arrays displays a strong dependence on cell type and nuclear morphology, with granulocytes penetrating a smaller distance than lymphocytes and interacting with the lymphocytes in a self-exclusionary manner. The physical distortion of the cells is the same as they experience in vivo, and and we propose that this complex non-random behavior is due to a hydrodynamic shear and deformation activated change in the cells relevant to observed *in vivo* behavior. Because we use reversibly sealed silicon arrays, in the near future we will be able to probe differences among individula stuck cells, either physically using techniques such laser tweezers or atomicf force microscopy, or via blotting transfer techniques to explore the biochemical variations among cells.

Tu-Pos281

ACTIN MONOMER DELIVERY TO THE FRONT OF RAPIDLY EXTENDING FILAMENT NETWORKS. ((**D. J. Olbris** and J. Herzfeld)) Brandeis University, 415 South St., Waltham MA 02254-9110.

The acrosomal process of the sea cucumber *Thyone* extends at speeds exceeding 10 μm/s. Goldfish keratocytes crawl much more slowly, with a top speed of about 0.5 μm/s. Though both polymerize actin at the moving front, the acrosomal process manages to do so far more rapidly, so rapidly that actin should be depleted faster than diffusion can replenish it. We propose a model to address this dilemma. When polymerization draws down the local actin concentration, water may escape through the cell membrane to areas of higher solute concentration. If the volume of the acrosomal process, stabilized by the framework of the actin polymers, is to remain constant, actin-rich solution will be drawn to the polymerization region, delivering actin at a rate faster than that of diffusion alone. *Thyone* sperm seem engineered specifically to take advantage of this process while the goldfish keratocytes are not, explaining the large difference in extension speeds.

Supported by NIH grant HL-36546

Tu-Pos282

Evaluating the in vivo elastic properties of different strands of Dictyostelium Discoideum using small shear forces. ((**R.Simson**, A.R.Bausch, F.Ziemann, E.Sackmann)) Technische Universität München, Germany.

We developed a new method for measuring elastic properties of cells, combining a parallel plate flow chamber and Reflection Interference Contrast Microscopy (RICM). RICM together with digital image processing allows reconstruction of the cell topography to a height of about 1μm. The cell shape changes in response to a laminar flow. From this change we were able to calculate tension and bending energy as well as the adhesion energy of the cell. The applied shear stress (0.4 to 1.2 Pa) was large enough to probe the elasticity of the cell, yet small enough to prevent detachment. For red blood cells we found a bending energy of ≈ 10 kT in good aggreement with previous results. For wildtype *Dictyostelium discoideum* we found a bending energy of ≈ 400 kT. Markedly reduced values were found with a mutant lacking an important actin binding protein. In additional experiments paramagnetic beads were incorporated into the cells and exposed to a magnetic field gradient. The applicability of this technique to measure the cell viscosity is explored.

Tu-Pos283

THE LEADING LAMELLUM OF CRAWLING CELLS GENERATES TRACTION FORCES IN A RADIAL ARRAY TO PULL CELLS FORWARD. ((K. Burton, J. Park, & D.L. Taylor)). Center for Light Microscope Imaging and Biotechnology, Carnegie Mellon University, Pittsburgh, PA, 15213.

The angular distribution of traction forces generated by crawling metazoan cells has been studied by observing patterns of wrinkles produced in silicone rubber substrata. The method of Harris *et al.* (*Science* 208:177, 1980) for measuring traction forces has been extended by fabricating silicone sheets from methyl phenyl polysiloxane, which improves the optical properties of the substratum, especially for Interference Reflection Microscopy (IRM), and permits the use of UV light (λ=254 nm) to adjust its compliance to match the strength of the cells. Cells and wrinkles in the silicone substrata were imaged using several modes of light microscopy, including Nomarski DIC, IRM, and fluorescence of microinjected rhodamine-labeled myosin II. The compliance of the silicone substrata has been calibrated by using flexible glass microneedles to distort the sheet in response to known forces. Elastic moduli estimated in this way have been used to measure single cell forces ranging from nanonewtons to micronewtons. Mouse Swiss 3T3 fibroblasts (37°C) and goldfish keratocytes (room temperature) were studied on silicone sheets sufficiently compliant to be wrinkled by lamellipodia. Wrinkles in the substrata extended in a radial pattern from the lamellum of cells during free locomotion and during respreading following cytokinesis, indicating forces normal to the leading edge and directed approximately towards the center of the cell. The angular distribution of forces generally conformed to the shape of the lamellum, and under some conditions included forces near the midline of the cell body acting to pull the cell forward. The magnitude of traction force varied with orientation, and was generally symmetric about the midline of the cell, except when changing direction when force was briefly greater on the side to which the cell turned.

Tu-Pos284

PHASE TRANSITIONS, ANISOTROPY, AND SIMULATED ASPIRATION OF MODEL MEMBRANE NETWORKS. ((**Dennis Discher,*** David Boal, and Tony Boey)) Dept. of Physics, Simon Fraser University, Burnaby, BC, V5A 1S6 Canada and *University of Pennsylvania, Philadelphia, PA 19104 USA. (Spon.D. Discher)

Membrane network models of various types have been simulated and analysed under large deformation both in- and out-of-plane. Experiments such as micropipette aspiration have shown that membrane networks are capable of sustaining large and reversible strains – relating this behavior to a discrete membrane network of proteins is the current challenge. In the case of a triangulated network, a first approximation to the red cell's network, analysis has focused on networks composed of either (i) symmetric n-monic springs (n=2 is Hookean) with a non-zero force-free length or (ii) polymer-like elements with a force-free length of zero that balances a two-vertex chain elasticity against a three-vertex excluded volume. The tension response of n-monic spring networks is found to be highly dependent on the direction of strain, and this anisotropy contributes to a structural transition in the n-monic model under modest compression, up to very high temperature. Similar instabilities are described for square nets relevant perhaps to networks in other cells. The polymer-like model is also anisotropic in extreme tensions, but lacks a phase transition. In comparing simulated aspiration of these network models to experiments, we find the phase transition behavior of n-monic networks is a limitation whereas better agreement is obtained with the network models where excluded volume provides stability.

Tu-Pos285

MICRORHEOLOGY IN ACTIN GELS: EXPERIMENT AND THEORY. ((B. Schnurr, F. Gittes, P.D. Olmsted, F.C. MacKintosh, C.F. Schmidt)) Dept. Physics & Biophys. Res. Div., University of Michigan, Ann Arbor, MI 48109.

Cytoskeletal polymer networks differ substantially from conventional synthetic polymers. The main cytoskeletal protein polymers are semi-flexible chains which convey unique viscoelastic properties to cells. Aiming at a basic statistical mechanical understanding of these unique properties, we used microscopic probes to locally measure the elasticity of entangled solutions of in vitro reconstituted actin filaments. Microscopic probes (comparable and larger than the average mesh size) allowed us to probe shear and compressional deformations and to map local variations in elasticity. Protein concentrations were between 1 and 2 mg/ml, the average mesh size of the gels was below 0.5 micrometers. Two methods were used: i) Thermal fluctuations of entrapped silica beads (between 0.5 and 5 micrometers) were measured by laser interferometry with nm spatial and <ms time resolution. ii) Beads were displaced with calibrated forces by optical tweezers, while the instantaneous force was measured by laser interferometry. Thermal fluctuation amplitudes were on the order of tens of nm, while the power spectrum exhibits an unexpected power-law behavior. Control experiments with polyacrylamide gels surprisingly show a similar exponent of about -1.5 in their spectra. The elastic response of the networks was calculated in a continuum elastic approximation, including shear and compressional deformation and the appropriate boundary conditions for a sphere. Using these results we determined Young's moduli for the gels from the different experiments. We discuss the dependence of the elastic moduli on polymer density. Dynamic models are discussed to explain the shape of the power spectra.

This work was supported by the Whitaker Foundation and the NSF (BIR-9512699).

Tu-Pos286

MECHANICAL FLUCTUATIONS OF THE MEMBRANE-SKELETON ARE DEPENDENT ON F-ACTIN ATPase IN HUMAN ERYTHROCYTES

((Shmuel Tuvia, Shlomo Levin, Arkady Bitler and **Rafi Korenstein**)) Dept. of Physiology and Pharmacology, Sackler Faculty of Medicine, Tel-Aviv University, 69978 Tel-Aviv, Israel

Submicron mechanical fluctuations of the cell membrane of erythrocytes, measured by point dark field microscopy, were shown to depend, to a large extent, on intracellular MgATP (Levin and Korenstein, *Biophys. J.* 60:733-737, 1991). We extended this investigation showing that cell membrane fluctuations (CMF) are associated with F-actin's ATPase activity. MgATP was found to reconstitute CMF in red blood cell (RBC) ghosts and RBC skeletons to their levels in intact RBCs, with an apparent K_d of 0.29mM., However, non-hydrolyzable ATP analogues (AMP-PNP, ATPγS) or hydrolyzable ones (ITP, GTP), were unable to elevate CMF levels. The inhibition of ATPase activity associated with the RBC's skeleton, carried out either by the omission of the MgATP substrate or by the use of several inhibitors (vanadate, phalloidin and DNase I), resulted in a strong decrease of CMF. We suggest that the actin's ATPase, located at the pointed end of the short actin filament, is responsible for the MgATP dependent stimulation of CMF in RBCs.

Tu-Pos287

MOLECULAR ORIGIN AND CONTROL OF F-ACTIN VISCOELASTICITY AND ITS IMPACT ON CELL SHAPE AND MOTILITY.

((J. Böhm[*], F.C. MacKintosh[f], J.V. Shah[a], L.E. Laham[a], P.A. Janmey[a], J. Guck[*], D. Humphrey[*] and **J. Käs**[*])) [*]Dept. of Physics, Univ. of Texas, Austin, TX78712, [a]Brigham and Women's Hospital, Harvard Medical School, Boston, MA 02115 and [f]Dept. of Physics, Univ. of Michigan, Ann Arbor, MI 48109.

ACTIN is the most abundant protein found in living cells. Shape and mechanical stability of eukaryotic cells are due primarily to the cytoskeletal rim, a meshwork of actin filaments (F-actin) that also plays a crucial role in cell motility. Our recent work shows that the mechanical response of actin networks *in vitro* is strongly dependent on the bending stiffness of the constituent filaments and is up to a 1000x stronger than the response of artificial polymers. In agreement with recent theoretical predictions this proves the role of individual filament properties for F-actin elasticity. The presented data also demonstrate that filament stiffness is a function of both solution adenosine triphosphate (ATP) as well as divalent cations. The sensitivity of the bending modulus to the phosphorylation state of the adenine nucleotide provides evidence for a second nucleotide binding site on F-actin. These results illustrate that the elastic behavior of F-actin is different to conventional flexible polymers and suggest that cells are able to modulate the elasticity of their outer rim by local changes in filament stiffness.

To elucidate the microscopic mechanism which allows F-actin to generate such outstanding properties we integrated a rheometer within an inverted fluorescence microscope. Due to the stiffness of actin filaments no knot-like entanglements like in flexible polymer solutions can be formed in F-actin. The sterical interactions, which allow F-actin solutions to resist shear, are of a collective nature and require multi-filament interactions. In particular, filament length is a crucial parameter. Only, filaments, whose length exceeds several times the mesh size of the network, contribute to the elastic response of a F-actin solution. This result also implies that actin filaments in the cytoskeletal rim, which are relatively short, have to be crosslinked by actin binding proteins to form a mechanical stable network.

Tu-Pos288

THEORETICAL DESCRIPTION OF THE TRANSMEMBRANE COOPERATIVITY DUE TO CYTOSKELETON INTERACTIONS OF ADHESION PROTEINS

((W. Baumgartner[1], D. Drenckhahn[2])) [1]University of Linz, A-4040 Linz and [2]University of Würzburg, D-97070 Würzburg.

A simple thermodynamic approach based on the theory of diffusion limited reactions was used to describe the phenomenon of transmembrane cooperativity observed for adhesion proteins like cadherins. These are proteins responsible for cell-cell-interactions of epithelial cells. It is known, that these cadherins interact with the cytoskeleton. This interaction is due to binding with plaque-proteins. In previous studies it was found, that the intercellular binding strength due to cadherin interactions can be altered by modifying the kinetics of the plaque-protein linkage to the cytoskeleton.

Our model predicts, that a change in the binding kinetics of transmembrane adhesion proteins and the cytoskeleton may result in a proportional increase in extracellular binding strength. Especially, if the affinity of the adhesion proteins (to other adhesion proteins or to a substrate) is low, a decrease in the translational entropy due to cytoskeleton binding results in a large amplification of the cell-cell (or cell-substrate) interaction. This explanation of transmembrane cooperativity seems more likely than a description assuming transmembrane conformational changes of adhesion proteins.

(Supported by FWF-project S6607-MED and SFB 182)

Tu-Pos289

DYNAMIC RATES OF CYTOSKELETAL PROTEIN BINDING AT THE SUBMEMBRANE OF LIVING CELLS.

((Susan E. Sund and Daniel Axelrod)) Biophysics Research Division and Dept. of Physics, University of Michigan, Ann Arbor, MI 48109. (Spon. by Geneva M. Omann)

Binding/unbinding kinetic rates of cytoskeletal proteins to the cytofacial surface of the plasma membrane in living 3T3 cells are measured by Total Internal Reflection/Fluorescent Recovery After Photobleaching (TIR/FRAP). Cells are first microinjected with a fluorescently labeled protein such as rhodamine annexin or rhodamine actin or the fluorescent actin marker rhodamine phalloidin. After an incubation time, fluorescence at a cell-substrate contact region is photobleached with a bright flash of evanescent light; the subsequent recovery under dim evanescent illumination is a measure of the residency time of protein reversibly bound at the submembrane surface. The general morphology and position of the cells after injection is also monitored with time-lapse CCD imaging under TIRF illumination. Kinetic behavior of proteins at the cytoskeletal membrane is important to our understanding of cell motility and the plastic and mechanical properties of the cytoplasm and cell membrane. These experimental and analysis techniques have not previously been combined in the study of living cells, and technical protocols and problems are discussed. Supported by NSF MCB 9405298.

Tu-Pos290

LACK OF ANTAGONISM AMONGST CALPONIN, α-ACTININ, AND FILAMIN IN BINDING TO ACTIN.

((**B. Leinweber** and J.M. Chalovich)) East Carolina University School of Medicine, Greenville, NC, 27858-4356.

The smooth muscle protein calponin colocalizes with α-actinin in dense bodies and with filamin in dense plaques (North *et al.* 1994a,b). All of these proteins bind to the carboxyl terminus of actin. Simultaneous interactions of calponin, α-actinin, and filamin with actin were measured by high-speed equilibrium sedimentation followed by polyacrylamide gel electrophoresis, Coomassie staining, and quantification of the resulting bands. At 150 mM ionic strength, calponin binding to actin appears to consist of a high-affinity interaction that saturated at approximately one calponin per two actin monomers together with a low affinity, possibly non-specific interaction. α-Actinin association with actin under the same conditions saturated at approximately one α-actin to three or four actin monomers. The apparent K_A was 1.4×10^6 M^{-1}. Filamin association with actin saturated at one filamin per two or three actin monomers. The apparent K_A was 5.6×10^5 M^{-1}. α-Actinin displaced filamin from actin. Both filamin and α-actinin displaced the lower affinity component of calponin from actin, but not the higher affinity component. The presence of saturating calponin resulted in at best a slight decrease in the affinity and stoiciometry of filamin and α-actinin for actin. Thus calponin and filamin or calponin and α-actinin can coexist on actin filaments. However, neither filamin nor α-actinin appear to target calponin to the cytoskeleton.

Tu-Pos291

PRELIMINARY EVIDENCES FOR A BIOLOGICAL ACTIVITY OF ADHALIN

((L. Senter, S. Ceoldo and G. Salviati)) CNR Unit for Muscle Biology and Physiopathology - Department of Biomedical Sciences, University of Padova, 35121 Padova, Italy

Adhalin is the protein of dystrophin-glycoprotein complex (DGC) which is missing in limb-girdle muscular dystrophy 2D (LGMD-2D). We have demonstrated that adhalin binds ATP in a Mg^{2+} dependent and Ca^{2+} independent manner. The binding is completely inhibited by 3'-O-(4-benzoyl)benzoyl ATP (BzATP) and ADP and it is slightly reduced by GTP, whereas UTP and oxidized ATP (oATP) have no effects. Moreover, the DGC preparation shows a Mg^{2+} dependent and Ca^{2+} independent ATPase activity that is highly inhibited by covalent binding of BzATP and is not inhibited by thapsigargin, cyclopiazonic acid and vanadate, like other ecto-ATPases. Finally, monoclonal anti-adhalin antibody inhibits both ATP labeling of adhalin and the ATPase activity of the DGC preparations. We suggest that adhalin is an ecto-ATPase whose possible role is the buffering of the extracellular ATP concentration. Since we have demonstrated the presence in the sarcolemma membrane of a P_{2Z}-type purinergic receptor, we speculate that in limb-girdle muscular dystrophy the concentration of extracellular ATP remains elevated because of the absence of the ecto-ATPase activity. This leads to a persistent activation of P_{2Z}-type purinergic receptors with a consequent intracellular Ca^{2+} overload causing muscle fiber necrosis. Supported by Telethon Italy (# 692), CNR and MPI.

Tu-Pos292

INTERACTION OF CALPONIN WITH DESMIN

((K. Mabuchi*, **B. Li***, W. Ip# and T. Tao*)) *Muscle Research Group, Boston Biomedical Research Institute, 20 Staniford Street, Boston, Ma 02114; #Dept. of Cell Biology, Neurobiology and Anatomy, University of Cincinnati College of Medicine.

Our previous immunogold electron microscopy (IEM) studies of chicken gizzard smooth muscle cells showed that in certain areas of a cell the distribution of anti-calponin (anti-CP) exhibits high degree of overlap with antibodies against ß-actin, filamin, and in particular, desmin, suggesting that *in situ* a fraction of CP may be associated with intermediate filaments (IFs) of the cytoskeleton. In this work we further explore this idea by studying the interaction between CP and desmin *in vitro*. We found that at physiological salt concentrations CP bound only weakly to preformed synthetic desmin IFs. On the other hand, CP bound strongly to non-filamentous, tetramers of desmin as judged by affinity chromatography and IEM, suggesting that CP may compete with IF subunits during assembly. Indeed, co-polymerization experiments showed that CP was stably incorporated into IFs when the two proteins were mixed in a buffer containing 6M urea and dialyzed into a buffer containing 0.15 M NaCl. Differential extraction experiments showed that CP co-purifies with dense body-IF fractions. IEM examination of these fractions showed that anti-CP decorated portions of IF/dense body complexes. Our findings suggest that in chicken gizzard smooth muscle cells CP may be an integral component of desmin IFs in the vicinity of dense bodies. Since CP is also known to bind actin, we hypothesize that one of CP's functions might be to bridge IFs with actin in dense bodies. (supported by P01-AR41637)

Tu-Pos293

PROTEOLYSIS AND DEGRADATION OF DESMIN DURING POST-ISCHEMIC REPERFUSION IN ISOLATED RAT HEARTS.

((**Fabio Di Lisa***[1], Roberta Menabò*, Maurizo Vittadello# and Luisa Gorza#)) CNR Unit for Biomembranes* and and Depts of Biochemistry# and Biomedical Sciences#, University of Padua, Italy. (Spon. by M.C. Sorgato)

In isolated rat hearts subjected to 10, 30, 60 or 90 min of global normothermic ischemia followed by reperfusion, desmin fragments (Mr 47-50 kDa) were visible only in immunoblots from reperfused hearts irrespective of the ischemic duration. Reperfusion was associated also with desmin cross-linking as shown by the appearance of two higher molecular weight peptides (111 and 105 kDa). Protelytic or cross-linking products could not be detected by using monoclonal antibodies anti α-actinin, vinculin, and β-tubulin. Desmin changes similar to those produced by reperfusion were obtained both by perfusing hearts with the Ca-paradox protocol and by incubating whole heart homogenates in the presence of 1 mM Ca^{2+}. Thus the rise in intracellular Ca^{2+}, which occurs in the irreversibly damaged myocardium, appears to be sufficient to produce the reported desmin changes. Calpain and transglutaminase are likely activated by calcium overload. Indeed, in tissue homogenates desmin fragmentation was inhibited by calpeptin, a specific inhibitor of calpain, which did not affect the formation of the larger peptide. On the other hand, acrylamide a specific inhibitor of transglutaminase, prevented the cross-linking but not the proteolysis. Desmin might represent a sensitive and precocious marker of calpain and transglutaminase activation

Tu-Pos294

CHARACTERIZATION OF THE TITIN PEVK FRAGMENT FROM DIFFERENT SPECIES

((**E. Berri**, J. Wolff* and M.L. Greaser)), Muscle Biology Laboratory and *Department of Molecular Genetics, Waisman Center, University of Wisconsin, Madison, WI 53706

Titin is a high molecular weight sarcomeric protein which is believed to be responsible for passive tension in heart and skeletal muscle. The human cardiac cDNA sequence revealed that the protein consists of a large number of 100 amino acid motifs of the IgG and FN3 types (Labeit and Kolmerer, Science 273:293, 1995). A different structure was found near the center of the I-band portion of titin and was referred to as the PEVK segment, because proline, glutamate, valine and lysine residues constitute about 70% of its sequence. This PEVK region was suggested to be important for muscle elasticity because it is expressed in different length versions in cardiac, psoas and soleus muscles and the lengths correlate with the passive tension properties of the different muscle types. Since passive tension differences have been shown between ventricular myocytes of different species (Fabiato, J. Gen. Physiol. 72:667, 1978), we hypothesized that there may be species differences in the lengths of their respective PEVK regions. RT-PCR was used to characterize the PEVK segment from rabbit, dog, pig, and rat ventricular and atrial muscle. A single major 740-bp fragment was amplified from rabbit, pig, and rat RNA while two fragments (a major 615-bp and a minor 740-bp) were amplified from dog RNA. Similar sized PCR fragments were obtained using ventricular and atrial muscle. The nucleotide sequences of the amplified fragments show a high homology between species and with the human cardiac titin PEVK sequence. These results suggest that PEVK sequence length is not the primary basis for species differences in passive tension in cardiac muscle. (Supported by HL 47053)

Tu-Pos295

MICROTUBULES IN CULTURED CHICK CARDIAC MYOCYTES.

((D.R. Swartz[1], E. Chernoff[2], S.-S. Lim[1])) Anatomy Dept.[1], Biology Dept.[2], Indiana University, Indianapolis, IN 46202.

Recent studies implicating a change in microtubule density with contractility suggest that microtubules may play a role in myofibrillogenesis in cardiac myocytes. To investigate this, embryonic (4 - 7d) chick cardiac myocytes were isolated and cultured for 3 - 7 days in vitro. Cells were immunostained with anti-tubulin, phalloidin, and anti-titin to localize cytoskeletal proteins and myofibrillar elements. During culture, most cells spread and develop a rounded morphology with a thin periphery. In the peripheral region, there was a circular orientation of both microtubules and actin filaments, the latter being more stress-fiber-like (SFL) in structure. The SFL structures show different degrees of myofibrillar maturation as shown by the periodicity of titin immunostaining which is specific for a myofibrillar element. The more peripheral SLF structures showed less maturation in terms of titin periodicity than the more centrally located structures. Localization of both microtubules and poorly developed myofibrils in the peripheral region suggests that microtubules may stabilize the nascent myofibril. To test this, cells were treated for 1 - 4 hours with nocadozole to depolymerize microtubules and immunostained with anti-tubulin and phalloidin. This treatment did not result in major changes in the SFL structures even though microtubules were depleted from the cells. This result does not support a major role for microtubules in myofibrillogenesis but treatment with nocadozole for longer durations are needed to rule this out. Supported by AHA, Indiana Affiliate.

Tu-Pos296

SUPPRESSION OF PP120FAK INHIBITS MORPHOLOGICAL CHANGES OF HUMAN ENDOTHELIAL CELLS IN RESPONSE TO CYCLIC STRETCH.

((**K. Naruse**, and M. Sokabe)) Department of Physiology, Nagoya University School of Medicine, Nagoya 466, Japan.

We have previously reported that cultured human umbilical endothelial cells (HUVECs) subjected to uni-axial cyclic stretch exhibited remarkable morphological changes associated with an increase in the level of tyrosine phosphorylation of focal adhesion proteins including $pp125^{FAK}$ and paxillin. To examine the role of $pp125^{FAK}$ in the stretch dependent morphological response, we introduced an antisense oligo-dioxynucleotide against $pp125^{FAK}$ into HUVECs to deplete $pp125^{FAK}$ protein. The expression level of $pp125^{FAK}$ in the antisense treated cells was suppressed to less than 10 % as compared to that in the sense treated cells. The expression level of other proteins, such as actin, was not changed significantly. The depletion of $pp125^{FAK}$ was detected at 24 hours and peaked at 48 hours after the antisense treatment. HUVECs cultured on a silicon membrane were treated with the antisense $pp125^{FAK}$ for 48 hours and were subjected to uni-axial cyclic stretch for 1 hour. The antisense treated HUVECs did not show any detectable morphological changes in response to mechanical stretch at any time points in contrast to sense treated HUVECs which showed normal response to cyclic stretch. These data show that $pp125^{FAK}$ is indispensable in the stretch dependent morphological changes in HUVECs.

Tu-Pos297

VISUALIZATION OF COCHLEAR OUTER HAIR CELL LATERAL WALL COMPOSITE STRUCTURE.

((**J.S. Oghalai**, A.A. Patel, T. Nakagawa, W.E. Brownell)) Dept. of Oto/Com Sci, Baylor College of Medicine, Houston, TX 77030

The motor element responsible for outer hair cell (OHC) electromotility resides in the lateral wall. The lateral wall is a composite, trilaminate structure composed of a plasma membrane (PM), an actin-spectrin network called the cortical lattice, and a multi-layered membranous organelle (similar to golgi and endoplasmic reticulum) called the subsurface cisternae (SSC). We visualized the lateral wall components during a controlled deformation produced by micropipette aspiration using confocal microscopy. Fluorescent staining of the PM with Di-8-ANEPPS and of the SSC with NBD-Ceramide demonstrated overlapping of these layers with low suction pressures. As the pressure was increased, the PM separated from the SSC and started to form a vesicle. The stiffness decreased by more than 50% at this point. This demonstrates that under tension, the PM can be peeled away from the lateral wall to form a vesicle which does not contain SSC membranes. To evaluate the contribution of the cortical lattice, OHCs were demembranated with saponin and labeled for actin with rhodamine-phalloidin. Aspiration on these cells revealed deformation, but no vesiculation, even with very high negative pressures. These findings suggest that the rigid skeleton of the cortical lattice remains with the lateral wall to buttress the SSC, rather than entering the vesicle. We conclude that the cortical lattice/SSC complex is the major contributor to lateral wall stiffness, and that vesiculation occurs when tethering between the PM and this complex is released. These data may be used to estimate the maximum amount of force that could be transmitted to the structural support of the cell from motor elements which are postulated to reside in the PM.

Tu-Pos298

ENERGETICS OF INCLUSION INDUCED MEMBRANE DEFORMATION.

((C. Nielsen[1], M. Goulian[2] and O. S. Andersen[1])) [1]Depart. Physiol. Biophys., Cornell Univ. Medical College New York, NY 10021, [2]Center for Studies in Physics and Biology The Rockefeller University New York, NY 10021. (Spon. by O.S. Andersen)

In order to understand how the material properties of a lipid bilayer determine membrane protein function, we have investigated theoretically the free energy changes associated with a hydrophobic mismatch at the contact surface between a phospholipid bilayer and imbedded inclusions. Analytical and numerical solutions to the membrane deformation energy are obtained using a liquid crystal model where the total free energy of deformation is a sum of three components: compression-expansion; splay-distortion and spontaneous monolayer curvature; and surface tension. The results show that the overall membrane deformation can be approximated by a linear spring model. In the radial decomposition of the deformation free energy (the component energy per unit length), the splay-distortion component dominates close to the interface, whereas the compression-expansion component is more prominent further away from the inclusion. The relative and absolute contributions depend on the choice of boundary conditions. In addition, when evaluating the interrelation between the energy components, we find that a change in e.g. the compression-expansion modulus affects not only the compression-expansion energy but also the splay-distortion energy and vice versa.

Tu-Pos299

EXPERIMENTAL STUDIES ON POLYPEPTIDE TRANSFER INTO MEMBRANES: TEMPERATURE-DEPENDENT PARTITIONING AND BACKBONE MEMBRANE AFFINITY.

Charles J. Russell, Thorgeir Elfs Thorgeirsson, and Yeon-Kyun Shin. Department of Chemistry, University of California, Berkeley, CA 94720.

Detailed experimental determinations of the forces governing peptide insertion into and stability within lipid bilayers should aid in understanding, predicting, and designing membrane protein/peptide structure. Our latest efforts toward this aim include (a) a study of the temperature dependence of the partitioning of 25-residue host peptides with four residues varied at a guest site and (b) an experimental determination of the energetic cost of burying the peptide backbone in the membrane using various spin labels attached to a 25-residue host peptide.

Electron Paramagnetic Resonance spectroscopy was used to measure the membrane/water partitioning of the spin-labeled peptides, which are derivatives of the mitochondrial presequence of subunit IV of yeast cytochrome c oxidase. The water-to-bilayer transfer of these peptides increases as the temperature is increased from 3 to 40 °C. The results are consistent with the hydrophobic effect being the major driving force behind membrane insertion. The value for the cost of burying the peptide backbone in the membrane will be presented.

Tu-Pos300

THE LIPID INTERACTIONS OF A PEPTIDE DESIGNED TO INSERT SPONTANEOUSLY INTO LIPID BILAYERS.

((L. A. **Chung** and T. E. Thompson)) University of Virginia, Biochemistry Department, Charlottesville, VA 22908.

The process of spontaneous incorporation of proteins into membranes from an aqueous compartment is poorly understood. Spontaneous insertion has been demonstrated for some proteins, the best known example being cytochrome b_5. To study this complex process, a *de novo* peptide sequence, H_2N-Ala_2-Leu_5-Ala_{22}-Tyr-Lys_4-$CONH_2$, designed to be both soluble in aqueous solution and capable of spontaneous insertion into lipid bilayers, was synthesized and purified. In a previous publication, we reported the temperature dependence of peptide structures in solution using a combination of circular dichroism and infrared spectroscopies (Chung and Thompson, *Biochemistry*, 35, 1996). Both surface-bound and inserted (transmembrane) conformations for the lipid-bound peptide were detected using attenuated total reflectance infrared spectroscopy. Here we report the effects of temperature on the peptide binding to phosphatidylcholine large unilamellar vesicles. The lipid-binding of the *de novo* peptide is both temperature-dependent, with increasing binding at higher temperatures, and affected by the physical state of the lipid, showing poor binding to lipids in the gel phase. (This work was funded by NIH grant GM-18628.)

Tu-Pos301

MECHANISM OF ALAMETHICIN INSERTION INTO LIPID BILAYERS

((H.W. Huang, K. He, S. J. Ludtke, W.T. Heller)) Physics Department, Rice University, Houston, Texas 77005-1892

Alamethicin adsorbs on the membrane surface at low peptide concentrations. However above a critical peptide-to-lipid ratio P/L, a fraction of the peptide molecules insert in the membrane. This critical ratio is lipid dependent. For diphytanoyl phosphatidylcholine it is about 1/40. At even higher concentrations, P/L≥1/15, all of the alamethicin inserts in the membrane and forms well-defined pores as detected by neutron in-plane scattering. A previous x-ray diffraction measure-ment showed that alamethicin adsorbed on the surface has the effect of thinning the bilayer in proportion to the peptide concentration. A theoretical study showed that the energy cost of membrane thinning can indeed lead to peptide insertion. This study extends the previous ones to a high concentration region P/L>1/40. X-ray diffraction shows that the bilayer thickness increases with the peptide concentration for P/L>1/23 as the insertion approaches 100%. The thickness change with the percent of insertion is consistent with the assumption that the hydrocar-bon region of the bilayer matches the hydrophobic region of the inserted peptide. The elastic energy of a lipid bilayer including both adsorption and insertion of peptide is discussed. The Gibbs free energy is calculated as a function of P/L and the percent of insertion in a simplified one-dimensional model. The model exhibits an insertion phase transition in qualitative agreement with the data. We conclude that the membrane deformation energy is the major driving force for the alamethicin insertion transition.

Tu-Pos302

BINDING OF PEPTIDES TO LIPID MEMBRANES INVESTIGATED BY INNER FIELD COMPENSATION

((**Günther Bähr**, Guy Vergères, and Mathias Winterhalter)) Dept. of Biophysical Chemistry, Biozentrum, University of Basel, Switzerland

We investigate how the boundary potential of a lipid bilayer influences the binding behaviour of peptides to lipid bilayers.
The method of Inner Field Compensation (IFC) is widely used (e.g. by Sokolov and Ermakov) for measuring changes in the boundary potential on one side of a planar lipid bilayer upon binding of small inorganic ions.
We used this method to compare the binding of the basic peptides corresponding to the PSD[a] of MARCKS[b] and MRP[c], two proteins essential for brain development. The PSD of these proteins binds to membranes and to calmodulin, crosslinks actin filaments and is phosphorylated by PKC[d]. Since a serine residue in the middle of the PSD of MARCKS is replaced by a proline in MRP, we have investigated whether this change effects the binding behaviour of the two peptides. To estimate the contribution of hydrophobic residues to binding we have compared the PSD peptides with pentalysine, a reference substance with no hydrophobic groups.
We discuss our quantitative binding measurements at different salt concentrations and at various percentages of negatively-charged lipids in the membrane.

[a]phosphorylation site domain
[b]Myristoylated Alanine-rich C Kinase Substrate
[c]MARCKS-related protein
[d]Protein kinase C

Tu-Pos303

ALTERING ALAMETHICIN-LIPID BILAYER INTERACTIONS BY CHANGING THE SIZE OF THE LIPID HEAD GROUP.

((W.T. Heller, K. He, S.J. Ludtke, T. Harroun, and H.W. Huang)) Rice University, Houston, TX 77251-1892.

When associated with lipid bilayers, alamethicin can adopt one of two different orientations. It can either be adsorbed into the head group region of the lipid bilayer, or it can insert across the bilayer, resulting in the formation of pores. Recently, it has been shown that the transition of alamethicin from the surface state to the inserted state is driven by the free energy cost of adsorbing into the head group region versus inserting across the bilayer. In this poster, we show that it is possible to continuously perturb the energy cost of alamethicin adsorbing into the head group region of the lipid bilayer by changing the average size of the lipid head group. We can apply a simple argument relating the energy cost of peptide adsorption to the average size of the lipid head group, allowing us to predict the critical concentration for insertion as a function of head group size. Using oriented circular dichroism to detect the orientation of an alpha-helix in an oriented bilayer, the fraction of peptide in the inserted state was measured as a function of both average lipid head group size and peptide concentration. The critical concentration for peptide insertion was determined for bilayers possessing different average lipid head group sizes. The experiment agrees with the prediction.

Tu-Pos304

THE EFFECTIVE SIZE OF LIPID POLAR HEAD GROUPS AND GRAMICIDIN CHANNEL FUNCTION

((**A. M. Maer**, L. L. Providence, O. S. Andersen)), Dept. of Physiology and Biophysics, Cornell University Medical College, New York, NY 10021 (Spon. by E. E. Windhager)

Gramicidin channel function varies with changes in the effective size of the lipid head groups, a maneuver that is expected to change the equilibrium monolayer curvature. Head groups'size can be varied by altering either the lipid composition or the electrostatic interaction between charged head groups. In the former case, replacing the bulky phosphatidylcholine (PC) with the less bulky phosphoethanolamine (PE) causes a two-fold decrease in the average channel duration (τ) when going from DOPC to DOPE:DOPC (4:1). In the latter case, the electrostatic repulsion between charged head groups can be modulated by titrating groups. We have previously shown that in DOPS, a negatively charged lipid, decreasing the pH from 8 to 3 reduces τ ten-fold. We now extend these experiments to DOPE:DOPC (4:1) bilayers. At pH 3-5, DOPE is zwitterionic. Increasing the pH to 9 or 10 increases τ two-fold, as the PE head groups become more negatively charged. Decreasing the pH from 3 to 0 increases τ three-fold, as the PE head group charge become more positive. The electrostatic repulsion between the head groups becomes stronger at the extremes of the pH, and the changes in single-channel duration can be related to the effective head group size.Importantly, alamethicin channels respond to similar maneuvers as gA channels do, but in an opposite way (Keller et al., Biophys. J. 65:23-27, 1993; Bezrukov et al., Biophys. J. 68 A341, 1995). This suggests that the changes in channel function result from alterations in the material properties of the surrounding lipid bilayer.

Tu-Pos305

CUBIC PHASES INDUCED UPON INTERACTION OF GRAMICIDIN S WITH LIPID BILAYERS. - A CLUE TO ITS MECHANISM OF ACTION?

((**E.J. Prenner**, R.N.A.H. Lewis, R.N. McElhaney, L.H. Kondejewski, R.S. Hodges, K.C. Neuman and S.M. Gruner)) Dept. of Biochemistry, and PENCE, University of Alberta, Edmonton, Alberta, CA. and Dept. of Physics, Princeton University, Princeton, New Jersey, U.S.A. (Spon. by L. Fliegel)

The interactions of gramicidin S with single-component lipid bilayers and with polar lipid extracts of the microorganism *Acholeplasma laidlawii* B were examined with ^{31}P-NMR spectroscopy. Mixtures of gramicidin S with lipids such as phosphatidylcholine, phosphatidylserine, cardiolipin and sphingomyelin exhibit ^{31}P-NMR powder patterns characteristic of lamellar phases throughout the temperature range examined (0-90°C). In mixtures of gramicidin S with either phosphatidylethanolamine or phosphatidylglycerol, axially symmetric ^{31}P-NMR powder patterns characteristic of lipid bilayers were also observed at low temperatures. However, at high temperatures an isotropic component appears in their ^{31}P-NMR spectra, whose relative intensity increases with temperature. This component exhibits a marked cooling hysteresis and disappears only when the sample is recooled below the gel/fluid phase transition. Gramicidin S appears to induce cubic phases upon interaction with some types of lipids, a suggestion supported by x-ray diffraction studies. It can also induce cubic phase formation in complex lipid mixtures such as found in the *A. laidlawii* B membrane. We suggest that interaction of gramicidin S with lipid bilayers results in a localized increase in bilayer curvature stress which may be an important part of the mechanism for the hemolytic and antibiotic activities of the peptide.
(Supported by the Medical Research Council of Canada, the Alberta Heritage Foundation for Medical Research and the Protein Engineering Network of Centers of Excellence [PENCE])

Tu-Pos306

CHANGES IN BILAYER THICKNESS INDUCED BY GRAMICIDIN AND α-HELICAL PEPTIDES IN MODEL MEMBRANES OF DIACYL-PHOSPHATIDYLCHOLINE

((**M.R.R. de Planque**[a], H. Schäfer[b], R.E. Koeppe II[c], D.V. Greathouse[c] and J.A. Killian[a])) [a]Department Biochemistry of Membranes, Utrecht University, Padualaan 8, 3584 CH Utrecht, The Netherlands; [b]Fakultät für Physik und Geowissenschaften, Universität Leipzig, Linnéstraße 5, D-04103 Leipzig, Germany; [c]Department of Chemistry and Biochemistry, University of Arkansas, Fayetteville, Arkansas 72701

The effect of gramicidin and of transmembrane α-helical model peptides on the average lipid acyl chain length of different diacylphosphatidylcholines was investigated as a consequence of hydrophobic mismatch. The model peptides are completely uncharged hydrophobic transmembrane peptides. The WALP16 sequence is AWW(LA)$_5$WWA, whereas WALP19 has a three amino acids longer hydrophobic stretch. Order profiles for the perdeuterated lipid *sn*2-chains were obtained by solid state ^{2}H NMR measurements and dePakeing. From these order parameters average acyl chain lengths were calculated. The hydrophobic thickness of a dilauroylphosphatidylcholine bilayer is smaller than the total length of the peptides. As a reaction to this hydrophobic mismatch, the two WALPs induced a small and similar increase in bilayer thickness upon incorporation. Gramicidin had a much larger effect, although this peptide has about the same length as WALP16. Lipid bilayers of which the hydrophobic thickness exceeds the total peptide length were also studied. Surprisingly, for all three peptides in these cases a minor increase in bilayer thickness was measured.

Tu-Pos307

EFFECTS OF PENTOBARBITAL ON GRAMICIDIN A CHANNEL FUNCTION IN PLANAR BILAYERS

((**Aaron D. Laskey**, Lyndon L. Providence, and Olaf S. Andersen)) Dept. Physiol. Biophys., Cornell Univ. Med. Coll., New York, N. Y. 10021

In order to examine whether the "lipid theory" of general anesthetic mechanisms could apply to barbiturate-induced anesthesia, we tested the ability of the barbiturate pentobarbital to alter gramicidin A protein function in planar phospholipid bilayers. Due to the differential lengths of the membrane's hydrophobic core and the hydrophobic length of the protein channel, gramicidin channel formation is associated with a deformation of the host bilayer. As channel formation kinetics are dependent upon the energy costs associated with this deformation, we predicted that these agents would increase both channel lifetime (τ) and the rate of channel formation by perturbing the host bilayer, hence mitigating the energy costs of dimerization. Indeed, at pharmacologically relevant concentrations (100-500 μM), pentobarbital both increased τ and increased the association rate in bilayers formed from diphytanoylphosphatidylcholine (DPhPC) and dioleoylphosphatidylcholine (DOPC). These effects did not result from bulk changes in membrane properties: surface tension and membrane thickness were unchanged by barbiturate addition. Thus, the effects of pentobarbital on gramicidin channel function may provide a rationale for understanding its effects on $GABA_A$ receptor function in excitable cells.

Tu-Pos308

MEMBRANE DEPENDENT CHANGES IN CONFORMATIONAL PREFERENCE OF GRAMICIDIN A CHANNELS.

((C. Nielsen, N. Mobashery and O. S. Andersen)) Depart. Physiol. Biophys., Cornell Univ. Medical College New York, NY 10021. (Spon. by A. M. Weinstein)

There is increasing evidence, that the material properties of the lipid bilayer affect integral membrane protein function and it is recognized that quaternary conformational changes in membrane proteins are associated with reciprocal changes in the structure of the surrounding bilayer. We provide direct experimental evidence that changes in lipid bilayer thickness affect the conformational preference of ion conducting gramicidin A (gA) channels and induces an additional conductance state in the standard gA channels. When gA is incorporated into di-C18:1-PC or di-C20:1-PC bilayers there is a single predominant channel type - the standard single stranded (SS) $\beta^{6.3}$-helical channel. In di-C22:1-PC bilayers the pattern of channel appearances changes profoundly there are several different channel types some of which appear as series of repetitive transitions from the baseline to one, or more, conducting levels and back to the baseline. The predominant channel structure is a double stranded (DS) dimer. This shift in structural preference results from an increased mismatch between channel length and membrane thickness which destabilizes the SS channels because they are pulled apart at the join between monomers. DS channels, which are joined by 26 intermolecular hydrogen bonds, are less affected by the increased mechanical mismatch.

Tu-Pos309

THE EFFECT OF MEMBRANE TENSION ON GRAMICIDIN A CHANNEL KINETICS

((M. Goulian[1], D. Feygenson[1] , O. N. Mesquita[2], E. Moses[2], C. Nielsen,[3] O. S. Andersen[3], and A. Libchaber[1,2])) [1]Center for Studies in Physics and Biology, The Rockefeller University, New York, NY 10021; [2]NEC Research Institute, 4 Independence Way, Princeton, NJ 08540; [3]Department of Physiology and Biophysics, Cornell University Medical College, New York, NY 10021. (Spon. by M. Goulian)

We study the effect of membrane tension on the channel-forming peptide gramicidin A, a model system which is well suited to explore the role of tension in membrane-protein interactions. Large unilamellar vesicles containing gramicidin are aspirated into a micro-pipet electrode. Channel activity is monitored by measuring the current in a voltage clamp, while tension is controlled via the aspiration pressure. For vesicles that intrude a long distance into the pipet, the background resistance is sufficiently stable to detect single channels. Tight seals between the membrane and pipet are avoided and we work with single-component lipids (DOPC). We therefore avoid the possibility of local lipid phase separation. Preliminary results suggest an increase in channel lifetime with increasing tension. As the gramicidin dimer is shorter than the equilibrium membrane thickness, channels deform the bilayer. The resulting elastic energy will affect both the partitioning and kinetics of channel formation. Membrane tension contributes to this elastic energy both directly, by controlling the cost of increasing membrane area, and indirectly, by thinning the membrane.

Tu-Pos310

COMPUTATIONAL STUDIES OF PEPTIDE-MEMBRANE SYSTEMS

((**See-Wing Chiu**, Michael Kellen, Shankar Subramaniam, and Eric Jakobsson)) Department of Molecular and Integrative Physiology, Center for Biophysics and Computational Biology, National Center for Supercomputing Applications, Beckman Institute, University of Illinois, Urbana, IL 61801.

Computer simulations have been used to study the behavior of two peptide-membrane systems. One is a gramicidin channel. The other is the signal sequence of the E. coli outer membrane protein lamB. In both cases the lipid is fluid phase DMPC, simulated at a constant surface tension boundary condition. The gramicidin-membrane behavior is compared with simulations in vacuum and the signal peptide-membrane behavior is compared with simulations in both water and vacuum. In both cases the membrane environment is seen to stabilize the peptide secondary structure. The gramicidin beta-helix is completely during the lifetime of the simulations in the membrane but not in vacuum. The signal peptide alpha-helix is completely stable during the lifetime of the simulation in the membrane but not in either water or vacuum. The lipid-peptide interactions are analyzed, including peptide-lipid hydrogen binding, correlations of lipid and peptide fluctuations, radial distribution functions for lipid-peptide interactions, and the effect of peptide on surrounding lipid configurations in the hydrocarbon and interfacial regions. In the case of the gramicidin channel, the effects of the lipid on the water mobility within the channel are shown. A water permeability is computed for the gramicidin channel and compared with experimental water permeabilities.

Supported by the National Science Foundation and by computer time from the National Center for Supercomputing Applications

Tu-Pos311

MEMBRANE MEDIATED PEPTIDE-PEPTIDE INTERACTION: GRAMICIDIN IN-PLANE DISTRIBUTION BY X-RAY SCATTERING.

((T. Harroun, W.T. Heller, K. He, S.J. Ludtke, and H.W. Huang)) Rice University, Houston, TX 77251-1892.

While there has been much speculation on the role the lipid matrix plays in controlling and mediating the inter-molecular dynamics of proteins, there has been little direct evidence for how the lipid bilayer can mediate the supra-molecular organization of these proteins. With the technique of X-ray in-plane scattering, we can directly measure the correlation function of gramicidin channels in the plane of the bilayer. We have studied the simple case of gramicidin incorporated into model Dilauroyl and Dimyristoyl - Phosphocholine (DL-,DMPC) membranes, and have seen how changing the membrane thickness changes peptide-peptide correlation. In the fluid phase, DLPC and DMPC present an elastic medium that can perhaps match the hydrophobic length of the peptide. The resulting membrane deformation energy is expected to cause inter-peptide attraction. Indeed, the scattering data shows that the gramicidin-gramicidin correlation distance is smaller in DMPC than in DLPC. Thus we have obtained direct evidence of membrane mediated peptide-peptide interaction. As the temperature drops and DMPC approaches its main transition temperature, gramicidin exhibits close packing. This may indicate that the channels are being excluded from gel lipid regions and are packing closer together.

Tu-Pos312

THE EFFECT OF POLAR RESIDUES AND MEMBRANE THICKNESS ON TRANSMEMBRANE ORIENTATION OF HYDROPHOBIC HELICES.

((S. Lew, J. Ren, Z. Wang, and **E. London**)) Dept. of Biochemistry and Cell Biology, SUNY at Stony Brook, Stony Brook NY 11794-5215.

We studied helix-forming hydrophobic peptides to determine the rules that govern transmembrane insertion of membrane protein α-helices. Peptides in which Lys residues flank poly Leu core long enough to span the hydrocarbon core of a normal bilayer were used. Previous investigators have shown these peptides form transmembrane helices. Variations of this structure were studied in which a single polar substitution was introduced close to the center of the poly Leu core, in addition to a single Trp at the center of the peptide introduced to monitor the location of the peptides in the membrane via parallax analysis of fluorescence quenching and λ_{max}. Transmembrane insertion of these peptides is significantly destabilized by loss of the charges on the Lys residues flanking the core. This is shown by a shift in Trp depth at high pH. In addition, transmembrane insertion is found to be destabilized in bilayers with a thick hydrocarbon core. This presumably results from "hydrophobic mismatch" between the hydrophobic thickness of peptide and bilayer. Interestingly a single Cys, Asn or Asp could be tolerated in the transmembrane orientation. This is shown by the Trp maintaining a depth in the center of the bilayer. However, at high pH or in thicker membranes a strongly polar substitution could significantly decrease the degree of transmembrane insertion relative to that of a helix without a strong polar substitution. This approach provides a method for analyzing the energetics of various aspects of membrane protein insertion.

Tu-Pos313

WHY PEPTIDES FORM SECONDARY STRUCTURE IN MEMBRANES.

((**William C. Wimley**, Alexey S. Ladokhin and Stephen H. White)) Department of Physiology and Biophysics, University of California, Irvine, CA, 92697-4560

Many membrane-active peptides partition into membrane interfaces where they gain secondary structure. Here we explore the thermodynamic coupling between these two processes using our experimentally-determined "Interfacial Hydrophobicity Scale" (W.C. Wimley and S.H. White, Nature Structural Biology (1996) 3:842-848). This scale provides information on the interfacial energies of free peptide bonds as well as the amino acid sidechains. The interfacial hydrophobicities are based on measurements of water-to-bilayer transfer free energies of small model peptides that are unstructured in membranes and therefore represent an unfolded reference state. Of particular importance is the observation that transfer of a free peptide bond into a bilayer interface is strongly unfavorable by ~1.2 kcal/mol. Even a small reduction in this high cost, through the formation of hydrogen bonds, will strongly favor the formation of secondary structure in peptides that are bound to membrane interfaces. We present two examples in which the Interfacial Hydrophobicity Scale is used to address the energetics of secondary structure formation in membranes. First, we show that the hexapeptide $AcWL_5$ forms hydrogen-bonded β-sheet or β-barrel oligomers that are unique to bilayers, and we examine the energetics of this β-structure formation in membranes. Second, we use the peptide melittin as an example of membrane binding and secondary structure formation in an α-helical peptide. We estimate that a net reduction in the free energy of an interfacial peptide bond of only 0.2 - 0.3 kcal/mol is sufficient to explain the secondary structure propensity of peptides bound to membranes. Taken together these results suggest the importance of peptide bond energetics to secondary structure formation in membranes. Supported by NIH GM46823.

Tu-Pos314

SIMULATION OF THE INTERACTIONS OF α-HELICES AND α-HELICAL HAIRPINS WITH MEMBRANES.

((**P.C. Biggin**, G.A. Woolley# and M.S.P. Sansom.)) Laboratory of Molecular Biophysics, University of Oxford, Oxford. U.K. and #Department of Chemistry, University of Toronto, 80 George St, Toronto, M5S 3H6. Canada.

The association and subsequent insertion of α-helices and α-helical hairpins into lipid bilayers is central to the modes of action of channel-forming peptides (CFPs) and of pore-forming toxins. We have developed a simulation protocol based upon the CHARMm force field, whereby the lipid bilayer is represented by a hydrophobicity scale applied on a residue by residue basis which varies along *z*, the bilayer normal. An externally applied transbilayer voltage difference is also included in the force field. Studies on monomers of alamethicin (a 20 amino acid helical peptide), suggest that voltage-sensitive insertion is coupled to local conformation changes about the proline-induced kink, whereby the kink angle is reduced so lengthening the helix which enables it to more readily span the bilayer. This method has now been extended to a-helical hairpins, in particular, those of the δ-endotoxin produced by *Bacillus thuringiensis*, and also to covalently linked dimers of alamethicin, which have recently been shown to form channels similar to those formed by native alamethicin monomers. Particular attention in the analysis has been to applied to the initial starting conformation and whether this determines the subsequent behaviour of the pepide, and also to the conformation of the loop (or linker) region of the hairpin (or dimer). The work provides insight into the mechanisms of hairpin insertion and also provides an indication of the features of a peptide which promote insertion.

Tu-Pos315

SOLID STATE NMR EVIDENCE FOR THE PRESENCE OF TWO DISTINCT BINDING MODES OF β-SHEET CARDIOTOXINS IN DPPC BILAYERS

((S. Sue, C. Hsieh, and **W.Wu**)) Department of Life Sciences, National Tsing Hua Univ. Hsinchu, Taiwan 30043

The interaction of the β-sheet cationic cardiotoxin with dipalmitoyl phosphatidylcholine (DPPC) bilayers has been investigated using ^{31}P and ^{2}H NMR. Cardiotoxin (CTX A3) from Taiwan cobra venom was found to promote isotropic ^{31}P NMR signal formation at temperatures near T_m and magnetically induced ellipsoidal deformation of the lipid bilayer above T_m. In addition, the ^{2}H NMR order parameter (S) profiles of fattyl acyl chain of d_{62}-DPPC became ordered or disordered depending on whether the interaction was studied right above or far above T_m. Since the ordering effect of this β-sheet polypeptide resembles that of other α-helix polypeptides with membrane penetratiing ability, we suggest that cardiotoxin may penetrate the membrane bilayers at temperatures near T_m. However, it changes into a peripheral binding mode at temperatures far above T_m. The transition of the binding mode further suggests that the magnetically induced ellipsoidal deformation of the lipid bilayer maybe a result of the disc formation near T_m. In this respect, β-sheet cardiotoxin resembles α-helical mellitin in its ability to cause disc formation. In conclusion, the binding of β-sheet cardiotoxin is found to undergo transition between the peripheral and penetrating modes in DPPC bilayers. Based on this observation, a novel membrane binding motif capable of penetrating membrane bilayers is identified in the β-sheet cardiotoxin. The results suggest a molecular basis for the general cytotoxic effect of snake cardiotoxins and indicate that cardiotoxins are a good model to study the interaction of β-sheet polypeptides with phospholipid membranes. (supported by NSC, Taiwan)

Tu-Pos316

THE ROLE OF HYDROPHOBIC MISMATCH AND INTERFACIALLY LOCALIZED TRYPTOPHANS IN PEPTIDE-LIPID INTERACTIONS
((**P.C.A. van der Wel**[a], M.R.R. de Planque[a], D.V. Greathouse[b], R.E. Koeppe II[b] and J.A. Killian[a])) [a]Dept. Biochemistry of Membranes, Utrecht University, Padualaan 8, 3584 CH Utrecht, The Netherlands; [b]Dept. of Chemistry and Biochemistry, University of Arkansas, Fayetteville, Arkansas 72701

The influence on lipid polymorphism of uncharged, hydrophobic, transmembrane α-helical model peptides -WALPs- containing interfacially localized tryptophans was studied by ^{31}P NMR. Length analogs of WALP were used that contained one tryptophan at each end of the peptide. These peptides proved capable of inducing the formation of non-bilayer structures in diacylphosphatidylcholine model membranes as a consequence of mismatch between the hydrophobic length of the peptides and the thickness of the membrane. Also their efficiency in inducing non-bilayer structures was shown to be mismatch-dependent. The obtained results furthermore suggested that the tryptophan-to-tryptophan segment is the determinant of the hydrophobic length of the peptides, rather than their total length. WALPs with a varying number and position of tryptophans as well as with modified tryptophan residues are being synthesized in order to further investigate the minimal requirement for non-bilayer phase induction and which properties of the tryptophans are responsible for the observed effects.

Tu-Pos317

STRUCTURAL MOTIFS THAT MODULATE PEPTIDE INTERACTION WITH NEGATIVELY CHARGED AND NEUTRAL MEMBRANES
((**M. Dathe**, L Maloy*, Wieprecht, T., M. Bienert)) Institute of Molecular Pharmacology, A. Kowalke Str. 4, D10315 Berlin, Germany; *Magainin Pharmaceuticals, Inc., Plymouth Meeting, PA 19462

Different interactions have been suggested to be responsible for the peptide induced disturbance of negatively charged and neutral lipid membranes.[1, 2] This study investigates the role of hydrophobicity, the hydrophobic moment and the polar angle of the amphipathic helix using a KLAL model peptide. Circular dichroism and fluorescence spectroscopic investigations describe peptide binding and dye release from vesicles. The antibacterial and haemolytic activity was tested. Changes in the structural motifs of the peptide were found to exhibit only slight influence on interaction with highly negatively charged lipid membranes. However, the pronounced membrane disturbing effect on neutral bilayers is correlated with the peptide features. The structural motifs were found to play a decisive role for membrane selectivity. The investigation support the hypothesis that the disturbance of the hydrophobic inner membrane region is much more effective in membrane permeabilization than the preferred binding and fixation of the cationic peptides at charged bilayer interfaces. The effects on model membranes show correlation with biological activity.
[1] Dathe,M., Schümann,M., Wieprecht,T., Winkler,A., Beyermann,M., Krause,E., Matsuzaki,M., Murase,O, Bienert,M (1996) Biochemistry 35, 12612-12622; [2] Wieprecht,T., Dathe,M., Schümann,M, Krause,E., Beyermann,M., Bienert,M. (1996) Biochemistry 35, 10844-10853.

Tu-Pos318

ORIENTATION AND DYNAMICS OF MEMBRANE ASSOCIATED PEPTIDES BY NMR
((**Judit A. Losonczi,** James H. Prestegard)) Department of Chemistry, Yale University, New Haven CT 06511

Field-oriented phospholipid bilayer disks, or bicelles, can mimic the environment of biological membranes while allowing unique spectroscopic measurements of structural and dynamic properties. In NMR, dipolar couplings and CSA data for various magnetic isotopes yield information on conformations and motional properties of bilayer anchored molecules. Moreover, these parameters can be measured with adequate resolution to work with multiple isotope labels in single molecular entities. These methods have been successfully used in studies of membrane bound carbohydrates. The applicability to the study of surface-associated peptides and proteins is now being explored. Preliminary results will be presented for N-myristoylated peptides which are based on the N-terminal sequence of ARF, a protein involved in membrane trafficking.

Tu-Pos319

LOCATION OF TRYPTOPHAN SIDECHAINS IN MEMBRANES STUDIED WITH ^1H MAS NMR
((**K. Gawrisch**, W.-M. Yau, W. C. Wimley* and S. H. White*))
NIH, NIAAA Rockville, MD 20852, *University of California, Irvine, CA 92717

The location of indole, N-methyl indole, 3-methyl indole, and the pentapeptide Ac-W-L(^{15}N)-W-L-L in POPC-d_{31} and DMPC-d_{67} bilayers has been investigated by ^1H-MAS NMR. Magic-angle spinning together with the rapid molecular motion of membrane lipids result in excellent spectral resolution which facilitates application of multidimensional high-resolution NMR techniques. Intensity of NOESY crosspeaks between lipid and indole resonances is strongest for lipid protons from headgroups, glycerol, and upper chain methylene groups suggesting a preferential interaction between indole and the lipid-water interface. Confirmation of indole location is provided by the indole ring current effect on lipid chemical shifts which moves resonances from the lipid interface to higher field. Methylation of the indole ring does not alter indole location. Tryptophan sidechains of the pentapeptide, also located at the membrane-water interface, increase the lateral spacing of POPC which is reflected by a decrease of ^2H NMR order parameters of chain segments in the bilayer center.

Tu-Pos320

MECHANISMS BY WHICH THIONIN INDUCES SUSCEPTIBILITY OF S49 CELL MEMBRANES TO PHOSPHOLIPASE A2.
((**H.A. Wilson**, A.M. Judd, and J.D. Bell)) Dept. of Zoology, Brigham Young University, Provo, Utah 84602

Whereas cells normally resist attack by PLA_2, they become susceptible under certain pathological conditions. To ascertain the regulatory mechanisms that induce cellular susceptibility to PLA_2, the effect of thionin on S49 cells was examined in the presence of PLA_2. Thionin alone was unable to evoke hydrolysis of the lipid bilayer. Likewise, the addition of PLA_2 alone caused production of only a minimal amount of free fatty acid. However, thionin and PLA_2 together resulted in significant hydrolysis of the cell membrane. Thionin caused perturbation of the bilayer structure as suggested by the changes in the emission spectra of laurdan and the permeability of the membrane to propidium iodide. These changes correlated quantitatively with the susceptibility of the lipid bilayer to PLA_2. Furthermore, thionin induced a modest increase in intracellular Ca^{2+}. The source of this Ca^{2+} was the extracellular fluid since EDTA in the extracellular medium inhibited the Ca^{2+} influx. Moreover, cobalt chloride, a universal Ca^{2+} channel blocker, prevented the rise in intracellular Ca^{2+}, the uptake of propidium iodide, and the susceptibility to PLA_2 induced by thionin. In contrast, the changes in the laurdan emission caused by the thionin were not affected by the cobalt. We hypothesize that thionin causes S49 cell membranes to become susceptible to PLA_2 by a Ca^{2+}–dependent perturbation of the bilayer structure.

Tu-Pos321

THE EFFECT OF MEMBRANE PACKING AND HYDRATION ON PHOSPHOLIPASE C ACTIVITY
(**M. Bonhomme**, M. Rebecchi and S. Scarlata) Depts. of Anesthiology and Physiology & Biophysics, SUNY Stony Brook, Stony Brook, NY 11794-8661

Inositol-specific phospholipase C works at the membrane interface catalyzing the hydrolysis of phosphatidylinositol 4,5 bisphosphate into the two second messengers, inositol 1,4,5 triphosphate and diacylglycerol. Previous monolayer studies suggest that catalysis occurs by insertion of a portion of the protein into the membrane surface. We have also found that lipids which alter surface packing and hydration also alter enzymatic activity. To better understand the interplay between lipid packing and enzyme activity, we have studied catalysis under hydrostatic pressure. To accomplish this we first developed a real time spectrofluometric assay using a fluorescent pH probe which is sensitive to the protons released during catalysis. Interestingly, we find that the application of pressure results in a systematic increase of the catalytic rate both in micelles and bilayers implying that the membrane binding and penetration events which accompany enzyme activation occur during the loading time of the pressure cell. To isolate the effects of lipid packing on membrane penetration, we are currently initiating the reaction after pressurization has been achieved.

Tu-Pos322

ELECTROSTATICS MEDIATES THE MEMBRANE BINDING OF SRC: THEORY AND EXPERIMENT

((**D. Murray**, C.A. Buser, S. McLaughlin, N. Ben-Tal, B. Honig, L. Hermida-Matsumoto and M.D. Resh)) HSC, SUNY Stony Brook, NY 11794; Columbia University, New York, NY 10032 and Memorial Sloan-Kettering Cancer Center, New York, NY 10021.

Src, a nonreceptor tyrosine kinase, is involved in cell cycle control, and membrane association is crucial to its normal and oncogenic functions. Membrane binding of Src requires the synergism of two interactions: the hydrophobic insertion of Src's N-terminal myristate into the hydrocarbon interior of the membrane and the electrostatic interaction of Src's N-terminal cluster of basic residues with acidic phospholipid head groups. Previous work showed that peptides corresponding to the N-terminus of Src mimic the membrane binding of the native protein. Recent experiments show that phosphorylation of serines within Src's N-terminus by protein kinases A and C produces translocation of peptides corresponding to the N-terminal region from phospholipid membranes and of chimeric Src proteins from the plasma membrane of COS cells. Using atomic models of Src's N-terminus and phospholipid bilayers, we calculated the electrostatic component of the membrane binding of Src peptides by solving the Poisson-Boltzmann equation. The theoretical results compare well with experimental vesicle-peptide binding data: membrane association of Src peptides increases as the mole % acidic lipid in the membrane increases, as the number of basic residues in the peptide increases and as ionic strength decreases. The introduction of phosphate groups into the Src peptide decreases the electrostatic binding to acidic phospholipids by the amount observed experimentally.

Tu-Pos323

ACIDIC LIPID DEPENDENT BINDING, INSERTION AND AGGREGATION OF THE LANTIBIOTIC NISIN ARE INVOLVED IN PORE FORMATION

((**E. Breukink**[#], C. van Kraaij[#*], A. van Dalen[#], R.J. Siezen*, R.A. Demel[#], O.P. Kuipers* and B. de Kruijff[#])) [#]Department of Biochemistry of Membranes, Center for Biomembranes and Lipid Enzymology, Utrecht University and *Department of Biophysical Chemistry, Netherlands institute of Dairy Research (NIZO), The Netherlands.

Nisin is a 34 amino acid long antimicrobial peptide which is produced by several strains of *Lactococcus lactis*. The antimicrobial activity is primarily thought to arise from pore formation in the cytoplasmic membrane of the target organism. With the use of nisin mutants, obtained via site directed mutagenesis, with an unique tryptophan at positions 1, 17 or 32 (I1W, M17W, and V32W) or a glutamic acid at position 32 (V32E), the interaction of different domains of the nisin peptide with model membranes was examined. Binding studies using radioactively labeled nisin showed that binding of wild type nisin to vesicles is markedly dependent on the presence of negatively charged lipids. Introduction of a negative charge at the C-terminus of nisin resulted is a 3-16 fold loss of the antimicrobial activity. This was paralleled by an almost complete loss of the negatively charged lipid dependency of the vesicle-binding. This suggests that the C-terminus of nisin is responsible for the initial interaction of nisin with the target membrane. Tryptophan fluorescence studies showed that nisin inserts in the membrane and aggregates in the presence of negatively charged lipids. A correlation was found between the formation of nisin aggregates and the ability of the peptide to cause leakage of vesicle contents, demonstrating that peptide aggregation is essential for the membrane permeabilizing activity of the peptide.

Tu-Pos324

THE INTERACTIONS OF ADRENOCORTICOTROPIN AND NEUROKININ PEPTIDES WITH SODIUM DODECYLSULFATE AND DODECYL-PHOSPHOCHOLINE MICELLES AS STUDIED BY NMR. COMPARISONS WITH BILAYER STUDIES.

((Xinfeng Gao and **Tuck C. Wong**)) Department of Chemistry, University of Missouri, Columbia, Missouri 65211.

The partition of two series of biologically active peptides, the adrenocorticotropin (ACTH) and Neurokinin peptides, in sodium dodecylsulfate and dodecylphosphocholine micelles was studied by NMR pulsed field gradient diffusion. These two micelles have been used frequently in high resolution NMR as membrane mimicking media. The results show that there are significant differences in the partition of these peptides in the two micellar systems. Furthermore, the partition of these peptides in micelles also differs from that observed for some of these peptides in lipid bilayers from previous studies. The mechanism of partition of these peptides in micelles, and the role of electrostatic and hydrophobic interactions in the partition, will be discussed. The secondary structures of these peptides in the micelles have also been determined from two-dimensional NMR experiments, and compared with those in lipid bilayers. The assumption that these micelles are good membrane mimics will be examined based on whether i) the peptide partition and ii) the secondary structures of the peptides are similar between the micelles and the bilayers.

Tu-Pos325

THE MEMBRANE-INSERTED STATE OF EXPORT-DEFICIENT LAM-B SIGNAL SEQUENCE PEPTIDES.

((Y. Dang, J. Stader, and **A.F. Esser**)) School of Biological Sciences, University of Missouri, Kansas City, MO 64110.

Introduction of charged amino acids into the central hydrophobic core of the *E. coli* LamB (maltoporin) signal sequence decreases the rate of LamB precursor transport across the inner membrane (Stader et al. J. Biol. Chem. *261* [1986] 15075). This defect can be compensated for by suppressor mutations. One such suppressor, *prlZ1* (Wei & Stader, J. Bact. *176* [1994] 5704), corrects only mutations which are located on the same face of the signal peptide when folded into a putative α-helix. To ascertain the folding of the signal peptide in its membrane-associated state we used cysteine-dependent site directed spin labeling of LamB mutant peptides V14D and M19R. The V14D mutation cannot be suppressed by *prlZ1* but the M19R mutation can be corrected. Peptides with a cysteine either at position 10, 13, 18, or 19 were synthesized and modified using a SH-specific methanethiosulfonate spin label reagent and the depth of insertion of the nitroxide group into a lipid bilayer (65% DOPC, 35% DOPG) was determined by EPR spectroscopy. Spectral analyses indicated that the wildtype signal peptide and the M19R mutant assumed a bound state in which the immersion depth of the different nitroxides varies between 0.5 and 1.2 nm, compatible with an α-helix parallel to the bilayer surface. In contrast, although the V14D mutant was firmly bound it remained in an extended state with all the nitroxides located at the same depth of about 0.2 to 0.4 nm. The extended state of the V14D mutant was confirmed by CD spectroscopy and by synthesizing peptides with two cysteines in positions 13 and 17 and measuring the distance between them. In the WT and M19R α-helices the spin labels bound to the two cysteines were sufficiently close to show lineshape broadening but no spin-spin exchange was detectable for the V14D peptide. These results indicate that the mutated signal peptides must be able to form an α-helix in the membrane to allow interaction with the suppressor gene product. (Supported by NIH grant AI-19478)

Tu-Pos326

STRUCTURAL STUDIES OF MEMBRANE PROTEINS USING MAS-NMR.

((**Melanie J. Cocco, Maria Javadpour, Ted Shieh, David K. Song, and Steven O. Smith.**)) Department of Molecular Biophysics and Biochemistry, Yale University, PO Box 208114, 266 Whitney Ave., New Haven, CT 06520-8114.

The amino acid sequence of most integral membrane proteins is characterized by one or more predominantly hydrophobic regions of 18-24 residues which often span the membrane in α-helical secondary structures. Helix-helix interactions are important in stabilizing the folded form of a protein with multiple membrane spanning domains and can drive the oligomerization of proteins with a single transmembrane domain. We have been interested in determining the structures of glycophorin A and phospholamban, which form dimeric and pentameric complexes, respectively. Towards this goal, we are evaluating methods of reconstitution of membrane proteins into lipid environments and developing methods for high resolution distance measurements using magic angle spinning NMR. We show that polarized FTIR provides a rapid assay of the secondary structure and orientation of transmembrane peptides. Both phospholamban and the transmembrane domain of glycophorin A span lipid bilayers with transmembrane α-helices oriented roughly 20-30° from the membrane normal. Internuclear ^{13}C-^{13}C distances are measured using rotational resonance NMR approaches over a range of temperatures to establish the local secondary structure and regions of helix-helix interaction in these systems. We present our current models of the dimer structure of the glycophorin A transmembrane domain and the pentamer structure of the phospholamban complex based on recent polarized IR and NMR results.

Tu-Pos327

AN HEPTAD REPEAT SEQUENCE FROM THE CYTOPLASMIC TAIL OF THE TRANSMEMBRANE PROTEIN OF HIV-1 ASSOCIATES WITH AND DESTABILIZES MEMBRANE BILAYERS

((Yossef Kliger and Yechiel Shai)). Department of Membrane Research and Biophysics, Weizmann Institute of Science, Rehovot, 76100 Israel (Spon. by Izchak Z. Steinberg)

HIV-1 transmembrane envelope glycoprotein (gp41) has unusually long cytoplasmic domain whose function and structure are mostly hidden. This domain contains two highly amphipathic α-helices, which were previously shown to interact with lipid bilayers. We have detected a highly conservative leucine heptad repeat motif between these α-helices. A synthetic peptide corresponding to this segment (residues 789-815) was found to be in an aggregated unstructured form in aqueous solution, but when exposed to phospholipid membranes it spontaneously inserts into them, dissociates into monomers, and adopts α-helical structure. The peptide is highly potent in destabilizing the bilayer structure as revealed by its ability to cause the dissipation of a membrane potential. Furthermore, it induces micelle formation and other non-bilayer structures, as revealed by negative staining electron microscopy. Tryptophan quenching experiments using brominated phospholipids, and enzymatic digestion experiments revealed that the peptide is inserted into the hydrophobic core of the membrane. The orientation of the peptide, when inserted into oriented lipid multibilayers, was determined using attenuated total reflection infrared spectroscopy (ATR-FTIR). It was found that the peptide α-helix axis is about 65° from the normal to the membrane plane. Integrating this with the knowledge about the membrane-associating features of neighboring segments, we suggest a structural model in which a large portion of the cytoplasmic tail of HIV-1 forms a secondary association with the membrane.

Tu-Pos328

THE DIFFERENT PEPTIDE-LIPID MEMBRANE INTERACTION OF NEUROMEDIN B (NMB) AND DELTA-SLEEP INDUCING PEPTIDE (DSIP) AS REVEALED BY SPECTROSCOPIC TECHNIQUES AND MOLECULAR SIMULATION. ((E. Polverini, R. Casadio, P. Neyroz* and L. Masotti*)) Dept.of Biology, Laboratory of Biophysics, and Dept.of Biochemistry*, University of Bologna, Via Irnerio 42/48*, I-40126 Bologna, Italy.

Two neuropeptides of similar small length (9/10 residues) and different physiological functions are investigated in relation to their interaction with the membrane phase using both micelles and lipid vesicles as model systems. Lipid-peptide interactions are determined with intrinsic static and dynamic fluorescence, circular dichroism and molecular dynamics. Upon addition of lipids, only for NMB the fluorescence emission spectra are blue-shifted; the fluorescence lifetimes and anisotropy values are significantly increased and quenching constants decreased, indicating lipid-peptide interaction. With CD spectra and molecular dynamics it is obtained that the lipid phase stabilizes an α-helix rich structure only for NMB and not for DSIP, whose folding seems to be indifferent to the lipid environment. Our results suggest a possible correlation between structure and functions for neuropeptides.

Tu-Pos329

SIZING MEMBRANE PORES IN LIPID VESICLES BY LEAKAGE OF CO-ENCAPSULATED MARKERS: PORE FORMATION BY MELITTIN AND INDOLICIDIN.

((**A.S. Ladokhin**[1,2], M.E. Selsted[2] and S.H. White[1]))
[1]Department of Physiology and Biophysics; [2]Department of Pathology University of California, Irvine, CA 92697.

Many toxins and antimicrobial peptides permeabilize membranes by forming relatively large multimeric pores. Determination of the size of such pores is an important first step for understanding their structure and mechanism of self-assembly. We report a simple method for sizing pores in vesicles based on the differential release (as determined by gel filtration chromatography) of co-encapsulated fluorescently labeled dextran markers of two different sizes. The method was tested using the bee venom peptide melittin, which was found to form pores 25-30 Å diameter in palmitoyloleoylphosphatidylcholine vesicles at a lipid-to-peptide ratio of 50. This result is consistent with observations on melittin pore formation in erythrocytes (Katsu et al. 1989. *Biochim. Biophys. Acta* **983**:135). We applied the method to study membrane permeabilization by the antimicrobial peptide indolicidin and its analogs. Unlike melittin, indolicidin does not form amphipathic helices when it binds to membranes (Ladokhin et al. 1996. *Biophys. J.* 71: in press). Nevertheless, it apparently forms pores of similar size. We find that release of dextrans correlates with the degree of indolicidin self-association in solution. Supported by GM-46823 and AI-22931.

Tu-Pos330

INFLUENCE OF STRUCTURAL PARAMETERS UPON THE MEMBRANE ACTIVITY AND SELECTIVITY OF THE ANTIMICROBIAL PEPTIDE MAGAININ 2. ((T. Wieprecht, M. Dathe, M. Beyermann, E. Krause and M. Bienert)) Forschungsinstitut für Molekulare Pharmakologie, A.-Kowalke-Str. 3, 10314 Berlin, Germany.

The antimicrobial peptide Magainin 2 amide (M2a) effectively permeabilizes negatively charged membranes but shows only a poor activity in the presence of electrically neutral membranes. Three sets of M2a analogs have been synthesized to investigate the influence of peptide hydrophobicity, hydrophobic moment and angle subtended by the positively charged helix face on membrane activity and selectivity. Only one of these parameters has been modified within a peptide set whereas the other two were almost kept constant. CD investigations of the peptides in the presence of vesicles revealed that all analogs retain the ability to fold into an α-helical conformation. All peptides permeabilized negatively charged POPG vesicles in a similar, submicromolar concentration range as determined by a dye-releasing assay. With decreasing amounts of POPG and increasing amounts of POPC the membrane-permeabilizing activity of the peptides becomes more differentiated. Analogs with slightly enhanced hydrophobicity or hydrophobic moment are highly active in permeabilizing POPC-rich vesicles and are not selective for negatively charged vesicles. Reduction of the angle subtended by the positively charged helix face from 120° (M2a) to 100° decreases the permeabilizing activity at POPC-rich vesicles. In contrast, analogs with an enhanced angle (140°, 160°) show an increased activity in the presence of POPC-rich membranes. Comparison of the membrane-permeabilizing ability and helicity on mixed POPC/POPG(3:1) vesicles revealed that no direct correlation exists. Correlation of peptide binding and membrane permeabilization of unselective analogs showed that the binding affinity of these peptides is higher on POPG vesicles whereas the permeabilizing efficiency of the bound peptide fraction is enhanced on POPC vesicles.

Tu-Pos331

MEMBRANE PORES INDUCED BY MAGAININ ((L.Yang, S.J.Ludtke, K.He, W.T.Heller, T.A.Harroun and H.W. Huang)) Physics Department, Rice University, Houston, Texas 77005-1892

Magainin, found in the skin of Xenopus laevis, belongs to a broad class of antimicrobial peptides which kill bacteria by permeabilizing the cytoplasmic membrane but do not lyse eukaryotic cells. The 23-residue peptide has been shown to form an amphiphilic helix when associated with membranes. However, its molecular mechanism of action has been controversial. Oriented circular dichroism has detected helical magainin oriented perpendicular to the plane of the membrane at high peptide concentrations, but Raman, fluorescence, differential scanning calorimetry, and NMR all indicate that the peptide only associates with the head groups of the lipid bilayer. Here we show that neutron in-plane scattering detects pores formed by magainin 2 in membranes only when a substantial fraction of the peptide is oriented perpendicular to the membrane. The pores are almost twice as large as the alamethicin pores. Based on the in-plane scattering data, we propose a toroidal (or wormhole) model, which differs from the barrel-stave model of alamethicin in that the lipid bends back on itself like the inside of a torus. The bending requires a lateral expansion in the head group region of the bilayer. Magainin monomers play the role of fillers in the expansion region thereby stabilizing the pore. This molecular configuration is consistent with all published magainin data.

Tu-Pos332

STRUCTURE-FUNCTION STUDIES OF CECROPIN A ACTIVITY IN LIPID MEMBRANES

((Loraine Silvestro, Jeffrey N. Weiser, and Paul H. Axelsen))
Departments of Pharmacology and Microbiology
University of Pennsylvania, Philadelphia PA

Cecropin A is a 37 amino acid peptide produced in the Hyalophora cecropia pupae as a part of its host defense mechanism. Cecropin A exhibits a broad antibacterial spectrum, killing both Gram-positive and Gram-negative bacteria, while eukaryotic cells remain viable. The basis for this selectivity is thought to lie at the level of the membrane, but the mechanism of action of cecropin A is unclear. The interaction between cecropin A and membrane surfaces is studied here in calcein-loaded liposomes using fluorescence spectroscopy, and in supported lipid membranes using internal reflectance infrared spectroscopy. The results indicate that cecropin A induced release of calcein from liposomes with a net negative surface charge is inhibited by 38 mole % cholesterol. The presence of valinomycin/K+ generated membrane potentials did not affect the cecropin A induced release of vesicle contents, but did demonstrate that cecropin A is capable of forming ion channels in liposomes. The minimum concentration at which channels are formed in these bilayers is at least two orders of magnitude less than that needed to induce lysis. The effects of cecropin A on bacterial cell viability indicate that concentrations which induce channel formation without lysis in liposomes cause significant death of bacteria.

Tu-Pos333

ANNEXIN INTERACTION WITH PLANAR LIPID BILAYERS. ((Y.V. Sokolov, N. Tranngo, W. Mailliard, H. Haigler, H. Luecke and J. E. Hall)) University of California, Irvine; Irvine, CA 92697-4560.

Annexins are a family of calcium- and phospholipid-binding proteins thought to be involved in a number of membrane processes including fusion and secretion. Recent studies of annexin XII showed that it forms a calcium-dependent homo-hexamer. To study phospholipid binding of annexin XII we used a lipid bilayer containing nonactin as a conductance probe. Annexin XII added to a solution bathing the lipid bilayer decreased the nonactin-induced conductance in a concentration-dependent manner. This dependence was well fit by an adsorption isotherm with an apparent pK of 6.8. Nonactin conductance reduction required phosphatidylserine in the lipid bilayer and was strongly dependent on calcium (but not magnesium) concentration in the range of 0.03 - 1 mM. Two annexin XII mutants which are not able to form hexamers (E105K and the double mutant, E105K/K68A) were much less effective. The conductance reduction of both could be fit by adsorption isotherms with pK of about 5.4. A third mutant (K132E) having a mutation in the central region of the molecule which did not affect hexamer formation had an effect on the nonactin conductance similar to that of wild type annexin XII. The possible mechanisms of annexin-phospholipid interaction are discussed.
This work was supported by NIH grant EY5661 to JEH.

Tu-Pos334

EFFECTS OF CECROPINS B, B1 AND B2 ON LIPOSOMES, BACTERIA AND CANCER CELLS. ((**H.M. Chen**, W. Wang and S.-C. Chan)) Department of Biochemistry, Hong Kong University of Science and Technology, Clear Water Bay, Kowloon, Hong Kong

Custom designed analogs of the natural anti-bacteria peptide, cecropin B (CB) have been synthesized. The anti-bacterial peptides cecropin B-1 (CB-1) was constructed by replacing the C-terminal segment (residues 26 to 35) with the N-terminal sequence of CB (positions 1 to 10 which includes five lysine residues). The second analog CB-2 is identical to CB-1 except for the insertion of a Gly-Pro residue pair between Pro-24 and Ala-25. These peptides were used to investigate their anti-liposome, anti-bacterial and anti-cancer activities. The strength of anti-liposome activity is about two- to three-fold reduced if the analogs are used instead of the natural CB based on DL_{50} analysis. Similarly, the potency of these analogs on certain bacteria is about two- to four-fold less than that of CB according to *LC* measurements. In contrast, on leukemia cancer cells, the potency of CB-1 and CB-2 is about two- to three-fold higher than that of natural CB based on IC_{50} measurements. CB, CB-1 and CB-2 have comparable helix content based on CD measurements. These results indicate that the designed cationic lytic peptides having extra cationic residues are more effective at lysing cancer cells but less effective in killing bacteria and breaking liposomes than native CB. It also suggests that the hydrophobic C-terminal segment of natural CB still contributes to its killing efficiency on bacteria.

Tu-Pos335

MOLECULAR DYNAMICS SIMULATIONS OF PEPTIDE-MEMBRANE INTERACTIONS. ((P.G. Pascutti, M.M. Cassiano, A.S. Ito and **P.M. Bisch**)) Inst. de Biofisica - UFRJ, Rio de Janeiro; Inst. de Física - USP, São Paulo, Brazil

Using a classical force field we perform molecular dynamics simulations to investigate partition and structural changes of peptide molecules at the membrane-water interface. Long-time dynamics (nanosecond scale) were performed by representing the membrane and the aqueous phase as continuum media with low (2) and high (80) dielectric constants, respectively. During the simulations, as expected, hydrophobic peptides (poli-lysine) do not cross the interface staying in the aqueous phase, although hydrophilic ones, like the α-MSH hormone, go into and stay in the membrane phase. A typical amphiphilic peptide, the α–helix from β-endorphin, does not go in the interior of the membrane, staying in the interfacial region. Structural changes are monitored, showing that α–helix structures are stabilized in the low dielectric constant medium, although they tend to disrupt in the aqueous medium. We show also that saline bridges are formed in the interior of the membrane preventing charged groups to be exposed in this phase. This picture allows us to understand the fundamental role played by the central sequence His-Phe-Arg-Trp of the MSH hormone and of its synthetic high-potent analogues, in interacting with the membrane. Short time dynamics (picosecond scale) were performed representing explicit water and lipid molecules. These simulations allow us to follow the molecular details of peptide-lipid interactions during the insertion process.

ERYTHROCYTE MEMBRANES

Tu-Pos336

REGULATION OF THE MOVEMENTS OF ERYTHROCYTE BAND 3 AS STUDIED BY SINGLE PARTICLE TRACKING AND LASER TWEEZERS. ((**M. Tomishige**, Y. Sako and A. Kusumi)) Dept. of Life Sciences, Univ. of Tokyo, Tokyo 153, Japan

We have proposed a "membrane skeleton fence model", in which close apposition of the membrane skeleton meshwork to the membrane gives effective barriers for free diffusion of membrane proteins due to steric hindrance. This model was examined by single particle tracking with a high speed camera and by laser tweezers.

(1) Erythrocyte band 3 was labelled by paucivalent colloidal gold (40-nm ϕ). The mobile fraction of band 3 was ≈ 65% at 37°C. These molecules undergo free diffusion ($D_{micro} \approx 5.3 \times 10^{-9}$ cm^2/s) within domains of ≈85-nm in diameter, and hop to adjacent domains every 260 ms on average. D_{MACRO} was one-sixtieth of D_{micro}.

(2) The cytoplasmic domain of band 3 was removed by brief trypsin treatment, which did not cleave spectrin and actin. The domain size and D_{micro} was the same after cleavage, but only the hop rate increased by a factor of 6 to once every 41 ms on average.

(3) When the membrane skeleton was dragged laterally by optical tweezers via attached latex bead (1-μm ϕ), mobile band 3 was also moved along with the membrane skeleton.

These results support the membrane skeleton fence model.

Tu-Pos337

Tu-Pos338

TRANSPORT OF HYDROXYUREA IN ERYTHROCYTES; IMPLICATIONS FOR HYDROXYUREA HANDLING IN THE KIDNEY. ((O. Fröhlich, R. T. Timmer, R. B. Gunn and J. Sands)) Depts. of Physiology and Medicine, Emory Univ. Sch. Med., Atlanta, GA 30322

Hydroxyurea (HU) is used in the treatment of several diseases including sickle cell anemia where it lessens the extent of hemoglobin polymerization through induction of fetal hemoglobin. Since HU is a derivative of urea, and because of the role of urea transport in the renal urine concentrating mechanism, it is important to understand the handling of HU in the kidney. In the renal medulla, urea concentrations can rise above several hundred millimolar, which is considered a cytotoxic level for HU. We studied HU transport in human erythrocytes by stopped-flow/light scattering, monitoring the osmotic changes in cell volume which occur during HU influx or efflux. The rate coefficient of osmotic re-swelling in a medium containing 200 mM HU (plus 100 mM NaCl) was 0.083 s^{-1} for HU versus 0.73 s^{-1} for urea under the equivalent condition, which means that the HU flux in erythrocytes is 9 times slower than urea flux. HU fluxes are mediated by the urea transporter since they were inhibited by the competitive urea transport inhibitor, thionicotinamide, with an affinity of about 200 μM. The rate constant of osmotic swelling by HU decreases with increasing HU concentrations, which means that influx of HU exhibits saturation. The half-maximal activation concentration of HU is 310 mM, and the maximal, extrapolated rate coefficient at zero HU concentration corresponds to a HU permeability of 6 x 10^{-6} cm s^{-1}. In the presence of a 100 mM gradient for both HU and urea, the swelling curve was biphasic, containing a rapid component due to urea and a slow component due to HU influx. The rates of HU net influx and efflux were approximately the same. The slower transport rate for HU in erythrocytes means that the accumulated HU would likely be washed out by the circulating red cells in the vasa recta if the renal countercurrent concentrating mechanism could accumulate HU. Furthermore, if the renal urea transporters exhibit a comparably slower transport rate for HU compared to urea, HU would not accumulate to significant (and toxic) levels in the medullary interstitial space. Finally, from these data one would not predict that HU would interfere with the accumulation of medullary urea under conditions of renal water conservation. (This work supported in part by grants HL28674 to RBG, HL08989 to RTT, and DK41707 to JMS).

Tu-Pos339

CONFORMATIONAL ORDER OF MEMBRANE PHOSPHOLIPIDS IN NORMAL AND SICKLE HUMAN ERYTHROCYTES ((**David J. Moore**[1,2], Richard H. Silts[1], Scott Gioioso[2] and Richard Mendelsohn[2])) [1]Department of Pediatrics, the Children's Hospital of N.J./University of Medicine and Dentistry of N.J., Newark, N.J. 07107 and [2]Department of Chemistry, Rutgers University, Newark, N.J. 07102

In recent reports we have demonstrated that acyl chain perdeuterated phospholipids such as dimyristoylphosphatidylcholine (DMPC-d_{54}) and dimyristoylphosphatidylserine (DMPS-d_{54}) can be incorporated by incubation into normal human erythrocytes. Using Fourier transform infrared (FTIR) spectroscopy the conformational behavior of these specific lipids has been measured in intact erythrocytes. Our initial investigations monitored the conformational order of phospholipids in echinocytic (spiculate) and stomatocytic (cupped) erythrocytes. The current work extends this research to the study of normal discocytic erythrocytes and sickle cell erythrocytes. In discocytic cells the conformational order of DMPC-d_{54} incorporated into the outer membrane leaflet is intermediate between an ordered and disordered phase: the same behavior is observed for DMPS-d_{54} incorporated into the inner membrane leaflet. These results are very different from the behavior observed in echinocytes and stomatocytes indicating that conformational order of phospholipids in intact erythrocytes is affected by cell shape. Studies of the effects of oxygenation and deoxygenation upon the conformational order of specific membrane phospholipids in sickle cell disease erythrocytes are also currently underway. Preliminary results indicate that DMPC-d_{54} incorporated into the outer membrane leaflet of oxygenated sickle cells exhibits a phase transition centered at 19°C. Upon deoxygenation of these same intact erythrocytes the DMPC-d_{54} phase transition is nearly abolished and the lipid becomes more conformationally disordered. This result demonstrates that FTIR spectroscopy can measure a change in conformational order of a specific lipid species in the membrane of intact erythrocytes. Furthermore, these results offer direct evidence that deoxygenation of sickle erythrocytes results in a conformational disordering of a lipid initially localized to the outer leaflet of the membrane.

(Supported by a grant from the American Heart Association)

Tu-Pos340

COMPLEX BEHAVIOUR OF THE SPECTRIN BASED NETWORK DURING MEMBRANE DEFORMATION ((**Knowles D.W.**, Gimm J.A., Oddone G., Mohandas N.)) Lawrence Berkeley National Laboratory, University of California, Berkeley, CA.

Micropipette aspiration is a well established technique for measuring elastic shear rigidity of the red cell membrane. Consideration of the compressibility of the membrane skeleton has added a new level of complexity to the analysis of these experiments. The recently developed technique of Fluorescence Imaged Microdeformation (FIMD) shows that aspiration of a single cell into a glass micropipette creates a local deformation of the underlying skeleton which must condense to enter the pipette and then dilate down the aspirated portion. This local membrane skeletal deformation drives molecular redistribution of the associated membrane components. A complete understanding of these processes will depend on our understanding membrane skeletal deformation at the molecular level. Our studies of rhodamine phalloidin labeled skeletal actin in human red blood cells show that the normalized skeletal density at the pipette entrance (Pe) and the aspirated cap (Pc) exhibit a linear increase and decrease, respectively, with increasing aspiration length scaled by the pipette radius (L/Rp), up to a moderate value of L/Rp which is measured from the aspirated cap. Analysis of the entrance and cap densities show that the skeletal density gradient is dependent on Rp and increases monotonically as Rp decreases. Most importantly, when the aspiration length exceeds a specific value, L_{2phase}/Rp, we measure a discontinuity in the actin density gradient. Analysis of Pe and Pc showed that this discontinuity results from a discontinuity in the slope of Pe, at L_{2phase}/Rp, whereas the slope of Pc remained constant. For normal cells this second deformation phase occurred at $L_{2phase}/Rp=5.8\pm0.6$ which was Rp independent. Since deformed membrane elements at the pipette entrance have a maximal (1) skeletal density; (2) skeletal azimuthal compression and (3) skeletal axial dilatation, it is plausible that the second phase of deformation be explained by a discontinuity in one or both of the azimuthal compression or axial dilatation of the skeleton. To obtain some insights into the mechanism(s) we calculate the principle stretch ratios from experimental density profiles. This shows that the second phase of deformation is accompanied by a discontinuity in the slope of the axial (dilatation) stretch ratio with almost no change in the azimuthal (compressive) stretch ratio. The analysis indicates that in the first phase of the deformation, skeletal elements at the pipette entrance reach a maximum limiting axial stretch which is then abruptly exceeded in the second deformation phase. This could result if molecular skeletal components are maximally stretched (first phase) and then fail (second phase). These data reinforce the complexities of membrane skeletal reorganization during micropipette aspiration and raise interesting issues regarding the behaviour of complex networks during mechanical deformation.

Tu-Pos341

BAND 3 PLAYS A CRITICAL ROLE IN RED CELL MEMBRANE STABILITY BUT IS NOT REQUIRED FOR MEMBRANE-SKELETAL ASSEMBLY. ((**Gimm J.A.**, Knowles D.W., Peters L.L., Lux S.E., Mohandas N.)) UCSF/UCB Bioengineering Graduate Group, Berkeley, CA. Lawrence Berkeley National Lab., University of California, Berkeley, CA. The Jackson Laboratory, Bar Harbor, ME. Harvard Medical School, Boston, MA.

Band 3 is a major red blood cell transmembrane protein which links the lipid bilayer to the underlying membrane-skeleton and plays a crucial role in regulating red cell membrane mechanical properties. Direct evidence for structural function of Band 3 can be seen in Southeast Asian ovalocytosis (SAO) red cells which have a mutant Band 3 and in Band 3/Glycophorin A cooperative interactions induced by anti-GlyA ligands in normal cells. In both cases, there is an increased interaction of the cytoplasmic domain of Band 3 with the membrane-skeleton which results in a marked increase in membrane rigidity. Recent development of mice with inactivation of Band 3 gene by homologous recombination has enabled generation of red cells with either partial (heterozygote) or complete (homozygote) deficiency of Band 3. These red cells enable us to establish the importance of Band 3 in regulating red cell membrane mechanical properties. The techniques of Fluorescence-Imaged Microdeformation (FIMD) and micropipette aspiration of individual red cells were used to evaluate Band 3 membrane-skeletal association in red cells from normal and heterozygote Band 3 mice and the membrane elastic rigidity of red cells from normal, heterozygote and homozygote mice. The FIMD experiments showed that an increased fraction of Band 3 interacts with spectrin based membrane-skeleton in red cells from heterozygote mice compared to normal mouse red blood cells. Elastic shear rigidity measurements showed that the homozygote red cells exhibit a near normal (~ 65%) elastic response during loading phase and small plastic response during unloading phase. Since spectrin-based membrane-skeleton is the dominant determinant of shear rigidity, this finding implies appropriate assembly of membrane-skeleton in red cells with complete deficiency in Band 3. However, the assembled membrane-skeleton appears to be weakly linked since small aspiration pressures used during the mechanical measurement were often enough to cause membrane fragmentation. These data imply that the interaction of Band 3 with the membrane-skeleton plays a critical functional role in membrane stabilization but is not essential for membrane-skeletal assembly.

Tu-Pos342

DOES α-TOCOPHEROL PARTICIPATE IN TRANSBILAYER ELECTRON TRANSFER FROM INTRACELLULAR ASCORBATE TO EXTRACELLULAR OXIDIZING AGENTS IN INTACT HUMAN ERYTHROCYTES? ((**C.E. Cobb**, Z-c. Qu, and J.M. May)) Dept. of Molecular Physiology & Biophysics, Vanderbilt University, Nashville, TN 37232.

The intracellular compartment of erythrocytes has multiple lines of defense against attack by water soluble oxidants, including protection via enzymatic (catalase, glutathione peroxidase, SOD) mechanisms and low molecular weight antioxidants (ascorbate, GSH). The erythrocyte membrane contains lipophilic low molecular weight antioxidants; the major one being α-tocopherol (α-toco), which are essential for preventing lipid peroxidation. We have previously shown that intracellular ascorbate is directly involved in reduction of the extracellular oxidant ferricyanide (FC) by a one-electron transfer mechanism since a monoascorbyl free radical (AFR) was formed (as detected by EPR spectroscopy; May, Qu, Whitesell, & Cobb, ***Free Radical Biology & Medicine, 20***, 543, 1996). However, the precise mechanism and participants in this net transfer of electrons from intracellular ascorbate to extracellular ferricyanide were not addressed. One potential mediator located in the erythrocyte membrane is α-toco; i.e., α-toco transfers an electron to extracellular FC and receives an electron from intracellular ascorbate. We have performed experiments with intact erythrocytes which have had their endogenous α-toco levels supplemented *in vitro* by incubation of washed cells with a α-toco emulsion; this procedure resulted in cells with an approximate 10-fold elevation in membrane α-toco concentration. Upon mixing of these α-toco supplemented erythrocytes with FC, FC reduction was increased ~ 20 % and an increase in the level of AFR as measured by EPR spectroscopy was observed as compared to control cells. This finding is consistent with the mechanism proposed above for transfer of electrons from intracellular to extracellular locations. Therefore, one role for erythrocytic intracellular ascorbate may be to protect against lipid peroxidation indirectly by maintaining lipid α-toco levels. Further studies are underway to conclusively define the relationship between these two antioxidant vitamins in erythrocytes. Supported by NIH Grants DK 50435, RR 04075, and HL 34737.

Tu-Pos343

THE FACILITATED AND NON-FACILITATED MEMBRANE TRANSPORT OF D- AND L-2'-FLUORO-5-METHYL ARBINOFURANOSYLURACIL IN HUMAN ERYTHROCYTES: A ^{19}F NMR STUDY. ((**Arron S.L. Xu**[†], Chung K. Chu[†] and Robert E. London[‡])).[‡] Laboratory of Structural Biology, National Institute Environmental Health Sciences, P.O. Box 12233, Research Triangle Park, NC 27709-2233. [†]Department of Medicinal Chemistry, College of Pharmacy, University of Georgia, Athens, GA 30602.

2'-Fluoro-5-methyl-β-L-arabinofuranosyluracil (L-FMAU) has potent anti-Hepatitis B and Epstein-Barr virus activities (Chu et al.1995. Antimicrob. Agents Chemother. 39: 979-981). In suspensions of human erythrocytes L-FMAU and its D-enantiomer both showed well-resolved ^{19}F NMR resonances arising from the respective nucleoside populations in the intra- and extracellular spaces. This phenomenon allowed their transmembrane distribution to be monitored by ^{19}F NMR. D- and L-FMAU transport readily across the membranes of human erythrocytes by facilitated and non-facilitated pathways. Although the transport of FMAU was significantly inhibited (60-70 %) by nitrobenzylthioinosine (NBTI) and dipyridamole, these inhibitors did not achieve complete blockage of FMAU uptake under conditions that are sufficient to completely inhibit the nucleoside transporter. FMAU transport was neither affected by inhibition of the nucleobase transporter nor by simultaneous uracil transport. Furthermore, the NBTI-insensitive transport did not show evidence of a saturability. The transport measured in the presence of maximal NBTI inhibition was found to be sensitive to the alteration of membrane permeability by butanol. The significant (30-40 %) contribution of non-facilitated membrane diffusion to the transport of FMAU is consistent with the large partition coefficients determined in octanol/PBS system. The enantiomeric preference of the nucleoside transporter for D- and L-FMAU is also discussed.

Tu-Pos344

INTERACTION OF THE CARBOXYL-TERMINUS OF HUMAN BAND 3 WITH RED CELL PROTEINS. ((**John W. Vince**, Jeremy M. Grushcow and Reinhart A. F. Reithmeier)) MRC Group in Membrane Biology, Department of Medicine and Department of Biochemistry, University of Toronto, Toronto, Ontario, Canada, M5S 1A8.

The interaction of the cytosolic carboxyl-terminus (Ct) of human Band 3, the erythrocyte anion exchanger, with red cell proteins was examined. A GST-fusion protein containing the 30 amino acid, highly acidic, Ct domain was produced in *E. coli*. Various red cell protein fractions (ghost membranes, hemolysate, etc.) were separated by SDS gel electrophoresis and transferred to nitrocellulose. The transfers were probed with the purified fusion protein which bound to several protein bands. One of these red cell proteins was putatively determined to be carbonic anhydrase by its electrophoretic mobility. Far Western blotting showed that the GST-fusion protein bound to purified carbonic anhydrase. Antibody binding showed that a fraction of carbonic anhydrase remained associated with the red blood cell membrane following extensive washing and that this fraction could be solubilized along with Band 3 by detergent. The effect of membranes, purified Band 3 and the Ct fusion protein on the activity of carbonic anhydrase was determined. The binding of carbonic anhydrase to Band 3 may increase the efficiency of CO_2 removal from the red cell by tethering the supplier of bicarbonate, carbonic anhydrase, to the chloride/bicarbonate exchanger, Band 3. (Supported by the Medical Research Council of Canada).

Tu-Pos345

PHOSPHOLIPID COMPOSITION OF THE RED CELL MEMBRANE IS SURPRISINGLY WELL PREDICTED BY THE LIPID HEAD-GROUP SUPERLATTICE MODEL.

((J. A. Virtanen[§], K. H. Cheng[#], **P. Somerharju**[*])) [§]Department of Chemistry, UCI, [#]Dept. of Physics, Texas Tech University and [*]Institute of Biomedicine, University of Helsinki, Finland (Sponsored by Josef Eisinger).

The erythrocyte membrane phospholipid composition is remarkably stable despite a continuous exchange of phospholipids with serum lipoproteins having a very different composition. The reasons for such compositional stability of the erythrocyte membrane are not clear. We report here that the phospholipid composition of the human erythrocyte membrane, as a whole as well as at the level of the individual leaflets, is remarkably well predicted by a model assuming that phospholipid head-groups *tend* to adopt regular, superlattice-like lateral distribution. Also the phospholipid compositions of the erythrocyte membrane from other mammalian species agree closely with the values predicted with such head-group superlattice model, as do those of the human and pig platelet plasma membranes. Statistical calculations show that the similarity of the observed and predicted compositions is highly significant thus strongly supporting the model. Furthermore, theoretical considerations indicate that formation of phospholipid head-group superlattices is feasible even in the presence of integral proteins and glycolipids in the membrane. Finally, it is suggested that lipid superlattices may universally involved in the regulation of membrane compositions as well as other important functions like membrane traffic and cell-cell interactions.

Tu-Pos346

DETERMINATION OF TOPOLOGY AND PORE-LINING RESIDUES IN THE TRANSMEMBRANE SEGMENT 8 REGION OF AE1, THE HUMAN ERYTHROCYTE ANION EXCHANGE PROTEIN ((**J.R. Casey**. X.-B. Tang and R.R. Kopito*)) Department of Physiology, University of Alberta, Edmonton, Canada T6G 2H7 and *Department of Biological Sciences, Stanford University, Stanford, CA 94305.

AE1 protein transports Cl^- and HCO_3^- across the erythrocyte membrane, by an electroneutral exchange mechanism. Glu681 is essential for Cl^- transport and can be accessed from either side of the membrane, suggesting that it is located at the permeability barrier. We have focused on the region surrounding Glu681 to identify other residues of the anion translocation pathway. Previously we showed that a cysteineless mutant of AE1, called AE1C$^-$, is fully functional. To map the anion translocation pathway, we have individually replaced each residue of the Ser643 (adjacent to the glycosylation site) to Ser690 region of AE1C$^-$ with cysteine. Mutant AE1 molecules were expressed by transient transfection of HEK293 cells. The effect of cysteine- introduction was assessed by measuring anion exchange activity in transfected whole cells. The anion translocation pathway was mapped by measuring the inhibition of anion exchange after covalently labelling with the small hydrophillic compound, (2-aminoethyl) methanthiosulfonate hydrobromide (MTSEA). Topology of the region was determined by comparing cysteine labelling with the membrane-permeant cysteine-directed reagent biotin maleimide, with or without prior labelling with membrane-impermeant stilbene maleimide. Our results indicate that the current topology model for AE1 is not accurate since labelling with MTSEA at position 651, predicted to be in an extramembranous loop, results in inhibition of anion exchange. Labelling with biotin maleimide indicates two regions that are readily-labelled with biotin maleimide separated by a region that is poorly labelled. The poorly-labelled region may correspond to the transmembrane region.

Tu-Pos347

TOPOLOGY STUDIES OF THE MEMBRANE DOMAIN OF THE HUMAN ERYTHROCYTE ANION EXCHANGER, AE1 ((**J. Fujinaga** & J. R. Casey)). Department of Physiology, University of Alberta, Edmonton, AB, Canada.

The erythrocyte anion exchange protein (AE1), also called band 3, facilitates the electroneutral transport of Cl^- and HCO_3^- across the plasma membrane. AE1 spans the membrane twelve to fourteen times. The topology of the first half of the membrane domain of AE1 is well defined, but the topology of the second half is much less clear. Therefore our goal is to better define the topology of the last half of the membrane domain of human AE1. To this end, all five cysteine codons of human AE1 were replaced with serine codons. Mutants, each with a single introduced cysteine codon, were constructed in this cysteineless background. Sulfhydryl-directed methodologies can be applied to these mutants. The anion transport activity of the mutant proteins was measured to ensure their structures were native. Anion exchange activity was monitored in HEK293 cells transiently transfected with the mutated cDNA, by following the fluorescence of the pH-sensitive dye BCECF-AM. Mutants retained 80 to 100% of the activity of cysteineless AE1. The intra or extra-cellular location of the cysteine residues was determined by incubating transfected cells with the sulfhydryl-directed compound biotin maleimide, either with or without preincubation with membrane-impermeant stilbene maleimide. Biotinylated AE1 was detected after immunoprecipitation with anti-AE1 antibodies. Our results confirm the topology of the first half of the protein. Similarly, Tyr904 is cytosolic, in agreement with the established cytosolic location of the C-terminal fourteen amino acids of AE1. In contrast, we found that the residue 745 was extracellular, in contradiction to most current models, which place the residue inside the cell. We propose a new model for the membrane domain of human AE1, which differs significantly from current models for trans-membrane segments 9 - 12.

Tu-Pos348

Measurement of External Cl^- Affinity of Band 3 and Determination of Transport Site Asymmetry at 0°C. ((D. Liu, P. A. Knauf, and S. D. Kennedy)) Dept. of Biochemistry and Biophysics, Univ. of Rochester, Rochester, NY 14642.

Flux measurements indicate that a far greater number of unloaded band 3 anion transport sites face the cytoplasm than face the external medium, but the reason for this striking asymmetry has remained obscure. To resolve this question, we have measured the apparent transport site Cl^- affinity of the human red blood cell band 3 protein under various conditions by analyzing the ^{35}Cl NMR free induction decay (FID). The $[Cl^-]$ that half-saturates the transport sites with $[Cl_i] = [Cl_o]$ ($K_{1/2}$) in RBC membranes (ghosts) is 46±5 mM at 0°C, while the $K^\circ_{1/2}$ (for half-saturation with $[Cl_o]$ at constant $[Cl_i]$) of intact cells is 3.2±2.1 mM. When cells were pretreated with eosin-5-maleimide (EM), an inhibitor of band 3 anion exchange that does not prevent external Cl^- from binding to the transport site, the $K_{1/2}$ and $K^\circ_{1/2}$ are 41±14 and 46±12 mM, respectively. The EM-induced increase in $K^\circ_{1/2}$ with little change in $K_{1/2}$ can be most simply explained if EM "fixes" the orientation of the transport sites so that $K^\circ_{1/2}$ and $K_{1/2}$ now both reflect the true dissociation constant, K_o, for binding of Cl^- to the external transport site. The fact that K_o for a slowly-transported anion, iodide, is nearly the same in EM-treated as in control cells indicates that EM does not significantly affect K_o. Our K_o measurements indicate that the true dissociation constants for Cl^- at the inside and outside are very similar, but that the rate constant for inward translocation is much larger than for outward translocation. For this reason, both unloaded and Cl-loaded transport sites are asymmetrically oriented toward the inside, and $K^\circ_{1/2}$ (in untreated cells) is much lower than K_o. (Supported by NIH (NIDDK) grant DK27495.)

Tu-Pos349

GENERAL MEMBRANE MECHANISMS OF ERYTHROCYTE HEMOLYSIS BY AMPHIPHILES.
((**Gregory V. Kaler** and Irina V. Yamaikina)) Institute of Photobiology, Belarus Acad. Sci., Minsk 220072, Belarus

The time course of isotonic hemolysis by a number of amphiphiles (detergents) varying in charge of polar group and critical micelle concentration (CMC) was studied. Under variations of experimental conditions (temperature, composition of the medium, concentrations of amphiphile and cells) the detergents were capable of inducing hemolysis with both mono- and bi-phase kinetics. The 1st phase starts without a lag-period and as a rule stops before completing the lysis, the 2nd phase has a distinctive lag-period and exponential hemolysis kinetics and always reaches 100% lysis. At low amphiphile concentrations hemolysis proceeds entirely by the 2nd phase mechanism. The kinetic parameters of the two phases were differently dependent on temperature and presence of non-permeating osmolyte in the medium. 1st phase appeared to be colloid osmotic in its mechanism, the osmotic component being less involved in 2nd phase. A general two-stage mechanism of amphiphile-membrane interaction is proposed. During the former stage, amphiphile bound initially on the outer surface of the cell membrane equilibrates across the membrane. If the amount of amphiphile bound per cell is sufficiently high, 1st phase hemolysis takes place in the beginning of this stage, with the rate decreasing sharply in the course of transmembrane equilibration. After reaching equilibrium distribution of detergent within membrane, the hemolysis proceeds slowly by the 2nd phase mechanism.

Tu-Pos350

INTERACTIONS OF N-TERMINAL α-SPECTRIN PEPTIDES WITH THE β-SPECTRIN SUBUNIT ((**Lisa Cherry**, Nick Menhart, L. W.-M. Fung)) Department of Chemistry, Loyola University of Chicago, Chicago, IL, 60626

Spectrin α and β subunits consist of repetitive, homologous sequence motifs of approximately 106 amino acid residues. These α and β subunits assemble in an antiparallel, side-to-side orientation to form heterodimers. Two heterodimers assemble in a head-to-head orientation to form a tetramer, the predominant form on the erythrocyte membrane. The head-to-head interaction involves the association of the N-terminus of the α-subunit with the C-terminus of the β-subunit. The precise binding sites and properties in the head-to-head association are not well understood, yet many hereditary hemolytic anemias involve deficient tetramer formation due to mutations in spectrin.

We have radiolabeled various recombinant α-spectrin fragments to study the binding affinity of these N-terminal fragments of various lengths with intact β-spectrin subunit bound to mirotiter plates. Peptides with sequences corresponding to 1-156, 1-262, and 1-368 residues in α-spectrin bound to the β-spectrin subunit. However, peptides with sequences corresponding to 52-156, 52-262, or 52-368 did not bind to the β-spectrin subunit. Equilibrium association constants of these systems at 4 °C in 10 mM Tris buffer with 20 mM NaCl, 130 mM KCl, and 1 mM β-mercaptoethanol at pH 7.4 were obtained to determine structural effects on α–β association. K_a of approximately 10^6 M^{-1} was measured for the 1-368 peptide, with similar values for the other 1-x peptides.

Tu-Pos351

DEVELOPMENT OF A NEW BINDING ASSAY FOR STUDIES OF SPECTRIN TETRAMER ASSOSIATION.(**Senthil Ranganathan**, Nick Menhart, Leslie. W.-M. Fung, Dept. of Chemistry, Loyola University Chicago, 6525 N.Sheridan road, Chicago, IL-60626)

The α–spectrin contains a number of homologous sequence motifs of approximately 106-amino-acid-residues that are folded into triple helical bundles. The N-terminus of the α–spectrin contains a fractional motif responsible for tetramer formation, by binding to a complimentary fractional motif at the C-terminus of the β-spectrin. To study the binding of α N-terminus with β C-terminus, we developed a binding assay in yeast that does not require the purification of α and β subunits or peptides.. Fragments of α- and β-spectrin were cloned into yeast expression vectors. The expression of pGAD-f provided the activation domain of the β-galactosidase transcription factor,GAL4, while the expression of pGBD-f provided the binding domain of GAL4. These two fragments are each not functional in themselves, or in combination *in-vivo*,since they cannot form an intact transcription factor. However, when these fragments are expressed as fusion proteins with two other proteins that assosiate, a functional GAL4 transcription activat or may be reconstituted. Their expression in yeast was coupled to the regulation of β-galactosidase. When the α-spectrin fragments containing the first fractional motif (α-spectrin peptide) binds to the corresponding β-spectrin fractional motif (β-spectrin peptide), the activation and binding domains are brought together to form a functional β-galactosidase transcription factor that initiates the transcription of the lac Z gene and produces β-galactosidase. Protein interaction was quantitated spectrophotometrically by an assay for the activity of β-galactosidase,using *o*-nitro-phenyl-β-D-galactopyranoside. The inhibition of histidine synthesis by 3-aminotriazole in the yeast strain HF7c was also used as a means to quantitate gene expression and so the α-β interaction. It provides quantitative information on α-β spectrin association, *in vivo*.

Tu-Pos352

AMIDE MODES OF THE α HELIX: RAMAN SPECTROSCOPY OF *Ff* FILAMENTOUS VIRUS CONTAINING ^{13}C- AND ^{2}H-LABELLED PEPTIDE GROUPS. ((**Stacy A. Overman** and George J. Thomas, Jr.)) School of Biological Sciences, University of Missouri, Kansas City, MO 64110.

The *Ff* filamentous virus, which is sheathed by ≈2700 copies of a 50-residue α-helical subunit (pVIII), represents a stable assembly of α-helical protein subunits. Isotopic substitutions in pVIII have been employed to advance amide band assignments for the α-helix and to facilitate structural interpretations of the *Ff* Raman spectrum. ^{13}C has been introduced into main chain carbonyl groups of 37 pVIII residues by growth of *Ff* in media containing ^{13}C-labelled amino acids. Also, ^{2}H (D) has been substituted for virtually all peptide NH groups by prolonged exchange of *Ff* in D_2O solution at elevated temperatures. The results indicate two, heretofore unrecognized, Raman amide bands of the α-helical pVIII subunit: (1) an amide III mode at 1340 cm^{-1}, and (2) an amide IV mode at 741 cm^{-1}. Amide modes of the isotopically labelled viruses have also been assigned. Notable is the multicomponent amide I″ band of ^{13}C-labelled *Ff*, which presumably reflects decoupling of the extensive transition-dipole interactions normally present in the unlabelled 50-residue pVIII α-helix. Examination of the temperature and time dependencies of NH → ND exchange dynamics reveals that *Ff* coat subunits contain several classes of exchange-protected peptide groups. [Supported by NIH Grant GM50776.]

Tu-Pos353

CONFORMATION AND INTERACTIONS OF THE PACKAGED ssDNA GENOME OF Pf1 VIRUS PROBED BY ULTRAVIOLET RESONANCE RAMAN SPECTROSCOPY ((**Zai Qing Wen** and George J. Thomas, Jr.,)) Division of Cell Biology and Biophysics, School of Biological Sciences, University of Missouri, Kansas City, MO 64110.

The filamentous bacteriophage *Pf1* contains a ssDNA genome of 7349 nucleotides, which comprises only 6% of the total virion mass. Accordingly, with conventional fiber diffraction and solution spectroscopic methods, it has proven difficult to obtain information about the structure of the packaged ssDNA molecule and its interactions with the viral coat protein. We have employed ultraviolet resonance Raman (UVRR) spectroscopy with 257-nm excitation to probe selectively the DNA bases of the packaged *Pf1* genome. UVRR spectra of high quality have been obtained and interpreted. Raman intensities (scattering cross sections) of packaged *Pf1* DNA are dramatically greater than those of unpackaged ssDNA and dsDNA molecules. The results indicate a minimally stacked arrangement of the bases. A diagnostic Raman marker band at 682 cm^{-1} shows, nevertheless, a strong preference for C2′-*endo/anti* nucleoside conformations. Extraordinary Raman markers are revealed for the carbonyl groups of dT and dC, implying unusual interactions with hydrogen-bond donor groups of the virion. UVRR spectra excited at 244, 238 and 229 nm provide complementary information on the coat protein tyrosine residues. Implications for the organization of ssDNA and coat protein subunits in the virion will be discussed. [Supported by NIH grant GM50776.]

Tu-Pos354

STRUCTURE-FUNCTION CORRELATIONS IN PROTEASOME-PA700 COMPLEXES ((**George Adams**[1], George DeMartino[2], Clive Slaughter[3], Alfred Goldberg[4], Edward Gogol[1])) [1]Division of Cell Biology and Biophysics, University of Missouri-Kansas City, Departments of [2]Physiology and [3]Biochemistry, University of Texas Southwestern Medical Center, Dallas TX, [4]Department of Cell Biology, Harvard Medical School, Boston, MA.

The eukaryotic 20S proteasome serves as the focal point in the degradation of cytosolic proteins. The cylindrical 20S core protein is structurally and catalytically modified by interaction with macromolecular regulatory complexes. We have shown that one of these, PA700, forms a capped structure on the 20S proteasome that closely resembles the 26S proteasome. PA700 increases the peptidase activity of the proteasome and broadens the range of substrates to include ubiquitinated proteins. Electron microscopy and a fluorescence-based peptidase assay were used to correlate appearance of capped proteasomes with proteolytic activity. The peptidase activity of proteasome-PA700 mixtures is further increased by addition of a modulator protein complex. An increase in the number of capped proteasomes was observed in the presence of modulator protein, without visible modification of the structures. The proportion of capped proteasomes in the presence of modulator also correlates with increased activity. These observations indicate that the modulator protein promotes formation of capped proteasomes, paralleling enhanced proteolysis.

Tu-Pos355

CHARACTERIZATION OF FACTOR XIII-γA/γ′ FIBRINOGEN COMPLEXES. ((D.H. Farrell, **M.G. Fried** and L.A. Falls)) Department of Biochemistry and Molecular Biology, Penn. State University College of Medicine, Hershey, PA 17033. (Sponsor: K. Lanoue)

About 10% of human plasma fibrinogen is present as a heterodimer of composition (αβγ′)(αβγA). The two different types of γ chains, the γA chain and the γ′ chain, are a consequence of alternative mRNA processing. The γ′ chain contains a 20-amino acid extension at the C-terminus that replaces a 4-residue sequence in the γA chain. Siebenlist and Mosesson (*Blood Coag. Fibrinol.* 4: 833 (1993)) have shown that the γ′ chain, but not the γA chain, binds to the b subunit of factor XIII. Our results show that fibrin clots are resistant to fibrinolysis, but only if factor XIII is present during clotting. This suggests that the binding of factor XIII to γ′ chains stabilizes clots, possibly by concentrating the factor XIII at the surface of the growing fibrin matrix. We have therefore investigated the binding interactions of factor XIII and γ′ fibrinogen. Sedimentation equilibrium analysis indicates that 2 γA/γ′ fibrinogen molecules can bind to each molecule of factor XIII, but that fibrinogen containing only γA does not form detectable complexes. These results suggest the involvement of the C-terminal extension of the γ′ chain. Garnier-Robson analysis predicts that the C-terminal 20 residues fold into an α-helix; helical wheel projections of this structure indicate that seven negatively-charged residues, including two tyrosine O-sulfates are clustered on one face of the helix. We propose that these residues mediate the interaction of γ′ fibrinogen with factor XIII. Supported by funds from the American Heart Association, Pennsylvania Affiliate.

Tu-Pos356

ANALYSIS OF PRECRYSTALLIZATION AGGREGATION IN PROTEIN SOLUTIONS DURING CENTRIFUGATION. ((**J. Behlke** and A. Knespel)) Max Delbrück Center for Molecular Medicine, D-13122 Berlin, Germany.

Determination of the three-dimensional structure of proteins using X-ray diffraction requires well-ordered single crystals of about 0.3 mm in the length. Although methods for protein crystallization have been studied intensively under different conditions, not every experiment is successful. Whether proteins are able to form crystals from supersaturated solutions by addition of precipitants, changing of solvent conditions or temperature can be seen in few cases within several days or normally after weeks. For monitoring protein crystallization conditions we have carried sedimentation velocity runs on supersaturated solutions of lysozyme or papain to analyze the nucleation process as a prerequisite for crystal growth. The method is based on the estimation of oligomers from sedimentation patterns, the calculation of equilibrium constants for the different steps of association and the calculation of the free energy involved in such processes. The transition from the state of unfavorable free energy that is necessary for the formation of smaller oligomers to that of free energy released systems ensues in assemblies of fifhteen to twenty molecules for both proteins. We believe this method will promote greater understanding of the events during the crystallization and of conditions under which early crystal growth is to be expected. The observation of nuclei in about one hour allows this method to be used for early recognition of crystal growth.

Tu-Pos357

HIGH SYMMETRY IS AN ATTRACTOR

((**Christopher Marzec**)) Inst. for Biomolecular Stereodymamics, SUNY-Albany

There is no theory underlying the morphogenesis of the high symmetry found in disparate biological systems. The work reported here takes a step in that direction.

We treat the dynamics of structures made of interacting morphological units (MUs) either constrained to lie on a sphere or moving freely in 3-space; each has position and orientation coordinates. An MU is an arbitrarily shaped three-dimensional object; MUs interact pairwise, via a non-specific isotropic function of distance, with total mutual interaction $\mathcal{I}$. MU structure, interaction function, and $\mathcal{I}$ are all rendered in Fourier space. MUs move via gradient dynamics, minimizing $\mathcal{I}$: eg., $\frac{d}{dt}\vec{r}_j = -K\vec{\nabla}_j\mathcal{I}$, for the j'th MU. The set of coordinates of all the MUs of a structure determine an evolving point P in a high dimension morphological space.

Define a "warping" P_W of P_S, a high-symmetry local minimum of $\mathcal{I}$: each MU undergoes possibly *large* translations and rotations resulting from accrued *small* (first order) local variations in nearest-neighbor relationships (like a very distorted net). We show analytically that the change in $\mathcal{I}$ is second order and positive; so gradient dynamics restores the high symmetry. We find numerically that evolution to a warped structure from a random initial configuration can occur quickly; subsequent evolution to high-symmetry P_S, undoing the warping, is slow. Thus, **high symmetry itself is an attractor with a large basin**: $P_{initial} \xrightarrow{fast} P_W \xrightarrow{slow} P_S$.

The theory allows P_S *any* high symmetry consistent with the number N of MUs and their individual symmetries; ie., A T=7 icosahedral capsid needs 72 pentameric capsomere MUs; but N MUs in a finite helical structure need have no symmetry. Non-Platonic and non-helical symmetries are also consistent with the formalism.

Tu-Pos358

DIRECT DETERMINATION OF MEMBRANE PROTEIN STRUCTURES IN PROJECTION - THE PSEUDO-ATOM METHOD ((**Douglas L. Dorset**)) Hauptman-Woodward MRI, Inc., Buffalo, NY, 14203.

In 1953, David Harker proposed that the FT of 'glob' units in proteins would provide a more accurate normalization of observed intensities than the atomic scattering factors themselves, particularly for low resolutions. If the low resolution data (to e. g. 6 Å) are re-scaled ten-fold, then any Gaussian-like function (e. g. an atom scattering factor) might well serve as a good approximation of this glob transform so that the direct phase determination would reduce to a small molecule problem. The correctness of this premise has been demonstrated via centrosymmetric data from halorhodopsin (plane group p4gm), where an accurate phase set (20° deviation for 45 largest |F| in set of 101 reflections) was found by symbolic addition. For non-centrosymmetric data sets, a multi-solution technique is required. The Sayre equation applied to data from native bacteriorhodopsin, deoxycholate-treated bacteriorhodopsin (plane group p3 for both) and Omp F porin from E. coli (plane group p31m) again provides accurate phase sets by this approach. These results are a great improvement over earlier direct phasing attempts involving phase extension and annealing, comparing well with extensions of image-derived phases . (Supported by NIGMS GM-46733)

Tu-Pos359

FIBER DIFFRACTION STUDIES OF THE COLUMNAR CRYSTALLINE PHASE OF TMV ((**A. George**[1], D.L.D. Caspar[1], D.H. Van Winkle[2])) [1]Institute of Molecular Biophysics, [2] Dept. of Physics and Martech, Florida State University, Tallahassee, FL-32306. (Spon. D.L.D. Caspar)

Colloidal solutions of Tobacco Mosaic Virus (TMV), a rigid rod-like particle, exhibits several ordered liquid crystalline phases. With increasing virus concentration isotropic, nematic, smectic and hexagonal-columnar liquid crystalline phases are observed. Oriented TMV fibers of columnar crystalline ordering were prepared by dehydrating droplets of solution between two glass rods over several days in a controlled humidity environment while placed in a 5.8 Tesla magnetic field. The equatorial diffraction pattern of the columnar crystalline phase showed several strong reflections at small angles. The x-ray diffraction camera used for these studies produced an order to order resolution of 2500 A. The columnar crystalline specimens at a relative humidity of 92% has a hexagonal lattice constant of 159 A and showed Bragg reflections out to a resolution of 20 A. The increase in the width of the equatorial reflections indicate a diverging autocorrelation function. Hydration of these specimens to increase the interparticle separation leads to a decrease in the coherence distance.

Tu-Pos360

DIFFRACTION ANALYSIS OF A NOVEL TETRAGONAL CRYSTAL FORM OF AMPHIBIAN M FERRITIN. ((**Y. Ha**[1], E.C. Theil[2] and N.M. Allewell[1])) [1]Department of Biochemistry, University of Minnesota, St. Paul, MN 55108, & [2]Department of Biochemistry, North Carolina State University, Raleigh, NC 27695.

The ferritins are a multigene family of proteins that are responsible for iron storage in all prokaryotic and eukaryotic cells. The gene products have different biochemical properties and gene expression varies with development and tissue type. All ferritins are made up of twenty four monomeric subunits which fold as four helix bundles and assemble to form a protein shell with 432 symmetry within which ~4000 iron ions are stored as ferric hydroxide. Amphibian M ferritin crystallizes in a novel tetragonal crystal form which has an unusual diffraction pattern with a complex pattern of missing reflections. We have shown by simulation that its unusual features are generated by the combined effects of the molecular symmetry and molecular packing. The unit cell dimensions and the space group have been shown to be a=b=169.6Å, c=481.2Å; $\alpha=\beta=\gamma=90^{o}$ and either $P4_12_12$ or $P4_32_12$. The two space groups can not be distinguished for this crystal form at moderate resolution. This is a general result for all 11 pairs of enantiomorphic space groups: the presence of non-crystallographic symmetry elements may make the space group determination ambiguous, even when the molecule that has been crystallized is chiral. Supported by NIH grant DK-50727.

Tu-Pos361

CRYSTALLOGRAPHIC AND SOLUTION STUDIES OF ANABOLIC E. COLI ORNITHINE TRANSCARBAMYLASE **((Lei Jin, Michael Rynkiewicz, Barbara Seaton, and James F. Head)) Structural Biology Group, Department of Physiology, Boston University School of Medicine, Boston, MA 02118.**

We have solved the crystal structure of E.coli ornithine transcarbamylase (OTCase) at 3.0Å and are refining it to 2.5Å. The space group is $P3_2$ (a=b=103.3Å, c=86.1Å, $\alpha=\beta=90°$, $\gamma=120°$), with a trimer in the asymmetric unit. This is the first crystal structure of an anabolic OTCase, which is homologous to the catalytic trimers of aspartate transcarbamylase (ATCase) and to mitochondrial OTCase, a urea cycle enzyme in mammals. The structure of the dodecameric catabolic OTCase from P. aeruginosa is the only other known OTCase structure. The E. coli OTCase structure was solved using a combination of molecular replacement (using B. subtilis ATCase as a model), single isomorphous replacement, and three-fold symmetry averaging. We describe herein the salient features of the structure and compare it with E. coli ATCase and with catabolic OTCase. We will also discuss specific features of the enzyme as they relate to enzymic function. E. coli OTCase participates in arginine biosynthesis by catalyzing the production of citrulline and phosphate from carbamyl phosphate and ornithine. We have also shown that the inactivity of the point mutant, R57G, can be partially reversed by "chemical rescue" with guanidine and guanidine derivatives. The significance of this "rescue" for the mechanism of action of the enzyme will be discussed.

Tu-Pos362

Structure and Energetics of Odorant Recognition by the Odorant Binding Protein

((G. **Bains**, M. A. Bianchet, P. Pelosi, H. L. Monaco and L. M. Amzel.)) Department of Biophysics and Biophysical Chemistry. The Johns Hopkins School of Medicine. Baltimore, MD 21205

Mammalian odorant binding proteins (OBPs) are homo- or hetero-dimeric proteins (monomer 19-22 kD) secreted into the nasal mucosa where they bind odorants with micromolar dissociation constants solublizing the odorants before their interaction with odorant receptors in the membrane. Over 50 different odorants are known to bind to OBP with broad specificity and a range of association constants (10^4 - 10^9 M^{-1}). Recently, we have solved the x-ray crystal structure of 2 different crystal forms of OBP at 2.2 Å resolution in complexes with different odorants. In both structures, odorant binds inside a large cavity in each monomer. The OBP structures reveal a unique feature thusfar unobserved in other lipocalins (RBP,BLG, and MUP) - that of domain swapping. While the overall topology of each monomer is that of a β- barrel with an associated α-helix, the α-helix of each monomer crosses over to associate with the β–barrel of the other monomer. Domain swapping is pH-sensitive with a pK_a of 4.5 - the monomer appearing structurally quite similar to the dimer by CD, although the monomer does not bind odorant.

Bovine OBP has been cloned and overexpressed in this lab and several key mutants have been designed to test the functional importance of specific residues in binding odorant and dimerization. Calorimetric studies of odorant binding to recombinant OBP reveal that the observed enthalpy of binding of 8 different odorants to OBP is between -7 and -15 kcal/mol, involves no protonation of residues, and is consistent with a single non-cooperative type of binding site. In all measured cases, the binding entropies are unfavorable.

Tu-Pos363

NMR STRUCTURAL CHARACTERIZATION OF THE BINDING OF PT523 AND NADPH IN THE TERNARY COMPLEX WITH HUMAN DIHYDROFOLATE REDUCTASE. ((**J.M. Johnson**, E.M. Meiering, J.E. Wright, J. Pardo, A. Rosowsky, and G. Wagner)) BCMP Dept., Harvard Medical School, Boston, MA 02115 (Spon. by J. Wang)

The antitumor drug PT523 [Nα-(4-amino-4-deoxypterol)-Nδ-hemiphthaloyl-L-ornithine] inhibits human dihydrofolate reductase (DHFR) with a 15-fold lower inhibition constant (Ki = 0.35 ± 0.10 pM) than the classical antifolate methotrexate (MTX). The bound structure of PT523 was investigated using multinuclear NMR techniques to assign resonance signals from the PT523-DHFR and PT523-DHFR-NADPH complexes. NMR evidence suggested that the binary complex has two distinct conformations in solution, and that addition of NADPH stabilizes the ternary complex in a single conformation. Comparison of resonance assignments in the PT523 and MTX ternary complexes revealed that chemical shift differences were strongly localized to distinct regions of DHFR tertiary structure. Thirty-three DHFR-ligand NOEs, six ligand intramolecular NOEs, and 150 protein-protein NOEs were volume-integrated to create distance constraints for a simulated annealing and energy minimization protocol, which generated 33 structures of the ternary complex. The positions of the pteridine and benzoyl rings of PT523 and the nicotinamide and ribose rings of NADPH are similar in the calculated structures (RMSD = 0.59 Å). Though the orientation of the Nδ-hemiphthaloyl-L-ornithine sidechain of PT523 is not as well defined, the phthaloyl ring appears to provide additional contacts not possible in the MTX-DHFR-NADPH complex, which may explain the greater binding affinity of PT523.

Tu-Pos364

HOW IS THE MONOMER/DIMER TRANSITION OF ENZYME I OF THE PHOSPHOTRANSFERASE SYSTEM INVOLVED IN REGULATION? A STUDY BY ENERGY TRANSFER.

((**F. CHAUVIN**, D. TOPTYGIN, S. ROSEMAN and L. BRAND))
Dept. of Biology, The Johns Hopkins Univ. Baltimore, MD 21218.

The E.coli phosphotransferase system (PTS) concomitantly translocates and phosphorylates sugar substrates such as glucose. Its activity is stringently regulated. How? Maybe by Enzyme I (EI), the first of the four proteins of the PTS and the only known point for phosphate entry. It undergoes a monomer/dimer (M/D) transition and only the dimer can be phosphorylated by PEP. The M/D interconversion is very slow (15 min at 23° C). Furthermore, ligand addition changes the equilibrium constant 240 fold.

It should be possible to obtain information about the monomer/dimer transition by resonance energy transfer. Wild type EI contains two tryptophan residues at positions 357 and 498. We have made three mutant forms, W357F, W498F and the double mutant. Pyrene has been conjugated at Cys-575 and energy transfer has been measured with tryptophan as the donor and pyrene as the acceptor. Energy transfer was observed with the W498F-pyrene conjugate. Efficiency of the transfer depends on the degree of dimerization. Energy transfer should provide a means for determining the M/D fraction as the PTS actively transports sugar. Supported by grant GM38759.

Tu-Pos365

FLUORESCENCE ENERGY TRANSFER IN BRADYKININS.

((**Amando Siuiti Ito**[a] and Luis Juliano[b])) [a]Instituto de Física USP, C.Postal 66318, São Paulo 05389-970, and [b]EPM UFSP, São Paulo, Brazil.

A series of hormone peptides derived from bradykinins were prepared having the fluorescent donor o-aminobenzoic acid (Abz) linked to the amino terminal and the acceptor group dinitrophenylethylenediamine (Eddnp) attached to the carboxyl terminal. The intensity of fluorescence from Abz decreases in the peptides due to energy transfer to the Eddnp group. The efficiency of transfer is dependent on the separation between donor and acceptor groups, and measurements of the intensity of the donor, both in absence as in the presence of the acceptor, would allow the determination of that distance. However, time-resolved fluorescence measurements showed that the decay profiles of the peptides were not homogeneous and it was not possible to fit them to a monoexponential curve. This is in agreement with the knowledge of bradykinins as flexible structures, and the resulting fluorescence should be coming from a distribution of distances instead of a single and fixed separation. The lifetime results are discussed within this assumption, allowing the estimation of a mean value for the separation between N- and C-terminals in the peptide. Comparison of the distances in different peptides gives information about a turn in the bradykinin structure, involving the central amino acids in the chain.

Acknowledgment: ASI thanks to CAPES-Brazil for financial support.

Tu-Pos366

RESONANCE ENERGY HOMOTRANSFER IN EOSIN-LABELED BAND 3 IN ERYTHROCYTE MEMBRANES DEMONSTRATED BY TIME-RESOLVED FLUORESCENCE AND CONFOCAL MICROSCOPY.

((**S.M. Blackman**, B.W. Van der Meer, D.W. Piston, & A.H. Beth)) Dept. of Molecular Physiology & Biophysics, Vanderbilt University, Nashville, TN, 37232.

Fluorescence resonance energy homotransfer, which occurs between identical "donor" and "acceptor" molecules, can measure distances between ~20 and 80 Å, an appropriate scale for studying protein structure and oligomerization. In particular, homotransfer is well suited to detect oligomerization in a multimeric protein with identical subunits, each labeled with the same single fluorophore. The erythrocyte anion transport protein, band 3, forms C_2-symmetric dimers, which may interact to form tetramers or higher-order oligomers. Each monomer of band 3 can be labeled at a single reaction site, Lys-430, with eosin-5-maleimide (EMA), which has been widely used in phosphorescence studies of band 3 rotational dynamics. Other studies have suggested that the inter-eosin distance is 20-60Å, which is within the range of detectable homotransfer given the calculated R_0 of 42Å. We previously used polarized fluorescence confocal microscopy to show that EMA adopts a specific orientation when bound to band 3. Time-resolved fluorescence anisotropy revealed a depolarization of ~3 ns correlation time, which is now shown to represent homotransfer. Erythrocyte ghost membranes labeled to different extents with EMA demonstrate a progressive decrease in the steady-state fluorescence anisotropy as adjacent EMA sites are populated. This trend is preserved by solubilization in $C_{12}E_8$, a nondenaturating detergent, and eliminated by SDS denaturation. Red edge excitation spectroscopy, which reduces the fraction of eosins able to undergo homotransfer, attenuates the anisotropy decrease. Time-resolved fluorescence studies demonstrate that the residual anisotropy, r_∞, depends strongly on labeling stoichiometry, while the fluorescence lifetime is unaffected. Collectively these results unambiguously demonstrate resonance energy homotransfer in EMA-labeled band 3. The effect of substoichiometric labeling on the effective fluorophore orientation (which is altered by homotransfer) should help determine the relative contributions of intra- and inter-dimer homotransfer. When more fully characterized, homotransfer will offer a new method of probing band 3 oligomeric state. Additional studies use fluorescein-5-maleimide, which labels the same 17K proteolytic fragment as EMA, has a defined orientation, and also exhibits homotransfer. *Supported by HL34737 and DK07563.*

Tu-Pos367

"GOLDEN RULER": VERY LONG-RANGE RESONANCE ENERGY TRANSFER TO SURFACE PLASMON ACCEPTORS.

((**W. J. Walczak**,* J. M. Xiao,* E. S. Kopetz,* K. Lease,* H. Grau,* S. P. Lee,# M. K. Han# and J. R. Knutson*)) *LCB/NHLBI, NIH, Bethesda, MD 20892, #Dept. of Biochemistry and Molecular Biology, Georgetown University Medical Center, Washington, DC 20007.

Fluorescence resonance energy transfer (RET) is a widely used technique in biochemistry. Unfortunately, the effective range of RET has been limited to under 80 A by the overlap integral between donor fluorophore emission and acceptor extinction profiles. Ro, the distance for half transfer, is proportional to the sixth root of this overlap. We have located acceptors with extinctions ~ 1000-fold greater than normal; namely, the surface plasmon absorption of colloidal gold (and other metals). This leads to predicted Ro > 150 A and useful ranges out to > 200 A. We are currently calibrating this "golden ruler" by attaching fluorescein and biotin at different sites in double stranded oligonucleotides, then quenching with gold-streptavidin and similar complexes. Significant quenching has already been seen across a 30-bp gap. We will discuss geometric linkage considerations and the elimination of artifacts due to incomplete complexes.

Tu-Pos368

LONG LIFETIME METAL-LIGAND PROBES FOR BIOPHYSICS

((Z. Murtaza, L. Li, F. N. Castellano, H. Szmacinski and **J.R. Lakowicz**))
Center for Fluorescence Spectroscopy, University of Maryland at Baltimore, Dept. of Biochem. & Molecular Biology, 108 N. Greene St., Baltimore, Maryland 21201.
(Spon. by M. L. Johnson)

Fluorescent probes display lifetimes dominantly in the range of 1-10 ns, which limits the dynamic information content to phenomena which occur on nanosecond time scale. Few methods are available which provide information on the time scale from 100 ns to μs. We have already developed a lipid probe which displays lifetimes near 500 ns. We are also developing a variety of water soluble and conjugatable metal-ligand complexes (MLC) for use as long lifetime luminescence probes. Complexes of rhenium and osmium were found to display a high quantum yield (~0.5), long lifetime (~5-100 μs) in aqueous solution and high fundamental anisotropy (>0.3). Our efforts are also to use MLC for sensing pH, oxygen, calcium, sodium and glucose in physiological samples and have successfully developed a pH sensor.

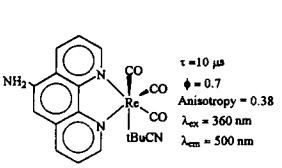

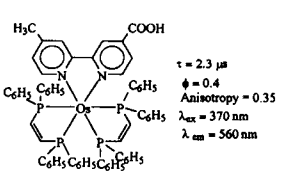

Tu-Pos369

Synthesis and Spectral Characterization of a Thiol-reactive Ru(II)-complex

((J.D. Dattelbaum, E. Terpetschnig, H. Szmacinski and J.R. Lakowicz))
Center for Fluorescence Spectroscopy, University of Maryland at Baltimore, Dept. of Biochem. & Molecular Biology, 108 N. Greene St., Baltimore, Maryland 21201.

Metal-ligand probes with microsecond decay times have numerous potential applications in the biophysical sciences. However, to date, only amine-reactive derviatives have been described. We report the synthesis and spectral properties of [Ru(II)bis(2,2'-bipyridyl)(1,10-phenanthroline-5-maleimide)]. The lifetime and anisotropy decays of this probe free and bound to reactive cysteines of human serum albumin (HSA) and IgG were measured using frequency domain fluorometry. The lifetime of this probe was found to be near 700 ns, which allows the hydrodynamic motions of larger molecular weight proteins to be determined.

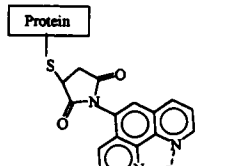

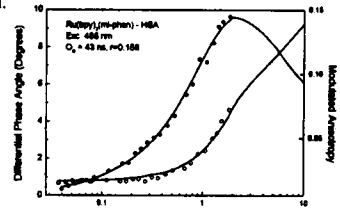

Tu-Pos370

APPLICATIONS OF NOVEL BROMINATED DETERGENTS TO THE STUDY OF LIPID-DETERGENT AND PROTEIN- OR PEPTIDE-DETERGENT INTERACTIONS. ((**B. de Foresta**, S. Soulié, P. Champeil and M. le Maire)) CEA and CNRS URA 2096, CE Saclay, F-91191 Gif-sur-Yvette Cedex France. (Spon. by M. le Maire)

We recently showed that the two brominated detergents 7,8-dibromododecyl-β-maltoside (BrDM) and 2-*O*-[10,11-dibromoundecanoyl]sucrose (BrUS) behave in many respects as satisfactory analogs of their parent detergents [B. de Foresta, N. Legros, D. Plusquellec, M. le Maire & P. Champeil, Eur. J. Biochem. (1996) in press]. Two of their applications for lipid- and protein-detergent interactions will be presented here: first, by stopped-flow experiments, we analyze the kinetics of the interaction of BrDM with sarcoplasmic reticulum (SR) membranes. The kinetics of SR Ca^{2+}-ATPase fluorescence quenching by BrDM, resulting from BrDM insertion into the membrane, exhibits a multiphasic behavior, which will be discussed in terms of rate of detergent partition into the membrane and flip-flop between the two bilayer leaflets. A second application is the assessment of Trp localization in solubilized complexes of protein or peptide and detergent, deduced from the extent of Trp fluorescence quenching in mixtures of brominated and non-brominated detergents. Examples will be given for Ca^{2+}-ATPase and derived peptides, and the results compared to those obtained with the model compound, tryptophan octyl ester.

Tu-Pos371

A HYBRIDIZATION PROBE CONTAINING A FLUORESCENT GUANOSINE ANALOG WITH INCREASED FLUORESCENCE INTENSITY UPON FORMATION OF A HAIRPIN.
((**M.E. Hawkins**, T.W. Schulte, and F.M. Balis)) NCI, NIH, Bethesda, MD

We developed a highly fluorescent pteridine nucleoside analog, 3-methyl isoxanthopterin, (3-MI, quantum yield, 0.88) which is formulated as a phosphoramidite and site-selectively inserted into an oligonucleotide using an automated DNA synthesizer. Fluorescence intensity of 3-MI within an oligonucleotide is quenched by neighboring bases, especially purines (presumably from base stacking) to quantum yields ranging from 0.04-0.30. Digestion of an oligonucleotide containing 3-MI with P1 nuclease results in a fluorescence intensity increase proportional to the difference between the quantum yield of 3-MI as a monomer and 3-MI in the oligonucleotide. We postulated that disruption of base stacking by forcing a one-base hairpin (consisting of 3-MI) would also result in an increase in fluorescence intensity. Hairpin formation, achieved by annealing complementary strands containing no base-pairing partner for 3-MI, yields an increase in fluorescence of up to 12-fold depending on the bases surrounding 3-MI. Melting temperature depression from the 3-MI hairpin is 1°C in an 18-mer. We are currently developing this technique for detection of PCR products.

Tu-Pos372

TRANSLATIONAL DIFFUSION OF MACROMOLECULE-SIZE SOLUTES IN CYTOPLASM AND NUCLEUS: EVIDENCE FOR DIFFUSION-RESTRICTING COMPARTMENTS WITHOUT SIEVING.
((**Olivier Seksek** and A.S. Verkman)) U.C.S.F. (Spon. by F. Szoka)

Fluorescence recovery after photobleaching (FRAP) was used to quantify the translational diffusion of microinjected FITC-dextrans (4-2000 kDa) in the cytoplasm and nucleus of MDCK epithelial cells and Swiss 3T3 fibroblasts. Absolute diffusion coefficients (D) were measured using a microsecond-resolution FRAP apparatus and solution standards. In aqueous media (viscosity 1 cP), D for the FITC-dextrans increased linearly from 1.5 to 45 x 10^{-7} cm^2/s with [molecular size]$^{-1/3}$. D in MDCK cells relative to that in water (D/D_o) was 0.26 ± 0.03 (cytoplasm) and 0.22 ± 0.02 (nucleus) and independent of FITC-dextran size. However, the fraction of mobile FITC-dextran molecules (f_{mob}) for spot photobleaching (20x objective lens) decreased progressively from 0.81 to 0.27 as dextran size increased from 4 to 2000 kDa. D/D_o for fibroblasts was 0.38 ± 0.04 (cytoplasm) and 0.40 ± 0.04 (nucleus) with f_{mob} values similar to those in MDCK cells. The independence of D/D_o on FITC-dextran size does not support the concept of solute 'sieving' in cytoplasm. To investigate the dependence of f_{mob} on dextran size, photobleaching measurements were carried out in concentrated dextran solutions, in swollen and shrunken cells, and using different bleach beam intensities and beam spot sizes. The data suggested that the low f_{mob} for the large FITC-dextrans was due to the presence of a diffusion-restricting compartment of characteristics dimensions of 1-2 μm. Smaller beam spot size did not change D/D_o, but increased f_{mob} for the 500 kDa FITC-dextran from 0.46 (4 μm diameter spot) to ~0.9 (0.8 μm). Our results indicate rapid diffusion of macromolecule-size solutes in cytoplasm and nucleus.

Tu-Pos373

PHOTOBLEACHING AND ANISOTROPY OF GREEN FLUORESCENT PROTEIN GFP-S65T IN SOLUTION AND CELLS: CYTOPLASMIC VISCOSITY PROBED BY GFP TRANSLATIONAL AND ROTATIONAL DIFFUSION. ((**R. Swaminathan**, C.P. Hoang and A.S. Verkman)). U.C.S.F.

The green fluorescent protein was used to non-invasively quantify the rheological properties of cell cytoplasm. Recombinant green fluorescent protein mutant S65T (GFP) was purified for solution studies, and expressed in CHO cell cytoplasm. Solution GFP was brightly fluorescent (λ_{ex} 490 nm, λ_{em} 508 nm) with lifetime 2.9 ns and rotational correlation time 20 ns. Exposure to a laser pulse (488 nm) gave irreversible photobleaching with efficiency ~2 fold less than that for fluorescein. In phosphate buffered saline, photobleaching recovery of GFP fluorescence was complete with a half-time ($t_{1/2}$) of 30 ± 2 ms (5 μm diameter spot). The $t_{1/2}$ was proportional to solution viscosity and dependent on spot diameter; in contrast to fluorescein, GFP photobleaching efficiency was not affected by solution O_2 content, triplet state quenchers (Mn^{++}, trp, MEA) or free radical scavengers (NaN_3, DABCO). In solutions of higher viscosity, an additional rapid GFP recovery process was detected and ascribed to reversible photobleaching. The $t_{1/2}$ for this process was 1.5-5.4 ms (relative viscosity 5-150), independent of spot diameter, and not affected by O_2 or triplet state quenchers. Time-resolved microscopy of GFP in cell cytoplasm indicated a lifetime of 2.6 ns and rotational correlation time of 36 ± 3 ns, corresponding to a relative viscosity of 1.8. Irreversible photobleaching of GFP in cytoplasm gave 82 ± 2% fluorescence recovery with a $t_{1/2}$ of 83 ± 6 ms (5 μm diameter spot), corresponding to a relative cytoplasmic viscosity of 2.8. The results define a reversible GFP photobleaching process and indicate 1.8-fold slowed GFP rotation and 2.8-fold translation in cytoplasm compared to aqueous solution.

Tu-Pos374

COMPETITION BETWEEN Li^+ AND Mg^{2+} IN HUMAN NEUROBLASTOMA SH-SY5Y CELLS ((Louis V. Amari, Joyce Nikolakopoulos, and Duarte Mota de Freitas)) Department of Chemistry, Loyola University Chicago, Chicago, IL 60626.

Lithium carbonate has been used in the treatment of manic depressive illness for a number of years. However the molecular mechanism of lithium action remains unknown. One hypothesis is that Li^+ competes with Mg^{2+} for Mg^{2+}-binding sites in biomolecules. Previous studies in our laboratory have shown that Li^+ competes with 10-20% of Mg^{2+}-binding sites on G proteins, the red blood cell (RBC) membrane, ATP, GTP and IP_3. Since manic depressive illness is a psychiatric disorder, a better model system than RBCs is the human neuroblastoma SH-SY5Y cell line, as the percentage composition of G proteins in SH-SY5Y cells is very similar to that in human brain cortex. If the lithium and magnesium competition mechanism is present in neuroblastoma cells, an increase in the total intracellular lithium concentration should result in an increase in the free intracellular magnesium concentration ($[Mg^{2+}]_i$). We have conducted both fluorescence measurements using the magnesium indicator magfura-2 and ^{31}P NMR measurements of $[Mg^{2+}]_i$ in lithium loaded SH-SY5Y neuroblastoma cells, which supports this hypothesis.

Tu-Pos375

INTERACTIONS BETWEEN AMILORIDE DERIVATIVES (AMI-D) AND FURA-2: STUDIES IN-VITRO AND IN CARDIAC MYOCYTES. ((**J.D. Rojas**[1], C.A. Hudson[2], N. Sarvazyan[1], D.E. Wesson[2], R. Martínez-Zaguilán[1])). [1]Departments of Physiology an [2]Internal Medicine, Texas Tech University, H.S.C., Lubbock, TX. 79430.

AMI-D are fluorescent molecules (Em_{max} = 410 nm; Ex_{max} = 286 and 360 nm) and their interactions with commonly used fluorescent ion indicators might complicate interpretation of fluorescence data obtained when using these indicators with AMI-D to inhibit Na^+/H^+- and Na^+/Ca^{2+}- exchange[1]. Our previous studies show that AMI-D decrease fluorescence of the pH^{in} indicator BCECF[2]. In the present studies we evaluate if interactions between AMI-D and Fura-2 (Em_{max} = 510 nm; Ex_{max} = 340 and 380 nm; isoexcitation= 360 nm) compromise the interpretation of Fura-2 data. *In vitro* data indicated that AMI-D decrease the fluorescence of Fura-2 at all its useful wavelengths, in a concentration dependent manner. The Fura-2 ratio 340/380 (used to estimate $[Ca^{2+}]$) also decreased with increasing AMI-D concentrations. Plotting the data in a Stern-Volmer relation suggested that this phenomenon was due to either static or dynamic quenching. However, varying temperatures (4 - 37°C) did not alter the Stern-Volmer constants, consistent with an alternative type of quenching, i.e., fluorescence resonance energy transfer. We evaluated the relevance of these interactions for the interpretation of *in situ* data using adult rat cardiomyocytes loaded with Fura-2. These cells exhibit Na^+/Ca^{2+} exchange as reflected by a rapid $[Ca^{2+}]^{in}$ increase following Na^+ removal. Pre-treatment of cells with benzylamiloride (BZA), a reversible inhibitor of the Na^+/Ca^{2+} exchanger (Ki ~ 10 μM) decreased the magnitude of Fura-2 ratios. Analysis of the individual Fura-2 useful wavelengths indicated that BZA at ≥25 μM, significantly altered the Fura-2 signal, consistent with the quenching effects noted *in vitro*. Altogether, these data indicate that AMI-D interact with Fura-2 *in vitro* and *in situ*. Therefore, caution must be exercised when interpreting the data derived from Fura-2 in conjunction with AMI-D.

1. Martínez-Zaguilán, et. al.; *Cell Calcium*, 19:337, 1996
2. Sanchez-Armass, et. al.; *J. Neurophysiol*, 71:2236, 1994

Tu-Pos376

SOLVATOCHROMISM IN SOME DICYANO-SUBSTITUTED AROMATICS
((A. Kutruff, J. Traver, G. Rehberg, and **B. W. Williams**)) Dept. Chemistry, Bucknell University, Lewisburg, PA 17837

Aromatic compounds possessing electron donor and electron acceptor substituents connected through conjugation often display solvatochromism, and can serve as spectral probes of polarity or viscosity in chemical or biological systems. We have begun investigation of the effects dicyano substitutents (serving as electron acceptors) have on spectral response, with the twin goals of better understanding the electronic properties of such molecules as well as obtaining better control of absorption wavelength characteristics. Synthetically, dicyano-substituted aromatics can often be easily prepared from precursor aromatic aldehydes and ketones using malononitrile via Knoevenagel type reactions (e.g.):

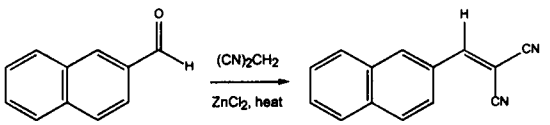

Here, we present data on the absorption and fluorescence spectral response of some dicyano-substituted aromatics we have recently characterized.

Tu-Pos377

Vibrational Analysis of Vanadate in Myosin S1 (S1·MgADP-Vi)
((J. H. Wang, H. Deng, R. Callender, J. C. Grammer* and R. G. Yount*)) Physics Department, City College of CUNY, New York, NY 10031 *Biochemistry/Biophysics Program, Institute of Biological Chemistry, and Department of Chemistry, Washington State University, Pullman, WA99164

In myosin, ATP binding initially reduces the affinity of myosin for actin, after which hydrolysis of ATP occurs rapidly and results in a metastable ternary complex between myosin, ADP, and inorginic phosphate. Release of the hydrolysis products is catalyzed by rebinding to actin which is accompanied by the energy transduction step. In the absence of actin, vanadate inhibits the myosin ATPase activity by forming a long-lived complex with MgADP that is believed to mimic either the transition state for hydrolysis or the ADP, Pi state. Raman Spectroscopy was used to determine the structure of vanadate moiety in S1·MgADP-Vi complex. The spectra of vanadate in solution and vanadate bound in S1 are taken. A complete vibrational analysis will be presented using both ab initio method and empirical method and the results will be compared with that from X-ray Crystallographic studies. Implications of our results on the mechanisms of ATP hydrolysis by myosin will also be discussed.

Tu-Pos378

FT-RAMAN SPECTROSCOPY OF HUMAN HAIR
((C. Pande)) *Clairol Inc. Stamford, CT. 06922.*

Human hair is primarily composed of keratin proteins. There are at least two distinct structural components of hair. The shingle-like cuticle scales form the protective exterior, and determine the surface properties of a fiber. Each cuticle cell is ~ 0.5 μ thick and 45 μ long. Typically the cuticle layer is 8 scales thick. The fiber interior is composed of cortical cells; each cell is ~ 8 μ thick and 100 μ long. The cortical cells, packed with α-helical protein in a fibrillar arrangement, provide the fiber its tensile strength.

We are developing *in situ* spectroscopic probes to fingerprint functional groups in hair to better characterize hair damage[1,2]. This, we feel, is the essential first step in reducing damage. We have now applied this technique to measure damage resulting from hair 'relaxing'. This process is used to straighten hair of African origin and involves treatment with alkaline solution (pH ~13.5) for ca.18 min. We find that about 35% cystine disulfide bonds in hair keratin are destroyed after a single treatment. Damage to the peptide bonds is also reflected by changes in the Amide-I band.

[1] Pande, C. *Biophys J.* 64, 2, A276, 1993; [2] Pande, C. *J. Soc. Cosmet. Chem.* 1994; 45, 257-268.

Tu-Pos379

CD, ABSORPTION AND MELTING TEMPERATURES OF REPEATING DINUCLEOTIDE DNA, RNA, AND HYBRID DUPLEXES, $[d/r(AC)]_{12}$•$[d/r(GT/U)]_{12}$, AND THE INFLUENCE OF PHOSPHOROTHIOATE SUBSTITUTION.
((**Christopher L. Clark**, Paul K. Cecil, Davinder S. Sekhon and Donald M. Gray)) Program in Molecular and Cell Biology, University of Texas at Dallas, Box 830688, Richardson, Texas 75083-0688. (Spon. by Claud S. Rupert)

Circular dichroism (CD) spectra and melting temperature (Tm) data for five sequences containing phosphorothioate linkages were compared with data for four unmodified sequences to assess the effect of phosphorothioate modification on the structure and stability of DNA•DNA and DNA•RNA duplexes. Sulfur modification on one strand did not contribute significantly to the absorption spectra of the separate single strands. Nine duplexes were formed by mixing oligomers that were 24 nucleotides long in 0.15 M K^+ (phosphate buffer) pH 7.0. Unmodified DNA•DNA and RNA•RNA duplexes were used as reference B-form and A-form structures. The CD spectra of the modified hybrids S-$d(AC)_{12}$•$r(GU)_{12}$ and $r(AC)_{12}$•S-$d(GT)_{12}$ were essentially the same as the spectra of the unmodified hybrids, and all were A-form in character. CD spectra of duplexes S-$d(AC)_{12}$•$d(GT)_{12}$ and $d(AC)_{12}$•S-$d(GT)_{12}$ were similar to that of $d(AC)_{12}$•$d(GT)_{12}$, except for a reduced long wavelength CD band. Sulfur modifications on both strands of the DNA duplex caused a pronounced effect on its CD spectrum. The order of thermal stability was: RNA•RNA > DNA•DNA > DNA•RNA > S-DNA•DNA > S-DNA•RNA > S-DNA•S-DNA. The effect of phosphorothioation of one strand was -7.8 ± 0.6 °C, regardless of whether the substitution was in a hybrid or DNA duplex.

Supported by the Texas Advanced Technology Program (#9741-036) and Cytoclonal Pharmaceutics, Inc.

Tu-Pos380

EFFECT OF CHAIN LENGTH OF HELICAL POLYPEPTIDES ON CIRCULAR DICHROISM AND INFRARED SPECTRA.
((S. Yu. Venyaminov and F.G. Prendergast)) Department of Pharmacology, Mayo Foundation, Rochester, MN 55905

Helical polypeptides of different lengths, from 7 to 37 residues and with the common formula Ac-W$(EAAAR)_n$-A-NH_2 where n=1,2,3,4,5,6,7, were investigated by circular dichroism (CD) and infrared (IR) transmission spectroscopy in aqueous (H_2O and D_2O) solutions. In an attempt to separate the effect of helix stability and nonhelicity of terminal residues from the chain-length dependence of measured spectral parameters, the continuous temperature dependence of ellipticity at 222 nm was measured, along with CD and IR spectra at different temperature in the range 0-94°C. These measurements were performed at low (5mM) and high (2.5M) ionic strength, at pH 7.0 and 2.0, and also in the presence of 25% trifluoroethanol. In this broad range of variables, the investigated polypeptides have difference secondary structure. The temperature dependence of the most helical and the most unordered peptides was used to normalize the experimental data set and caldulate chain-length dependence of position and amplitudes of bands in CD and IR spectra. The value of molar ellipticity per residue at 222nm for infinite helix is equal to -45500 deg cm^2 $dmol^{-1}$. The results are discussed in connection with existing methods of evaluation of secondary structure of proteins by CD and IR techniques. (Supported by GM34847-12).

Tu-Pos381

ELECTROROTATION STUDIES OF BABY HAMSTER KIDNEY FIBROBLASTS (C-13) FOLLOWING INFECTION WITH HERPES SIMPLEX VIRUS, TYPE I.
((S. Archer, H. Morgan and F Rixon*)) Bioelectronics Research Centre, Department of Electronics and Electrical Engineering and *MRC Virology Unit, University of Glasgow, Glasgow, UK G12 8QQ

Rotating AC electric fields have been used to characterise the dielectric properties of individual cells and to monitor physiological changes in the properties of cells. The rate of rotation of the cell varies with the applied frequency of the AC field and by modelling the cell as a series of concentric spheres it is possible to obtain the dielectric parameters of the cell. Rotating 4-phase electric fields in the frequency range 1kHz to 20MHz have been used to investigate the membrane properties of fibroblasts. Cells were exposed to the fields using microfabricated electrodes. The rotation spectrum of single BHK (C-13) cells was recorded and the change in this spectrum and hence the dielectric properties of the cell followed after infection with Herpes Simplex Virus (Type 1). The effect of virus infection on the biophysical properties of the cell is discussed in relation to the known biochemical life-cycle of the virus.

Tu-Pos382

NMR STUDIES ON A NOVEL PROTEIN-PROTEIN INTERACTION WHICH ACTIVATES TRANSCRIPTION IN YEAST. ((**P. Hidalgo**‡*, P. Schmidt‡, S. Farrell†, N. Simkovich†, M. Ptashne† and G. Wagner‡)) ‡Department of Biological Chemistry and Molecular Pharmacology, Harvard Medical School, Boston, MA 02115 and †Department of Molecular and Cellular Biology, Harvard University, Cambridge, MA 02138.

Transcriptional activation is a major stage of regulation during gene expression. Although eukaryotic transcription has been studied extensively, the precise mechanism of activation remains unclear. We use nuclear magnetic resonance (NMR) spectroscopy to study the specific protein-protein interaction between derivatives of the yeast transcriptional activators GAL4 and GAL11P.
GAL4 derivatives lacking activating region strongly enhance transcription in cells bearing a point mutation in the GAL11 protein. This observation lead to an attractive hypothesis of gene activation, the *simple recruitment hypothesis*, which proposes that the interaction between a protein bound to DNA (like GAL4 derivatives) and a single component of the holoenzyme (like GAL11P) suffices for transcription. Functional studies on the binding between GAL4 and GAL11P derivatives imply that amino acids 50 to 106, of GAL4, and 261 to 352, of GAL11P, are responsible for binding activity.
We have demonstrated, using NMR spectroscopy, that GAL4 (50-106) and GAL11P (261-352) interact with each other in solution with an stoichiometry of 1 GAL4 (50-106) dimer to 1 GAL11P (261-352) monomer. The residues in GAL4 (50-106) involved in the interaction with GAL11P (261-352), as indicated by HSQC spectra, are in agreement with site-directed mutagenesis studies. We are currently using NMR spectroscopy to solve the structure of the GAL4 - GAL11P complex.
*P.H is a Bristol-Myers Squibb Pharmaceutical Research Institute Fellow of the Life Sciences Research Foundation. This work was supported by NIH GM47467.

Tu-Pos383

STRUCTURE AND FUNCTION OF PHOSPHATIDYLINOSITOL-SPECIFIC PHOSPHOLIPASE C FROM *BACILLUS CEREUS*
((Tun Liu, Margret Ryan, Frederick W. Dahlquist, and **O. Hayes Griffith**)) Institute of Molecular Biology, Department of Chemistry, University of Oregon, Eugene, OR 97403

Recently, crystal structures of phosphatidylinositol-specific phospholipase C (PI-PLC) have been solved, and reveal two histidines at the active site [Heinz, D. W., et al. (1995) *EMBO J.* 14, 3855-3863; Essen, L.-O., et al. (1996) *Nature* 380, 595-602]. Here we present the first study of the pKa values of histidines of a PI-PLC. All six histidines of *Bacillus cereus* PI-PLC were studied by 2D ^{1}H-^{13}C NMR spectroscopy and site-directed mutagenesis. The recombinant protein was selectively labeled with ring-2-^{13}C-histidine. A series of ^{1}H-^{13}C HSQC NMR spectra were acquired over a pH range of 4.0 - 9.0. Five of the six histidines have been individually substituted with alanine to aid the resonance assignments in the NMR spectra. The active site histidines, His32 and His82, display pKa values of 7.6 and 6.9, respectively. His92 and His227 exhibit pKa values of 5.4 and 6.9, whereas His61 and His81 do not titrate over the pH range studied. These values are consistent with the crystal structure data in that His92 and His227 are on the surface of the protein, and His61 and His81 are buried in the three-dimensional structure. The pH profile of enzyme activity and the pKa value provide direct evidence that His82 acts as a general acid in the catalytic mechanism. His32 is essential to enzyme activity, but its putative role as the general base is uncertain due to its relatively high pKa value. The catalytic mechanism is compared to that of ribonucleases A and T_1. Substrate analog inhibitors of PI-PLC were designed to examine the importance of the lipid portion and the inositol phosphate head group for binding to the enzyme. Compounds were screened for their suitability to map the active site region of the enzyme by protein crystallography. Short chain lipids (dihexyl or dioctyl) that resemble most closely the natural substrate PI were the most potent inhibitors. Among dihexyl derivatives, a phosphonoinositol derivative was the strongest inhibitor (K_i =14 μM, inhibition is competetive). Inositols and inositol-derivatives that do not contain lipid moieties show IC_{50}s about three orders of magnitude above those of the short chain lipids.

Tu-Pos384

NMR STUDIES OF THE CONTIGUOUS SH3-SH2 DOMAINS FROM $PP60^{C\text{-}SRC}$, FREE AND COMPLEXED WITH A HIGH-AFFINITY PHOSPHOPEPTIDE ((**L. K. Nicholson**, M. Tessari†, L. N. Gentile, and G. Vuister†)) Biochem., Molec. & Cell Biol., Cornell U., Ithaca, NY 14853, †Bijvoet Center for Biomolec. Res., Utrecht U., Padualaan, 3584 Netherlands.

Multidimensional high resolution NMR techniques have been applied to study the structure and dynamics of a model protein comprised of the Src-homology (SH) domains SH3 and SH2 derived from chicken $pp60^{c\text{-}src}$ (Src). This SH3-SH2 fragment has been over-expressed and isotopically labeled with ^{15}N and ^{13}C in *E. coli*, and a repertoire of double- and triple-resonance experiments have been performed on 500, 600 and 750 MHz spectrometers. The resonance assignments and secondary structure of both the SH3 and SH2 domains within this fragment are very similar to those reported for the individual domains derived from Src, indicating that no large-scale structural changes result from covalent linkage of the two domains. Backbone dynamics studies reveal an intermediate time-scale motion (2 - 5 ns) across essentially the entire backbone, consistent with a flexible hinge linker region which would allow reorientation of whole domains. The addition of a high-affinity phosphopeptide (EPQpYEEIPIYL) yielded several significant peak shifts in the ^{15}N-^{1}H chemical shift correlation spectrum, which were restricted to the SH2 domain. Questions regarding the possible dimerization of the SH3-SH2 fragment and implications of these studies for the role of the SH3 domain in phosphopeptide binding will be discussed.

Tu-Pos385

NMR STRUCTURE OF THE AMYLOID PRECURSOR PROTEIN CARBOXY-TERMINAL DOMAIN CONTAINING SIGNALS FOR INTRACELLULAR TRAFFICKING. ((**T. Ramelot**, J. Reinking, N. Zambrano†, T. Russo† and L. Nicholson)) Section of Biochemistry, Molecular and Cell Biology, Cornell University, Ithaca, NY 14853, and †Dipartimento di Biochimica e Biotecnologie Mediche, Universitá degli Studi di Napoli "Federico II," via S. Pansini 5, I-80131 Napoli, Italy. (Spon. by J. Feigenson)

Amyloid precursor protein, APP, is an essential transmembrane glycoprotein which is the precursor to the 4 kDa amyloid β-protein, AβP, found in the senile plaques of Alzheimer's disease patients. All of the isoforms of APP contain an identical 47 residue intracellular carboxy-terminal tail containing the consensus sequence NPXY, essential for internalization of many plasma membrane receptors via coated pits. The major proteolytic product of APP is a large secreted extracellular domain, APPs, formed by the so called α-secretase pathway acting within the AβP and thus precluding AβP production. The AβP is produced by a different pathway involving the proteolytic processing of APP by β- and γ-secretases and possible endocytosis of APP from the plasma membrane. We have over expressed the 47 amino acid carboxy-terminal tail, APPc, in order to study the structure and dynamics of the endocytosis signal using high resolution NMR spectroscopy. Our preliminary NMR results obtained on a 600 MHz Unity INOVA spectrometer indicate a partially folded structure. Additionally, we are studying interactions of the intracellular domain of APP with other proteins. We are over expressing a phosphotyrosine interaction domain, PID, of a recently discovered protein, Fe65, shown to interact with this region of APP by two hybrid screens as well as co-precipitation experiments [Fiore, Zambrano, Minopoli, Donini, Duilio, and Russo, (1995), *J. of Bio. Chem.*, **270**, 30853-30856]. Structural and dynamics studies of the APPc/PID complex will be pursued.

Tu-Pos386

A CRITICAL STUDY OF ELECTRON SPIN ECHO MODULATION BY WEAKLY COUPLED ^{14}N FROM IMIDAZOLE: RAMIFICATIONS FOR COPPER COORDINATION AND ELECTRONIC STATES. ((C.J. Bender)) Einstein College of Medicine, Bronx, NY 10461 and Emory University, Atlanta.

Electron spin echo modulation spectra are interpreted as effective zero (Zeeman) field nuclear quadrupole interaction spectra and, as such, potentially reflect the valence shell orbital occupancy and local electric field of non-coordinating ligand nuclei that may be used as probes of the metal binding site in protein. The interpretations and studies of Mims & Peisach (1978) and Flanagan & Singel (1987) are reexamined in the context of *ab initio* SCF calculations with the density functional approximation of the electron correlation energy. The computed spin density and electric field gradient of the remote imidazole nitrogen do not match experimentally derived values unless certain assumptions are made concerning the electronic state of the copper-ligand system. Best correlation is made by using the starting assumption that the 'pruned' protein complex has a formal charge of $Z = +3$ and $S_{eff} = ½$. This configuration brings into play low-lying virtual states that lead to adequate spin delocalization onto the histidine ligand, and is consistent with the optical properties of Type I copper proteins. Geometric factors, *i.e.* distortion from a square pyramidal geometry, can account for the unusual oxidation state and its implications.

Tu-Pos387

SITE DIRECTED SPIN LABELING OF THE PROTON PORE AND CATALYTIC SITES OF THE *E. COLI* ATP SYNTHASE WITH CARBODIIMIDE AND SH-REACTIVE ESR SPIN LABELS ((Michael Kersten, Jakov Poiline, Thomas Schanding, Pia D. Vogel and **John G. Wise**)) Fachbereich Chemie, Universität Kaiserslautern, Erwin-Schrödinger-Straße, 67663 Kaiserslautern, Germany. Tel.: 49-631-205-4254, Fax.: 49-631-205-3419; Email: wise@chemie.uni-kl.de.

The reaction of newly synthesized cyclohexylcarbodiimide spin labels with specific residues of the F_0 proton pore and the reaction of SH-reactive spin labels with a site specific cysteine mutant of the catalytic site of the F_1 ATPase have been used to study the *E. coli* ATP synthase. The synthesis of a spin label cyclohexylcarbodiimide derivative and its initial use in labeling the proton pore of the ATP synthase has been recently described (Schanding, T., Vogel, P.D., Trommer, W.E. and Wise, J.G. (1996) Tetrahedron *52*, 5783-5792). Here we report the synthesis of additional cyclohexylcarbodiimide spin labels for use in the analysis of conformational changes within the F_0 sector of the ATP synthase. Covalent modification of F_0 by cyclohexylcarbodiimide spin labels inhibited ATP-driven proton-pumping in the ATP synthase and proton-translocation through F_1-depleted F_0-containing membranes. In related work, the labeling of a site specifically introduced cysteine residue in the catalytic nucleotide binding site of the F_1 ATPase sector of the ATP synthase (βTyr331→Cys) by SH-reactive spin labels has been accomplished. Reactive cysteine residues not in the catalytic site were first blocked by reaction of F_1 with NEM in the presence of ATP. SH-reactive spin labels were then introduced in the catalytic sites after removal of nucleotides from the enzyme. Conformational changes in the enzyme that are dependent on nucleotide binding were investigated by EPR spectroscopy. The combination of these two approaches, spin labeling of the F_0 sector with cyclohexylcarbodiimide labels and spin labeling of the F_1 sector with SH-reactive spin labels, promises to yield new information on the coupling of conformational changes between the proton pore and catalytic nucleotide binding sites of the ATP synthase.

Tu-Pos388

MEASUREMENT OF MOLECULAR DISTANCES USING DIPOLAR COUPLED NITROXIDE SPIN-LABELS: THE GLOBAL ANALYSIS OF MULTIFREQUENCY CW-EPR DATA. E.J. Hustedt[1], A.I. Smirnov[2], C.F. Laub[1], C.E. Cobb[1], and A.H. Beth[1]. [1]Department of Molecular Physiology and Biophysics, Vanderbilt University, Nashville, TN 37232 and [2]Illinois EPR Research Center, University of Illinois at Urbana, Urbana, IL 61801

For immobilized nitroxide spin-labels with well-defined geometry between the two nitroxides, resolved dipolar splittings can be observed in CW-EPR spectra for interelectron distances as large as 30 Å using perdeuterated probes. This is an important distance range for examining structural features of proteins and other macromolecular systems. Algorithms have been developed for calculating the CW-EPR spectrum for a pair of immobilized, dipolar coupled nitroxides. Calculations are presented which define the limits of sensitivity to the interelectron distance as a function of geometry and microwave frequency. Secondly, the CW-EPR spectra of N^4-spin-labeled coenzyme NAD^+ (SL-NAD^+) bound to microcrystalline, tetrameric glyceraldehyde - 3 - phosphate dehydrogenase (GAPDH) have been collected at 9.8, 34, and 94 GHz. These data have been analyzed, using a combination of the methods of simulated annealing and global analysis, employing a model with pairwise R-axis related dipolar interactions between the nitroxides of N^4-SL-NAD^+ bound to the enzyme tetramer. Using this approach, a unique determination of the distance and relative orientation between the two nitroxides has been obtained. These results do not violate any significant steric restraints as determined from a molecular model built from the known crystal structure of the GAPDH tetramer. Finally, the effect of rigid body isotropic rotational diffusion on the CW-EPR spectra of dipolar coupled nitroxides has been investigated using a newly developed algorithm based on the use of Brownian dynamics trajectories. These calculations, which assume axial A- and g-tensors and an interelectron vector aligned with the nitroxide z-axes, demonstrate the sensitivity of CW-EPR spectra to dipolar coupling in the presence of rigid body rotational motion. The further development of this and other more complex dynamic models, including local motion of the nitroxide relative to the protein backbone, will be critical to the rigorous quantitative analysis of nitroxide - nitroxide dipolar coupling in a wide range of biological systems. Supported by: NIH grants RO1 HL 34737, RR 04075, and RR 01811.

Tu-Pos389

THERMODYNAMIC STABILITY AND TERTIARY INTERACTION STUDIES ON FEPA USING DENATURANT UNFOLDING AND SITE-DIRECTED SPIN LABELING. ((Candice S. Klug, Wenyi Su, **Jimmy B. Feix**)) Biophysics Research Institute, Medical College of Wisconsin, Milwaukee, WI 53226

Previously, we have used site-directed spin labeling (SDSL) to characterized guanidine (Gdn) and urea-induced unfolding in the ligand binding domain of the ferric enterobactin receptor, FepA (Klug et al., *Biochemistry 34*, 14230-14236, 1995). Denaturation of the ligand binding domain converts the spin labeled side chains from a buried, rotationally immobilized environment into a freely mobile one. Thus, the attached spin label is able to detect the motional constraints imposed by the tertiary structure of the protein providing a sensitive monitor of changes in local structure. In this study, we have examined the unfolding of several spin labeled FepA mutants, several located in a transmembrane β-sheet and others in an extracellular loop proposed to contain the ligand binding domain. Significant variation is observed in the Gdn concentrations at which the different sites become rotationally unrestricted, even for neighboring residues in the primary structure. These results demonstrate that SDSL used in conjunction with chemical denaturation can provide information on both the thermodynamic stability of localized domains and on long range tertiary interactions.

Tu-Pos390

CHARACTERIZATION OF A PROPOSED β-STRAND LOCATED IN THE FERRIC ENTEROBACTIN RECEPTOR FEPA USING SITE-DIRECTED SPIN LABELING. ((**Candice S. Klug**, Wenyi Su, and Jimmy B. Feix)) Biophysics Research Institute, Medical College of Wisconsin, Milwaukee, WI 53226.

FepA is an 81kDa integral membrane protein responsible for transporting the iron siderophore, ferric enterobactin, across the outer membrane of gram-negative bacteria. The receptor is predicted to form a β-barrel structure (Murphy *et al.* (1990) *J. Bacteriol. 172*, 2736-2746). Previous studies have shown FepA to behave as a ligand-gated porin with the extracellular loops acting as the ligand-binding domain (Rutz *et al.* (1992) *Science 258*, 471-475; Liu *et al.* (1993) *PNAS 90*, 10653-10657). The proposed structure contains 29 antiparallel β-strands which span the bilayer and form the transmembrane channel. Site-directed spin labeling (SDSL), in which selected residues are mutated to cysteine and then modified with a nitroxide spin label, can give valuable information on the location and environment of an individual residue. In this study, seven consecutive residues located within a single proposed β-strand near the active site were characterized and mapped. This approach has the capability of proving a model correct, making small adjustments in a model, or helping to completely rebuild a simulated structural prediction. We confirmed that these residues do form a transmembrane β-sheet and that their mapped locations are fairly consistent with their predicted positions.

Tu-Pos391

STRUCTURAL CHANGES OF YEAST 3-PHOSPHOGLYCERATE KINASE UPON PHOSPHORYL TRANSFER ? ^{31}P and ^{13}C RELAXATION MEASUREMENTS ON ENZYME-BOUND REACTION MIXTURES. ((**Mei H. Chau** and B.D. Nageswara Rao)). Department of Physics, Indiana University Purdue University Indianapolis (IUPUI), Indianapolis, IN 46202.

3-Phosphoglycerate kinase (PGK) is a key enzyme in anaerobic glycolysis. Crystal structure data of this enzyme with substrate analogs have been available, but the location of the active sites is not unequivocally ascertained. Although it was suggested that the enzyme undergoes hinge-bending motion during catalysis, conclusive evidence has not been found. Structural changes of PGK during enzyme turnover, determined by measuring the paramagnetic enhancement of ^{31}P and ^{13}C nuclear spin relaxation on the enzyme-bound equilibrium mixture, E.Mn(II)ATP.3P-glycerate(3PG), are presented in this paper. Mn(II) is a substituent activating paramagnetic cation in place of Mg(II). Relaxation measurements were made at three different frequencies for each nucleus with the same sample at pH 7 and 1 °C. Since the relaxation rates are complicated by the enzyme turnover rate, the results of these measurements have been analyzed on the basis of a recently published theory (Nageswara Rao, B.D. (1995) *J. Magn. Reson.* B108, 289-293). The distance from Mn(II) to the 3P nuclei of 3PG and 1,3-dPG in the equilibrium mixture are both found to be 11.4 ± 0.3 Å, similar to that obtained for a dead end complex, E.Mn(II)ADP.3PG (Bruce D. Ray and B. D. Nageswara Rao (1988) *Biochemistry* 27, 5579-5585). This result indicates that hinge-bending, if it occurs at all, occurs even in the dead-end complex.

Tu-Pos392

ESTIMATION OF THE ELECTROSTATIC POTENTIAL AT THE AGONIST SITE OF THE ACETYLCHOLINE RECEPTOR ((George H. Addona and David S. Cafiso)) University of Virginia, Department of Chemistry and Biophysics, Charlottesville, VA 22901.

Electrostatic potentials at spin-labeled sites were measured using continuous wave power saturation EPR spectroscopy. The method was validated by measuring membrane surface potentials by power saturating the EPR spectrum of an ^{14}N spin probe located at the membrane interface in the presence of a neutral or positively charged ^{15}N spin probe. The potentials measured were in good agreement with other measurements and with predictions of the Gouy-Chapman-Stern theory. It has been postulated for some time that a negative subsite involved in ligand binding is present at the acetylcholine binding site in the nicotinic acetylcholine receptor(nAChR). In order to characterize the environment of the acetylcholine binding site on the nicotinic acetylcholine receptor a spin-labeled affinity probe, derived from the agonist site label maleimidobenzyltrimethylammonium (MBTA), was synthesized and derivatized to a sulfhydryl close to the agonist binding site on reconstituted nAChR. The spin probe was in significant contact with the receptor and an electrostatic potential of approximately -15 mV was determined, by power saturation EPR spectroscopy, to be located near the binding site labeled with spin label analogue of MBTA. Two other sulfhydryl probes used to derivatize the agonist site of reconstituted nAChR were found to have less contact with the receptor and reported reduced potentials. This indicates that there is a strong spatial dependence to the electrostatic potential at the acetylcholine binding site. The identification of a significant potential at the agonist binding site suggests a role for acidic residues in the acetylcholine binding pocket.

Tu-Pos393

PROTEIN AND LIPID STRUCTURAL CHARACTERISTICS ASSOCIATED WITH THE RECOVERY OF NORMAL BACTERIORHODOPSIN PHOTOCYCLE BEHAVIOR IN TRITON-TREATED PURPLE MEMBRANE

((**Steven M. Barnett**,[a] Swetlana Dracheva,[b] Salil Bose,[b] Richard W. Hendler,[b] and Ira W. Levin[a]))
[a]Laboratory of Chemical Physics, NIDDK, [b]Laboratory of Cell Biology, NHLBI, NIH, Bethesda, Maryland, 20892-0510.

Brief exposure of purple membrane to dilute Triton (0.1% Triton, 2 min) dramatically alters the bacteriorhodopsin photocycle while minimally affecting the trimer structure. Native photocycle behavior is recovered upon reconstitution with purple membrane lipids in the presence of high saline media (> 2M NaCl). Progressively less recovery is attained at lower NaCl concentrations. Infrared spectroscopic studies were performed on purple membrane both after exposure to Triton and after lipid reconstitution at different NaCl concentrations to identify the purple membrane structural features which are associated with the recovery of normal photocycle activity. Triton-induced infrared spectroscopic changes include decreases in the width of the α-helical component of the amide I mode at 1660 cm^{-1}, in the amide I/amide II intensity ratios, and in the intensity of specific spectral intervals in the C-H stretching mode region. The recovery of the various spectral parameters, and in particular the width of the α-helical component of the amide I mode, correlates with a gradual restoration of native bacteriorhodopsin photocycle function upon lipid reconstitution with increasing NaCl concentration. The purple membrane structural features essential for native photocycle behavior, including normal M intermediate decay and the ability of actinic light to modulate the bacteriorhodopsin photocycle, will be discussed in light of these observations.

Tu-Pos394

THE ROLE OF SALT IN RECONSTITUTING PHOTOCYCLE BEHAVIOR TO TRITON-DAMAGED PURPLE MEMBRANES BY ADDITION OF NATIVE LIPIDS

((**Salil Bose, Anup K. Mukhopadhyay, Swetlana Dracheva, and Richard W. Hendler.**)) LCB, NHLBI, NIH, Bethesda, MD 20892
(Spon. by M. R. Bunow).

We demonstrated recently that damage to the normal BR photocycle caused by brief exposure to dilute Triton X-100, which removes lipids from the membrane (Dracheva et al.(1996)FEBS Lett. 382,209-212), can be repaired by adding back an extract of PM lipids (Mukhopadhyay et al.(1996)Biochemistry,35,9245-9252). Reconstitution with lipids required the presence of high (>2M) concentration of NaCl at neutral pH. This presentation shows that reconstitution can be achieved with divalent and trivalent cations at much lower concentrations than were required for NaCl (i.e., ~10 mM for Ca^{2+} and ~0.5 mM for La^{3+}), indicating that negative surface charges must be neutralized to allow the added lipids to reach and be incorporated at the proper locus. Reconstitution in absence of salt can be accomplished by protons alone with an apparent pK near 5. The pH-dependence studies on reconstitution at various salt concentrations showed that the apparent pK of reconstitution increased with increasing salt concentration. This observation is opposite to what is expected from Gouy-Chapman charge screening. Attempt to explain the unexpected result considering specific cation-binding equilibria, has so far been unsuccessful.

Tu-Pos395

pH DEPENDENCE OF PROTON TRANSFER REACTIONS WITHIN BACTERIORHODOPSIN: A TIME-RESOLVED ATR/FT-IR STUDY

((C. Zscherp & **J. Heberle**)) Forschungszentrum Jülich, IBI-2, 52425 Jülich, FRG

The technique of attenuated total reflection (ATR) is combined with step-scan Fourier transform infrared spectroscopy. We obtained time-resolved infrared difference spectra (time resolution 5 μs) of biological samples in bulk aqueous media[1]. The ATR approach allows adjustment and variation of pH, substrate and salt concentration. Linear dichroism experiments yield information about structural changes in all three spatial dimensions in contrast to conventional transmission spectroscopy.
In this contribution, we investigated the photocycle of the light-driven proton pump Bacteriorhodopsin. Data in the range between 1900 cm^{-1} and 950 cm^{-1} have been collected for 4 < pH < 9.3. Difference spectra exhibit high signal-to-noise ratio. A firm data analysis shows the following results:

- The pK_a of Asp-96 drops from 11.4 in the ground-state[2] to 7.2 ± 0.3 in the N state.
- The O intermediate exhibits no major changes in secondary structure.
- The C=O frequency of Asp-85 in the M intermediate is upshifted by 2 cm^{-1} at acidic pH values as compared to neutral and alkaline.

References:
1) Heberle, J. & Zscherp, C. (1996), *Appl.Spectrosc.* 50, 588-596.
2) Szaraz, S., Oesterhelt, D., & Ormos, P. (1994), *Biophys. J.* 67, 1706-1712

Tu-Pos396

THE MUTATION K129H REVERSES THE ORDER OF PROTON RELEASE AND UPTAKE IN BACTERIORHODOPSIN; GUANIDINIUM RESTORES IT.

((R. Govindjee[1], E. Imasheva[1], S. Misra[1], S.P. Balashov[1], T.G. Ebrey[1], N. Chen[2], D.R. Menick[2], and R.K. Crouch[2])) [1]Center for Biophysics and Computational Biology, Univ. of Illinois at Urbana-Champaign, Urbana, IL 61801 and [2]Medical Univ. of S. Carolina, Charleston, SC 29425.

K129 is a residue located in the extracellular loop connecting transmembrane helices D and E of bacteriorhodopsin (bR). Replacement of K129 with a histidine affects the pK_as of two key residues in the proton transport pathway, D85 and E204. The pK_a of D85 is raised from ~2.6 to 5.1, while the pK_a of E204 is lowered from ~9.5 to 8.1 in the unphotolyzed state, as determined from the pH dependence of dark adaptation. From the pH dependence of proton release and uptake we estimate that the pK_a of E204 in the M state is 7.0 in K129H, compared to ~5.8 in the wild type (WT). In contrast to the wild type, at neutral pH and 150 mM NaCl, light-induced proton uptake precedes proton release, while it follows proton release at higher pH. These changes are similar to those seen in a related Halobacterial retinal protein, archaerhodopsin-1, which has a histidine in the position analogous to K129. We find that in K129H mutant the normal order of proton release and uptake is restored by the addition of millimolar amounts of guanidine hydrochloride, which lowers the pK_a of D85 and E204 in the unphotolyzed pigment by 0.5 pK unit, and pK_a of E204 in M by more than 1 unit, to a value close to that in the WT pigment, probably by binding to a specific site on bR with a 1:1 stoichiometry. We suggest that K129 may be involved in stabilizing the hydrogen bonding network that couples E204 and D85, since changes in the pK_as of these residues caused by replacement of K129 by histidine indicate that they are coupled more weakly in K129H than in the WT.

Tu-Pos397

PATH OF THE PUMPED PROTON AT THE SURFACE OF BACTERIORHODOPSIN

((**U. Alexiev**[1], R. Mollaaghababa[2], H. G. Khorana[2] and M. P. Heyn[1])). [1]Biophysics Group, Dept. of Physics, Freie Universität Berlin, D-14195 Berlin, Germany. [2]Dept. of Biology, Massachusetts Inst. of Technology, Cambridge, MA 02139, USA.

The time constants and activation energies for the proton release of the proton pump bacteriorhodopsin (bR), measured with surface bound pH-indicator dyes, differ for the detection sites at the extracellular and cytoplasmic surface (22±4μs and 61±4μs at 22°C, respectively) in monomeric bR-micelles. In purple membranes, the detection time for the proton release is similar on both protein surfaces (71±4μs and 76±5μs) and matches the deprotonation of the Schiff base (SB). By modification of the lipid composition of the purple membrane (insertion of DMPC), the deprotonation of the SB is accelerated. The proton release is accelerated only for an indicator bound on the extracellular side (44±4μs at position V130C) and remains unchanged on the cytoplasmic side (71±6μs at position A160C). The results indicate a similar energy barrier both for the bR micelle and the bR patch system at the interface between protein and lipid surface.
The proton transfer step from the bR surface into the aqueous bulk phase is strongly affected by the lipids and by the size of the membranes. Delipidation leads to a delayed transfer of the pumped protons into the bulk phase (3.7ms vs 0.8ms). The time constant for proton release is proportional to the size of the membranes and can vary between 270±10μs (membrane diameter: 0.1-0.2μm) and ~800μs (membrane diameter: 0.8-1.2μm).
A possible mechanism for these observations will be proposed.

Tu-Pos398

LONG-RANGE INTERACTION BETWEEN GLUTAMIC ACID 74 AND ASPARTIC ACID 85 IN BACTERIORHODOPSIN

((J. Rodriguez, X.-Y. Yin, L. Villarreal, E. Rodriguez, R. Needleman, and **R. Renthal**)) U. of Texas at San Antonio, San Antonio, TX 78249 and Wayne State U., Detroit, MI 48201

The bacteriorhodopsin (bR) proton pump consists of a series of H^+ transfer reactions that connect the retinal Schiff base at the membrane center to the membrane surfaces. A key step initiating proton release from the extracellular membrane surface is the transfer of a proton from the Schiff base to Asp 85. We previously found that chemical modification of Glu 74, at the extracellular surface, lowers the pK of Asp 85, at the membrane interior. We have now generated a new bR mutant, E74C, to further examine the interaction between Glu 74 and Asp 85. Positively charged, negatively charged, and neutral modifying groups were attached to the reactive thiol at position 74. The effect on Asp 85 was tested by measuring the conversion of the bR chromophore from its 570 nm purple form to the 605 nm blue pigment, which occurs when Asp 85 is protonated, either by deionization or acidification. Surprisingly, E74C itself shows a lower pK for Asp 85. Most of the modifying groups introduced at position 74 had little additional effect on the pK of Asp 85. We also found that E74C membranes contained a normal ratio of sulfated glycolipid to glycolipid, ruling out a surface charge effect caused by changes in sulfur metabolism. We conclude that a specific interaction between Glu 74 and another group or groups influences the pK of Asp 85. In a recent molecular model of bR, Glu 74 and Asp 85 were separated by 1.8 nm.

Tu-Pos399

Thr-89 Participates in the Active Site of Bacteriorhodopsin: Evidence for a Role in Color Regulation and Proton Transport ((Terence S. Russell, Matthew Coleman, Anders Nilsson, Parshuram Rath, Gary Ludlam and Kenneth J. Rothschild)) Department of Physics and Molecular Biophysics Laboratory, Boston University, Boston, MA 02215

A major factor in determining the visible absorption of light-adapted bacteriorhodopsin (bR_{570}; λ_{max} = 570 nm) is the existence of an active site which includes the protonated retinylidene Schiff base, residues Asp-85, Asp-212, Arg-82 and at least one water molecule. In this work we show that Thr-89, which is located one turn above the Schiff base counterion and proton acceptor, Asp-85, on the C-helix, also participates in this active site. The substitution Thr-89→Asn (T89N) results in a redshift of the visible λ_{max} from 568 to 580 nm and a downshift in the retinylidene C=N and C=C stretch frequencies along with a decrease in the C=O stretch frequency of Asp-85. In contrast, the λ_{max} of dark-adapted T89N is similar to wild type. Time-resolved visible absorption reveals that decay of the L intermediate is significantly slowed and that the λ_{max} of the M intermediate is blue shifted relative to wild type. These results are consistent with a direct interaction of Thr-89 with the Schiff base and Asp-85, thereby influencing the λ_{max} of bacteriorhodopsin. The substitution Thr-89→Asn appears to interfere with the ability of the Schiff base to transfer a proton to Asp-85 during M formation by disrupting these interactions. This work was supported by a grant from the NSF (MCB-9419059) to KJR. M.C. is supported by an NIH Training Grant (GM08291-06). T.R. is supported by an ASSERT award (DAAH04-93-G-0375) from the Army Research Office.

Tu-Pos400

HALORHODOPSIN SPECTRUM CHANGES INDUCED BY CHANGES OF THE ANION CONCENTRATION AND THE CATIONIC STRENGTH IN THE SOLUTION. ((**Jun Otomo**)) PRESTO, JRDC and Advanced Research Laboratory, Hitachi, Ltd., Hatoyama, Saitama 350-03, Japan.

The absorption maximum of shark halorhodopsin in the absence of chloride was found to be shifted to around 600 nm. By addition of anions such as chloride, bromide, or nitrate, its absorption maximum returns to 578 nm. Although this absorption maximum shift is almost the same as that for pharaonis halorhodopsin, half-maximal bindings with chloride, bromide, and nitrate were different. This difference is most likely due to the different amino acid sequence in shark and pharaonis strains. In the presence of anions with large Stokes radii, such as sulfate or bicarbonate, a change in absorption maximum was not observed. The photocycle reaction was also strongly dependent on the anion concentration. The half-maximal binding constant was found to increase when cations were added to the solution. These results suggest that the electrostatic interaction around the retinal Schiff base affects the anion binding of halorhodopsin.

Tu-Pos401

PROBING THE ACTIVE SITE OF PHOTOACTIVE YELLOW PROTEIN (PYP) FROM *ECTOTHIORHODOSPIRA HALOPHILA*.((**S. Devanathan***, U. Genick#, I. Canestrelli#, E. Getzoff#, T. Meyer*, M. Cusanovich* and G. Tollin*)) *Department of Biochemistry, University of Arizona, Tucson, AZ and #Department of Molecular Biology, Scripps Research Institute, La Jolla, CA.

Photoactive Yellow Protein (PYP) can be reversibly bleached by excitation with a laser flash through isomerization of the chromophore (*trans-p*-hydroxycinnamic acid; 446 nm absorption maximum) which is covalently bound to C69 via a thioester linkage. Two mutants, E46Q (buried in the active site) and R52A (separating the active site from the solvent) were constructed. PYP holoprotein was generated by chemical attachment of activated *p*-hydroxycinnamic acid chromophore to recombinant apoprotein. 3,4-Dihydroxycinnamic acid was also attached to the recombinant apoprotein to yield the variant dihydroxyPYP (DH-PYP). The ground state absorption maximum shifted from 446 nm to 462, 452 and 458 nm for E46Q, R52A and DH-PYP, respectively. The bleaching reaction (I_1 to I_2 transition) was accelerated 4-6 fold for the two mutants and about an order of magnitude for the DH-PYP, in comparison to native PYP. The speed of recovery (I_2 to P transition) was 7 fold slower for the R52A mutant and 40 fold for the DH-PYP, compared to native PYP. In contrast, there was an increase in the recovery rate of about 4 fold for the E46Q mutant at neutral pH, as well as a 700 fold increase in recovery rate with pH for E46Q (pK 8.0). The structural basis for these effects will be discussed. (Work supported by grants from the NIH and USAF Rome Laboratory.)

Tu-Pos402

PHOTOACTIVE YELLOW PROTEINS: BACTERIAL BLUE-LIGHT SENSORS. ((**K. J. Hellingwerf**, R. Kort, W.D Hoff, A.R. Kroon and W. Crielaard))
E.C. Slater Institute, University of Amsterdam, The Netherlands.

Photoactive yellow proteins (PYP's), also known as Xanthopsins [1,2], constitute a new family of eubacterial, cytoplasmatic blue-light photosensors with a rhodopsin-like photocycle. They are proposed to function as sensors for negative phototaxis [3]. Members have been isolated from three purple sulfur bacteria, among which the *Ectothiorhodospira halophila* protein is the best characterized. Recently, we also cloned the *pyp* gene from *Rhodobacter sphaeroides*, a genetically well-accessible organism. The chromophore of PYP is 4-hydroxy-cinnamic acid (e.g. [4]), which is thiol-ester linked to the unique cysteine of the protein. Blue light gives rise to *trans* to *cis* isomerization of the C=C bond of the chromophore [5], which subsequently leads to large conformational changes in this photoreceptor protein [6].

Here we report experiments of modification of PYP through: (i) reconstitution with chromophore analogues and (ii) through site-directed mutagenesis. Conclusions from this work are: (i) chromophore analogues that lack the 4-hydroxy group yield non-functional protein, (ii) bulky substituents can be added to the aromatic ring of the chromophore, without considerably affecting PYP's characteristics and (iii) mutant forms of PYP (e.g. R52K, G51S and E46D) can be reconstituted into photoactive chromoproteins.

Literature: 1] Kort, R. et al. (1996) EMBO J. 15, 3209-3218. 2] Hellingwerf, K.J. et al. (1996) Mol. Microbiol. 21: 683-693. 3] Sprenger, W.W. et al. (1993) J. Bacteriol. 175, 3096-3104. 4] Hoff, W.D. et al. (1994) Biochem. 33: 13959-13962. 5] Kort, R. et al. (1996) FEBS Lett., 382, 73-78. 6] Van Brederode, M.E. et al. (1996) Bioph. J. 71: 365-380.

Tu-Pos403

ESSENTIAL WATER MOLECULES IN THE PROTON PUMP BACTERIORHODOPSIN DETECTED BY NEUTRON DIFFRACTION AND LASER SPECTROSCOPY. ((T. Hauß*, G. Papadopoulos#, S.A.W. Verclas*, G. Büldt§ and **N.A. Dencher***)) *Inst. Biochemie, Technische Hochschule, Petersenstr.22, D-64287 Darmstadt and BENSC-NE, HMI, D-14109 Berlin, Germany; #University of Thessaly, Greece; §IBI-2, KFA, D-52425 Jülich.

Neutron diffraction (λ = 5.68 Å) and time-resolved (time resolution: 10 ns) laser-spectroscopic experiments on the light-driven proton-pump bacteriorhodopsin revealed the location and number of water molecules as well as their functional importance. For both experimental approaches, purple membrane films were prepared by drying membrane suspensions on quarz slides at controlled humidity. The decay of the photocycle intermediate M was strongly slowed down below 80% r.h.. Employing optical pH-indicators proved that for r.h. below 75% the proton pumping activity was decreased and no activity was observed at 50% or below. To locate and quantitate the water molecules in bacteriorhodopsin, neutron diffraction measurements were performed both in H_2O and D_2O atmosphere at 15, 57, 75, 86, and 94% r.h.. Our new approach to evaluate the number of water molecules in the projected density of the membrane, which considers a membrane model and avoids some inherent limitations of the Fourier difference method, yielded 6-8 water molecules present in the transmembrane proton pathway at 15% r.h., instead of 3-4 as previously calculated. At higher hydration, the number of water molecules in the channel was not greatly different compared to 15% r.h..

Tu-Pos404

ORIENTATION OF THE ELECTRONIC TRANSITION DIPOLE MOMENT IN THE PHOTOCYCLE OF BACTERIORHODOPSIN.
((**B. Borucki**, H. Otto, M. P. Heyn)) Biophys. Group, Phys. Dep., Freie Universität Berlin, Arnimallee 14, D - 14195 Berlin, Germany. (Spon. by H. Otto)

Time-resolved polarized absorption spectroscopy with isotropically excited magnetically oriented purple membranes is a sensitive method to determine changes in the chromophore orientation in the photocycle of bR [1]. The polarized absorption changes were measured with a sampling rate of 1 GHz (1ns - 100μs, first channel) and an effective time resolution of 20ns - 80ns. In addition to the standard measurements of $\Delta A_{\parallel}$ ($\theta = 0°$) and $\Delta A_{\perp}$ ($\theta = 90°$) we also measured the absorption changes at characteristic wavelengths as a function of the polarization angle θ. The dependence on the polarization angle in oriented patch samples is due to linear dichroism and linear birefringence. In wavelength regions, where the absorbance changes are small, the birefringence effects are even dominant. From the analysis of the time traces $\Delta A(\theta, t)$ at several wavelengths we obtained information about the absorbances and the anisotropies of the intermediates K,L,M and O, assuming a simplified kinetic model of the photocycle. We conclude that the angles between the electronic transition dipole moment and the membrane normal in the intermediates K,L,M and O are smaller than in the inital state: K $\sim$ 1°, L $\sim$ 2°, M $\sim$ 2° and O $\sim$ 1°. In the intermediate N the angle is also smaller than in the initial state, but the exact value depends strongly on the kinetic model of the photocycle.

[1] Otto, H.; Zscherp, C.; Borucki, B.;Heyn, M.P. (1995) *J. Phys. Chem.* **99**, 3847-3853

Tu-Pos405

X-RAY DIFFRACTION STUDIES ON BACTERIORHODOPSIN: LOCALIZATION OF LOOP- AND SULPHUR-CONTAINING RESIDUES

((**W. Behrens**, H. Otto, R. Mollaaghababa*, U. Alexiev, H.G. Khorana* and M.P. Heyn)) Biophysics Group, Dept. of Physics, Freie Universität Berlin, D-14195 Berlin, Germany. *Depts. of Biology and Chemistry, MIT, Cambridge, MA 02139, USA.

Single amino acids in the loops of bacteriorhodopsin were changed to cysteine by site-directed mutagenesis and labeled with the mercury-containing heavy-atom compound PCMB. On the cytoplasmic side position 101 (D96A/V101C-MB) in the CD-loop and on the extra-cellular side position 130 (V130C-MB) in the DE-loop were labeled. X-ray diffraction experiments were performed and the positions of the heavy atoms were determined. We conclude that both the CD and the DE-loops have well-defined structures (short loops).
The distribution of the sulphur-containing methionine residues in bR was investigated by MAD (multiple wavelength anomalous diffraction). X-ray experiments with synchrotron radiation were performed at the sulphur K-edge at λ=5Å. The sulphur positions of the methionine residues M32, M56 and M209 could be determined. An extra sulphur was inserted in the CD-loop in position 105 (cysteine mutant Q105C). MAD experiments allowed to determine this additional sulphur in good agreement with other known positions in this loop (101 and 103). While methionine occurs in nearly every protein, this method combined with cysteine mutants seems to be a powerful tool for structure investigations.

Tu-Pos406

LINEAR DICHROISM OF PURPLE MEMBRANES IN COMPRESSED GELS

((**J. Kappert**, B. Borucki, H. Otto, M. P. Heyn)) Biophys. Group, Phys. Dep., Freie Universität Berlin, Arnimallee 14, D - 14195 Berlin, Germany. (Spon. by M. P. Heyn)

A very efficient method of orienting purple membranes is the gel-squeezing technique, introduced by Abdourakhmanov et al.[1]. We reached an absorption anisotropy up to -0.34 for the main absorption band of the bR groundstate at 570nm. As a function of the compressing factor we obtained higher order parameters than the theory of Ganago et al.[2] predicts, even assuming the maximum of 90° for the angle θ between the transition dipole moment and the membrane normal. From the anisotropy of -0.34 with the maximal possible order parameter of 1 we conclude that θ must be larger than 71°. Time resolved measurements indicate that the photocycle is not perturbed by the pressing. The changes in the chromophore angle between the groundstate and the intermediates K,L and M are in agreement with measurements on magnetically oriented samples. Steady state measurements of the acid blue and the pink form show that the chromophore angle in the pink state is about 2° larger than in the blue state.

[1] Abdourakhmanov, I.A.; Ganago, A.O.; Erokhin, Yu.E.; Solov'ev, A.A.; Chugunov, V.A. (1979) *Biochim. Biophys. Acta* **546**, 183-186
[2] Ganago, A.O.; Fok, M.V.; Abdourakhmanov, I.A.; Solov'ev, A.A.; Erokhin, Yu.E. (1980) *Mol. Biol. (Mosc.)* **14**, 381-389

Tu-Pos407

SOLID-STATE NMR STUDIES OF THE ARGININE RESIDUES IN THE PROTON-MOTIVE PHOTOCYCLE OF BACTERIORHODOPSIN.

((**A.T. Petkova**, B.Q. Sun, M. Bizounok, J.G. Hu, R.G. Griffin, and J. Herzfeld)) Dept. of Chemistry, Brandeis University, Waltham, MA 02254, Dept. of Chemistry and Francis Bitter Magnet Laboratory, Massachusetts Institute of Technology, Cambridge, MA 02139.

Previous ^{15}N solid-state NMR studies of [$\eta_{1,2}$-$^{15}N_2$]Arg-bR in 0.1 M NaCl at pH=10 revealed the development of 'wing' peaks in the M photointermediate, which arise from a single arginine residue. These 'wing' peaks have since been observed in the M state trapped in NaBr and NaI at pH=10, in the acid blue form obtained in HCl at pH=2, and in the acid purple form obtained in HCl at pH=0. Additional spectra of [α-^{15}N]Arg-bR showed that changes in the M intermediate also include perturbation of an arginine peptide bond. CPECHO/REDOR difference spectroscopy of [1-^{13}C]Ala, [α-^{15}N]Arg-bR has isolated signals from the Ala81-Arg82 peptide linkage. Both ^{15}N and ^{13}C spectra showed two distinct resonances in the resting state of the protein, which may be related to crystallographic evidence for disorder in the Arg82 sidechain. Shifts of these signals in the M state are small, which indicates that the pertubation of the peptide backbone observed earlier is occurring at a different arginine residue. Further studies are in progress to identify this peptide bond, as well as the sidechain responsible for the guanidyl 'wing' peaks.

Tu-Pos408

SOLID STATE NMR DETECTION OF LOCAL STRUCTURAL CHANGE IN THE BACTERIORHODOPSIN PHOTOCYCLE

((J.G. Hu, B.Q. Sun, M. Bizounok, R.G. Griffin and J. Herzfeld)) Department of Chemistry, Brandeis University, Waltham, MA 02254 and Department of Chemistry and Francis Bitter National Magnet Laboratory, Massachusetts Institute of Technology, Cambridge, MA 02139.

Selectively detecting a specific active site in a large protein, such as bacteriorhodopsin (bR), is a challenge because it is difficult to specifically label one particular amino acid residue among many. In bR, there are 21 valine residues, six of which occur in the F-helix and one (Val49) in the middle of the B-helix and the proton channel. Electron diffraction indicates that the F-helix tilts away from the membrane normal during the photocycle, opening the cytoplasmic side of the proton channel. There is also evidence that Val49 plays important roles in proton-pumping and conformational change. The ^{13}C CP/MAS NMR difference spectrum between the LA state and M photointermediate of [1-^{13}C-Val],[^{15}N-Pro]-bR shows that the chemical shifts of at least two valine residues move upfield by at least 3 ppm. This implies that these valine residues are active during the bR photocycle. Selective observation of valines 49, 69 and 199 by heteronuclear dipolar recoupling and valines 179, 180, 187, and 188 by homonuclear dipolar recoupling shows that the chemical shifts of Val49 and the four valine residues in the F-helix (Val179, Val180, Val187 and Val188) remain constant during the LA→M transition. Therefore these are not the valine residues responsible for the changes observed in the NMR difference spectrum.

Tu-Pos409

THREE ELECTRONIC STATE MODEL OF THE PRIMARY PHOTOTRANSFORMATION OF BACTERIORHODOPSIN

((W. Humphrey*, **H. Lu***, I. Logunov*, H.-J. Werner#, and K. Schulten*)) *Beckman Institute, UIUC, Illinois and #Institut fur Theoretische Chemie, University of Stuttgart, Germany. (Spon. by R. Gennis)

Ab initio calculations on an analogue of a protonated Schiff base of retinal *in vacuo* reveal two closely lying excited states S1 and S2, the potential surfaces of which intersect along the reaction coordinate through an avoided crossing, and then exhibit a second weakly avoided crossing or a conical intersection with the ground state surface. The primary trans to cis photoisomerization of retinal in bacteriorhodopsin governed by the three potential surfaces, scaled to match the *in situ* level spacings, are described by means of combined classical/quantum mechanical simulations employing the density matrix evolution method. For a suitable choice of non-adiabatic coupling constants the simulations reproduce the observed photoisomerization quantum yield and predict the first state crossing at T1=330 fs and the crossing to the ground state at 460 fs after light absorption. The first crossing occurs after a 30 degree torsion on a flat S1 surface, while the second crossing follows after a rapid torsion by a further 60 degrees. The three level scenario is corroborated by simulations of D212N and D85N mutants of bacteriorhodospin for which T1 is found to increase by factors eleven and five, respectively, in qualitative agreement with observations.

Tu-Pos410

BINDING PATHWAY OF RETINAL TO BACTERIO-OPSIN; A PREDICTION BY MOLECULAR DYNAMICS SIMULATIONS.

((**B. Israelewits**, S. Izrailev and K. Schulten)) Beckman Institute, Dept. of Biophysics and Dept. of Physics, University of Illinois, Urbana, Illinois 61801

Formation of bacteriorhodopsin from the apoprotein and retinal has been studied experimentally, but the actual pathway, including the point of entry, is little understood. Molecular dynamics simulations provide a surprisingly clear prediction. A window between bR helices E and F in the trans-membrane part of the protein can be identified as an entry point for retinal. Simulated micromechanical manipulations, performed by applying a series of external forces of 200–1000 pN over a period of 0.2 ns to retinal, allow one to extract retinal from bR once the Schiff base bond to Lys216 is cleaved. Extraction proceeds until the retinal tail forms a hydrogen bond network with Ala144, Met145, and Ser183, side groups lining the entry window. The manipulation induces a distortion with a fitted RMS deviation of coordinates (ignoring retinal, water, and hydrogen atoms) of less than 1.9 Å by the time the entry window–retinal tail hydrogen bond network forms. The forces used are consistent with the friction expected for fast extraction and do not indicate significant potential barriers. We therefore suggest that the path followed in the simulated extraction of retinal also describes the binding of retinal. The simulation reveals that movement of a water molecule inbetween Lys216 and retinal's aldehyde group initiates unbinding. Water molecules also participate in hydrogen bond breaking on retinal entry into bacterio-opsin involving side groups. The simulations are consistent with the observed formation of stable water structures in retinal's binding site and with the observed pKa-dependence of retinal binding.

Tu-Pos411

Studies of Cation Binding in $ZnCl_2$ Regenerated Bacteriorhodopsin by XAFS

Ke Zhang#, Li Song*, Jun Dong#, and M. A .El-Sayed*
Illinois Institute of Technology, * Georgia Institute of Technology

The binding of Zn^{2+} in Zn^{2+} regenerated bacteriorhodopsin was studied under various conditions by X-ray absorption fine structures (XAFS). It was found that in aqueous bR solution, Zn^{2+} has an average of six oxygen or nitrogen ligands. Upon drying, two ligands are lost, suggesting the existence of two weakly bound ligands near the cation binding site in bacteriorhodopsin. When excess Cl^- ions were present before drying in the Zn^{2+} regenerated bR samples, it was found that two of the ligands are replaced by Cl^- ions in the dried film while two remain unchanged. The above observations suggest that Zn^{2+} has three types of ligands in regenerated bR (referred to as type I, type II and type III). Type I ligands are strongly bound. These ligands cannot be removed by drying but can be replaced by Cl^- ligands. Type III ligands are weakly bound to the metal cation and are most likely water molecules that can be removed by evaporation under vacuum or by drying with anhydrous $CaSO_4$. The results are discussed in terms of the possible binding sites of Zn^{2+} in bR.

The research is supported by DOE Grant DE-FG03-88ER-13828 and NIH Grant GM-47534.

OPTICAL SPECTROSCOPY

Tu-Pos412

MEMBRANE POTENTIAL CHANGES MEASURED FROM EMISSION SPECTRAL SHIFTS OF DI-8-ANEPPS USING WHOLE-CELL PATCH-CLAMP ((C.E. Davis, W.Y. Kao, J.M. Beach)) Department of Biomedical Engineering, University of Virginia Health Science Center, Charlottesville, VA 22908. (Spon. by R.C. Bogaev)

Voltage-sensitive dyes are used to monitor transmembrane potentials from cells *in vitro* and in intact organs. Transmembrane potential changes cause spectral shifts of fluorescence excitation and emission spectra of the voltage dye di-8-ANEPPS. Although dual-wavelength excitation has been employed for measurements in cells using the excitation shift mode, similar use of the emission shift mode has not been widely exploited. We have used the whole-cell patch-clamp technique to produce step changes in transmembrane potential while monitoring fluorescence changes produced by emission spectral shifts. Small cell lung cancer and bovine adrenal chromaffin cells labeled with di-8-ANEPPS (0.2-1 mM) were held at hyperpolarizing potentials of -80 mV and step-depolarized from -60 to + 90 mV for 5 seconds. Fluorescence was recorded simultaneously at 560 and 620 nm using a dual photomultiplier detector. In response to depolarization, opposing changes in fluorescence intensity from each channel were detected. An increase in the 560 nm signal and a decrease in the 620 nm signal corresponded to a blue-shift in the emission spectrum. The change in the fluorescence ratio F_{620}/F_{560} was proportional to the size of the membrane potential change. These results show continuous membrane potential recordings from cells can be obtained with single wavelength excitation of di-8-ANEPPS by exploiting shifts in the emission spectrum. Supported by HL49593.

Tu-Pos413

TRANSITION MOMENT DIRECTIONS IN AMIDE CRYSTALS ((Robert W. Woody)) Dept. Biochemistry & Molecular Biology, Colorado State Univ., Fort Collins, CO 80523.

Transition moment directions are critical for predicting CD and absorption spectra. Single-crystal polarized reflection spectra of a primary amide (propionamide, **1**) and a secondary amide (N-acetylglycine, **2**) have recently been analyzed, yielding transition moment directions for the first (NV_1) and second (NV_2) $\pi\pi^*$ transitions (L. Clark, *J. Am. Chem. Soc.* **117**, 7974 (1995)). In terms of the angle θ, measured from the C=O bond with the C-N bond at positive θ, the directions for the NV_1 transitions are -35° for **1** and -55° for **2**. INDO/S MO calculations give NV_1 transition moment directions that are too positive by 10° and 19° for **1** and **2**, respectively. When the mixing of excited states due to the crystal field and to dynamic correlations (exciton effect) are considered, the discrepancies are reduced to 0° and 13°, respect-ively. For the NV_2 transitions, the discrepancies are decreased from -13° to -3° for **1** and from -8° to -6° for **2**. Simplified charge models have been developed that give results for crystals of **2** essentially equivalent to those obtained with the detailed charge model. The method used in the prediction of the CD and absorption spectra of polypeptides for calculating the mixing of excited states under the influence of a static field was tested on crystals of **2** with satisfactory results. Calculations for an amide group in the middle of a 20-residue α helix give θ = -42°. (Supported by NIH grant GM22994 and by a Fogarty Senior International Fellowship, TW02122)

Tu-Pos414

TRANSIENT THERMAL PHASE GRATING SPECTROSCOPY AND THE CALORIMETRY OF REACTION CENTERS. ((M. McCauley[1,3], B. Luther[2], S.-Y. Tang[3*], C.C. Schenck[3], N.E. Levinger[2#]))[1]Dept. Physics,[2]Dept. Chemistry and [3]Dept. of Biochemistry and Molecular Biology, Colorado State University, Fort Collins, CO 80523.

The process of bacterial photosynthesis is understood to involve a bacteriochlorophyll-binding protein, the reaction center, that converts electromagnetic energy into chemical energy by catalyzing light-induced charge separation. However, the mechanism of this process has not been agreed upon. Theory suggests a relationship between reaction rate and energetics (and other parameters). The rapid rate of the first stages of the charge separation (typically 10^{-12}s) has made the energetics, and even the very path of the electron, difficult to determine.

The technique of transient thermal phase gratings offers a direct measurement of the dynamics and thermodynamics of photochemically-reactive systems. In this approach, degenerate pump laser pulses with different k vectors are temporally and spatially-overlapped in a resonant liquid sample, creating a spatially-modulated excited state population. Subsequent energy relaxation (primarily due to electron transfer, vibrational relaxation and internal conversion in reaction centers) releases heat into the nearby solvent. The spatially-modulated heat release causes a local variation in sample density and refractive index, which in turn serves as a diffraction grating for a nonresonant probe pulse as it impinges on the excitation region at the Bragg angle. Since the diffracted probe pulse is detected against zero background, the method is exquisitely sensitive, and it is capable of time-resolution approaching the acoustic period between fringes. By properly accounting for the terms driving the time-dependent index changes, one can extract the time-dependent energetics of the system. Results from simulations and recent experiments on reaction centers will be presented. Support by NIH, NSF and DOE. *NIH NRSA Fellow. #NSF NYI.

Tu-Pos415

PROTEIN STRUCTURAL CHANGES STUDIED BY NEAR-FIELD SPECTROSCOPY. ((M.K. Lewis, P. Wolanin, A. Gafni, D.G. Steel)) Institute of Gerontology, University of Michigan, Ann Arbor, MI 48109

Many critical structural biology questions such as those relating to studies of protein folding, transport, and interaction, are difficult to study with traditional experimental techniques. This results from the lack of synchrony that exists in traditional experiments which obtain information from averages over large ensembles. To address this problem we have been developing a new spectroscopic approach using the technique of near-field scanning optical microscopy (NSOM) to obtain structural information using spectroscopy rather than imaging. With a literature demonstrated spatial resolution as small as 12 nm and localization potentially as small as 1 nm, NSOM makes possible experiments designed to obtain structural information at the single protein level. Our studies focus on the development of this methodology with particular emphasis on its application to membrane bound proteins. Specific experiments include examination of large molecular motions such as those proposed during the functioning of ADP/ATP translocase and ATP synthase. Refinement of this technique will yield the ability to study protein interactions in a single cell. Studies of protein interactions *in vivo* are hampered by the difficulty in differentiating between the large number of different proteins present. Unfortunately, experiments on single proteins *in vivo* are difficult using present NSOM technology due to its limited depth of field. However, using two and three photon excitation the depth of field becomes limited to the order of the transverse resolution limit, thus providing a means to suppress optical excitation of proteins in the cell far below the membrane surface. These experiments could provide information on the sequence of folding events during and following protein translocation such as the translocation of alkaline phosphatase across the E. coli periplasmic membrane.
Supported by ONR N00014-91-J-1938 and NIA 2 T32 AG 00114-11.

Tu-Pos416

CONSTRUCTION AND CHARACTERIZATION OF PHOSPHOLIPID-ALKANETHIOL HYBRID BILAYER MEMBRANES. ((**C. W. Meuse** and A. L. Plant)) NIST, Gaithersburg, MD 20899.

A cell membrane is made up of an array of different molecules which influence each other in many intricate ways. Insights into the structures and functions of the components of the cell membrane are critical for understanding and controlling disease, drug delivery, integral membrane protein behavior and biosensor development. One method to simplify the complex cell membrane system is to produce a model phospholipid-alkanethiol hybrid bilayer on gold. The gold surface provides an electrode capable of monitoring the transport properties of the membrane as well as an internal standard for the determination of the orientation of membrane components. Most of the early work on planar bilayer systems has been conducted in aqueous environments. In order to obtain a more complete understanding of the structure, we have devised a method for the construction of phospholipid-alkanethiol hybrid bilayer membranes at an air-gold interface using a novel Langmuir-Blodgett transfer technique to coat a lipid monolayer onto the hydrophobic surface of a self-assembled alkanethiol-gold system. The hybrid bilayer membrane at the air-gold interface was carefully characterized using atomic force microscopy, X-ray photoelectron spectroscopy, and reflection-absorption infrared spectroscopy. These techniques reveal that the lipid overlayer induces structural changes in the self-assembled alkanethiols which are dependent on the length of the alkanethiol chains and that the lipid layer has an ordered structure similar to the well-packed structure of self-assembled alkanethiol systems.

Tu-Pos417

COMPARISON OF INFRARED METHODS TO STUDY THERMAL INDUCED STRUCTURAL CHANGES IN PROTEINS: ATR VS. TRANSMISSION SPECTROSCOPY ((J.J. Unruh, T.F. Kumosinski and Harold F. Farrell, Jr.)) ERRC, USDA, Wyndmoor, PA 19038-8598

FTIR has become a tool for the protein chemist to study the global secondary structure of proteins and their changes due to environmental stress. But for the novice the choice of which method to obtain the spectra may not be clear.

We have been studying the thermal induced changes in lysozyme and β-lactoglobulin using an ATR (Attenuated Total Reflectance) microcircle device and a traditional 6μm pathlength CaF_2 transmission cell. The 6μm pathlength CaF_2 transmission cell was prone to sample leaks from the spacer and upper gasket when filling and during acquisition of data at elevated temperatures (>50°C), and may exhibit window-protein interaction. Loss during acquisition required repeating the experiment. These factors were not present with the ATR device. Working in H_2O solutions, the ATR does not require as concentrated solutions as required by the transmission cell, and has the ability for greater sample recovery — an advantage when analyzing a protein of limited availability. The repeatable pathlength inherent in the ATR device made for easier spectral comparisons not obtained without necessary compensation for pathlength differences required with the transmission cell. Overall our results show the ATR microcircle device to be easier to use, and most likely to produce reliable data with fewer complications in a shorter time period.

Tu-Pos418

TETRAMETHYLRHODAMINE (TMRM) QUENCHING OF CALCEIN FLUORESCENCE LIMITS THE EVALUATION OF THE INTRACELLULAR DISTRIBUTION OF CALCEIN.

((**Valeria Petronilli**,[*] Gianni Miotto,[#] Raffaele Colonna,[1*] Paolo Bernardi,[1*] and Fabio Di Lisa[*#])) CNR Unit for Biomembranes[*] and and Depts of Biochemistry[#] and Biomedical Sciences[1], University of Padua, Italy. (Spon. by D. Pietrobon)

It has been proposed that the filling of mitochondria with calcein could be used to monitor the mitochondrial permeability transition (MTP) in situ even in cells loaded with other probes. We studied the interactions between calcein and TMRM which is commonly used to monitor the mitochondrial membrane potential. The fluorescence emission of an aqueous calcein solution (50 μM) was totally quenched by equimolar amounts of TMRM. Under these conditions the emission peak of TMRM was increased suggesting a process of energy transfer. A similar interaction could be observed in rat liver mitochondria loaded with calcein-AM. The calcein emission at 508 nm (exc = 488) was decreased by TMRM addition and was then restored by uncoupling agents. Finally, when we studied calcein-AM loaded hepatocytes by means of confocal microscopy, we consistently observed a diffuse cellular fluorescence with rare round fluorescent voids. The diffuse calcein fluorescence became punctate upon the addition of TMRM. Each void in the calcein fluorescence colocalized with a bright spot in the TMRM fluorescence channel. In conclusion, in double labelling experiment the colocalization of calcein with TMRM can hamper the reliability of this approach for the study of MTP in situ.

Tu-Pos419

PHOTOPHYSICAL CHARACTERIZATION OF THE DYE CY-5 BY FLUORESCENCE CORRELATION SPECTROSCOPY.

((**Jerker Widengren**,[*] Petra Schwille,[* #] and Rudolf Rigler[*])) [*] Dept. Medical Biophysics, MBB Karolinska Institute, S-171 77 Stockholm, Sweden and [#] Dept. Biochemical Kinetics, Max-Planck Institute for Biophysical Chemistry, D-37077 Göttingen, Germany

For immunofluorescence and ultrasensitive fluorescence detection purposes near-infrared (NIR) cyanine dyes have become popular owing to their relative brightness and the reduced level of cell autofluorescence at their absorption wavelengths. Also, the instrumentation for NIR fluorescence detection can be made very simple by use of inexpensive laser diodes and avalanche photodiodes. Although used frequently as a label in many different fluorescence microscopy studies, very few investigations concerning the photophysical properties of Cy-5 have been undertaken. It has earlier been shown how FCS provides a useful tool to investigate triplet state properties of dyes as well as their photodestruction yields. In this investigation, Fluorescence Correlation Spectroscopy (FCS) was used to determine these properties of Cy-5. In addition, fluorescence fluctuations arising due to trans-cis isomerization could be used to determine rates of isomerization and back-isomerization taking place in the hydrocarbon chain connecting the two headgroups of the dye. This study illustrates the use of FCS to photophysically characterize dye molecules.

Tu-Pos420

SPATIALLY-LOCALIZED BALISTIC TWO-PHOTON EXCITATION IN SCATTERING MEDIA.

((**H. Szmacinski**, I. Gryczynski and J.R. Lakowicz)) Center for Fluorescence Spectroscopy, Univ. of Maryland at Baltimore, Dept. Of Biochemistry & Molec. Biology, 108 N. Greene St., Baltimore, Maryland 21201, (Spon. R. Agbaria)

Using femtosecond pulses at 770 nm from a Ti:Sapphire laser, we were able to provide two-photon excitation of fluorophores in capillary tubes under up to 2 mm of 0.5% intralipid suspension. Displacement of the laser beam relative to the embedded samples indicates that highly localized excitation was possible with two-photon excitation, whereas one-photon excitation resulted in loss of spatial resolution due to excitation by the diffusely scattered photons. These results indicate that two-photon excitation in the scattering solution is due only to the ballistic photons, a result confirmed by frequency-domain time-resolved measurements. Selective excitation of adjacent samples was found possible for two but not one-photon excitation.

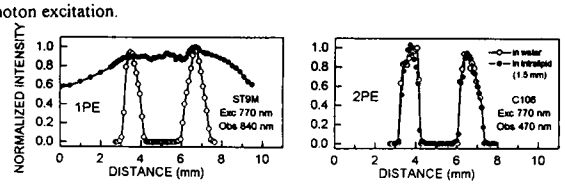

Tu-Pos421

MAPS FOR KAPPA-SQUARED

((**B. Wieb Van der Meer**)) Western Kentucky University, Bowling Green, KY 42101, and Vanderbilt University, Nashville, TN 37232.

Formulas have been derived for maximum and minimum values for kappa-squared in terms of d, a and θ: d is the depolarization factor for the donor, a is that for the acceptor, and θ is the angle between the donor and acceptor axes. There are two cases: θ=known and θ≠known. The figure below refers to the case θ≠known. In each region of this "map" the minimum and maximum is given by a simple expression linear in a and d, except in the parallellogramlike region where the minimum is not linear.

In the case θ=known the minima and maxima are given by 6 different formulas, 5 of which are not linear, and the borders between the regions depend on θ. Using such maps in the two cases is an alternative for using the contour plots derived by Dale *et al.* (Biophysical. J. 26(1979) 161-194).

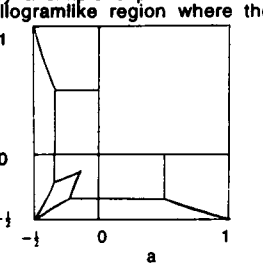

Tu-Pos422

FREQUENCY-DOMAIN PUMP-PROBE STIMULATED EMISSION SPECTROSCOPY USING A FLUORESCENCE MICROSCOPE. ((**C. Y. Dong**, C. Buehler, P. T. C. So, and E. Gratton)) Laboratory for Fluorescence Dynamics, Department of Physics, University of Illinois at Urbana-Champaign, 1110 West Green Street, Urbana, IL 61801.

We developed a pump-probe stimulated emission system for spectroscopic studies inside a microscope. Our pump-probe technique involves focusing two pulsed laser beams onto a fluorescent sample. One laser, the pump, is used to excite the fluorophores. The other laser, the probe, is used to induce stimulated emission from the molecules in the excited state. The repetition frequencies of the two lasers are offset by an amount small compared to the base laser repetition frequency; this results in a signal at the difference frequency between the two lasers and corresponding harmonics. There are several advantages of this technique. First, the high frequency content of pulsed lasers can be analyzed at a very low frequency. As a result, fast optical detectors are not needed to investigate ultrafast molecular phenomena. Second, optical overlapping of two laser beams is efficient inside the microscope. With relatively high numerical aperture objectives, tight focusing and effective signal collection can be achieved. Consequently, low laser power is necessary to observe the pump-probe stimulated emission effect. Furthermore, multiple harmonics can be acquired simultaneously resulting in reduced data acquisition time and improved signal-to-noise ratio. The instrument's temporal resolution is determined by the laser pulse width and relative jitter between the two lasers. We present time-resolved spectroscopic data acquired with this instrument including lifetime and polarization. (This work was supported by NIH RR03155.)

Tu-Pos423

FREQUENCY-DOMAIN LIFETIME SPECTROSCOPY IN THE MULTIPLE SCATTERING REGIME. ((**A Cerussi**, S. Fantini, M. A. Franceschini, and E. Gratton)) Lab for Fluorescence Dynamics, Department of Physics, University of Illinois at Urbana-Champaign, Urbana, IL 61801.

The fluorescence lifetime provides a useful quantitative spectroscopic parameter that is sensitive to the fluorophore local environment. A distinct advantage of the fluorescence lifetime over the fluorescence intensity lies with the independence of the lifetime with respect to the fluorophore concentration. A variety of fluorophores exist that exhibit measurable lifetime changes while in the presence of physiologically relevant analytes such as Ca^{++} and Mg^{++}, and as a consequence of variations in local environment conditions such as pH. There are many potential applications offered by the fluorescence lifetime's sensitivity in highly scattering environments such as tissues that are not amenable to traditional spectroscopic methods. It has recently been demonstrated that a model for fluorescence spectroscopy in multiple scattering media allows the accurate recovery of fluorescence parameters such as the lifetime. In the frequency-domain an analytic expression for the fluorescence signal has been obtained, whereas in the time-domain an analytical expression cannot be obtained. Using this frequency-domain model, we were able to recover the fluorescence lifetime of a uniformly distributed fluorophore from within a multiple scattering medium. The sensitivity of this method for lifetime determination is also discussed. This work is supported by NIH grants RR03155 and CA57032, and also a joint Whitaker-NIH grant RR10966.

Tu-Pos424

MEASUREMENT OF ABSOLUTE FLUORESCENCE QUANTUM YIELD IN TURBID MEDIA. ((**T. French**[†], A. E. Cerussi[‡], S. Fantini[‡], M. A. Franceschini[‡], and E. Gratton[‡])) [†]Advanced Optical Instrumentation Group, Sandia National Laboratories, Albuquerque, NM 87185-0986 and [‡]Laboratory for Fluorescence Dynamics, Dept. of Physics, University of Illinois at Urbana-Champaign, Urbana, IL 61801.

We demonstrate the measurement of the absolute fluorescence quantum yields performed inside a multiple scattering medium. A model for frequency-domain fluorescence spectroscopy in multiple scattering media that allows the accurate recovery of fluorescence parameters such as the quantum yield has recently been verified. Our work uses this model to determine the absolute quantum yield of a fluorophore that is uniformly distributed throughout a multiple scattering medium. Using this technique, it is not necessary to have a reference fluorophore of known quantum yield. The only reference compound that is necessary is one which is used to calibrate the spectral response of the detection system. This technique does not require the calibration of the excitation and emission light paths. Because of the multiply scattering of the medium (titanium dioxide particles suspended in water), the excitation and emission geometries are identical. We present the quantum yield of Rhodamine B in water measured in both infinite and semi-infinite geometries. Supported by NIH RR03155 and CA5702, a joint Whitaker-NIH grant RR10966, and Sandia CRADA SC93/01177.

Tu-Pos425

SIMULTANEOUS MEASUREMENT OF TIME RESOLVED FLUORESCENCE OF BOTH LINEARLY POLARIZED COMPONENTS OF ALL WAVELENGTHS IN AN EMISSION SPECTRUM. ((Lisa A. Kelly[†], John G. Trunk, Denise C. Monteleone, and **John C. Sutherland**)) Biology Department, Brookhaven National Laboratory, Upton, NY 11973

We describe a system that records the temporal profile of both linear polarization components of all wavelengths in a fluorescence emission spectrum simultaneously. Our excitation source was the vacuum ultraviolet storage ring of the National Synchrotron Light Source at Brookhaven National Laboratory, which provides a continuous spectrum of ultraviolet, visible and near-infrared light consisting of $\approx$ 1.5 ns full width at half maximum pulses at a repetition rate of $\approx$ 50 MHz, and with identical temporal profiles at all wavelengths, although any source with similar temporal properties could be used. A single excitation wavelength is selected by a monochromator and polarized before reaching the sample. Fluorescence can be monitored either along an axis perpendicular to the excitation beam, or at near normal incidence. A polarizer divides the fluorescence into components with polarizations parallel and perpendicular to the polarization of the incident beam. The emission spectrum is dispersed with an imaging spectrograph, and detected with a position sensitive photomultiplier operated in a single photon counting mode. The time of arrival of a photon is derived from signals originating in the "dynodes" of the photomultiplier, while the location of the centroid of the electron swarm on the position sensitive anode of the detector indicates both the wavelength and polarization of the detected photon. †Present address: Dept. of Chemistry, University of Maryland, Baltimore County Research Supported by the Office of Health and Environmental Research, USDOE. LAK was a DOE Distinguished Postdoctoral Fellow.

MICROSCOPY

Tu-Pos426

TRANSIENT INTRACELLULAR ALKALOSIS MEASURED IN EARLY ISCHEMIA IN RABBIT PAPILLARY MUSCLE USING CONFOCAL FLUORESCENT MICROSCOPY. ((**B.J. Muller-Borer**, H. Yang, J.J. Lemasters, W.E. Cascio)) The University of North Carolina, Chapel Hill, NC 27599.

Hydrolysis of creatine phosphate (CP) during early ischemia is predicted to cause a transient intracellular alkalosis. A novel method used ratiometric confocal fluorescent techniques, with high spatial and temporal resolution, to measure intracellular (pH_i) and extracellular pH (pH_e) in rabbit papillary muscle during arterial perfusion and no-flow ischemia. Cylindrical muscles (diameter=1.6±0.5mm, n=9) were suspended at an ~40° angle in an enclosed controlled atmosphere. Intracellular pH was recorded (n=5) after the muscles were loaded with C-SNARF-1/AM (10 µmol/L). To measure pH_e (n=4) C-SNARF-1 was continuously perfused to the muscle in a modified Tyrodes's solution. Diacetyl monoxime (20 mmol/L) inhibited contraction in the muscles. Single excitation-dual emission fluorescence ratios were acquired with a K2SBIO epifluorescent confocal microscope with cooled CCD camera. During arterial perfusion, the surface and subendocardial pH_i were 7.14±0.08 and 7.16±0.07, respectively. Ischemia was produced by removing O_2 from the atmosphere and arresting flow. During the first 3 min. of ischemia the surface and subendocardial pH_i increased by 0.03±0.02 and 0.05±0.01 units. Subsequently, surface and subendocardial pH_i progressively decreased and reached 6.99±0.10 and 7.03±0.11 after 10 min. By contrast, pH_e only decreased during ischemia and the transient intracellular alkalization was not observed after contemporaneous inhibition of the Na/H exchanger or Na/CO_3 symport. Taken together, these results are consistent with the hypothesis that the changes of pH_i are a result of H^+ producing and consuming processes. Hydrolysis of CP is likely to contribute to a transient intracellular alkalosis in ischemic myocardium. This initial alkalosis can be masked by inhibition of proton transport.

Tu-Pos427

CONFOCAL IMAGING OF TRANSCRIPTION FACTOR LOCALIZATION USING GREEN FLUORESCENT PROTEIN. ((**G. H. Patterson**, S. Schroeder, Y. Bai, K. Gerrish, P. A. Weil, and D. W. Piston)) Dept. of Molecular Physiology and Biophysics, Vanderbilt University, Nashville, TN 37232

The TATA binding protein (TBP) has been suggested to be rate-limiting for transcription *in vivo*. Studies of TBP overexpression indicate that it is not rate-limiting for yeast growth, but this could be due to overexpressed TBP not being localized in the nucleus. To address this issue, viable yeast strains expressing a TBP-green fluorescent protein(GFP) fusion as the sole source of TBP were quantitatively imaged by confocal microscopy. Use of different promoters allowed TBP-GFP to be expressed to 1X, ~20X, and ~30X normal TBP levels. The expression of TBP-GFP in each strain was similar to the TBP expression in the respective strains. For overexpressed strains, the nuclear content of TBP-GFP was limited to ~10-fold greater than wild type concentrations, while the "extra" TBP-GFP was localized throughout the cytoplasm with exclusion from the vacuole. The localization of the TBP-GFP throughout the cell cycle was also followed by time-lapse confocal imaging. Since in *Saccharomyces* the nuclear membrane does not disassemble during mitosis, the TBP-GFP remained localized to the nucleus. One surprising result from these studies was the unequal sharing of TBP-GFP between mother and daughter cells, resulting in a lower initial concentration in the buds. The TBP-GFP levels in the daughter cells reached mother cell concentrations within 30 min. The decreased TBP content in these buds suggests a lower limit for TBP in viable cells. We are currently working with yeast strains that underexpress the TBP-GFP to determine the lower limit of TBP acceptable for cell viability.

Tu-Pos428

DIRECT OBSERVATION OF SHEAR-INDUCED STRUCTURES IN WORM-LIKE MICELLES: A FREEZE-FRACTURE ELECTRON MICROSCOPY STUDY. ((**S.L. Keller**, P. Boltenhagen, D.J. Pine and J.A. Zasadzinski)) Department of Chemical Engineering, University of California, Santa Barbara.

Surfactant molecules in water above their critical micellar concentration (CMC) aggregate in spherical or elongated worm-like micelles (living polymers). Like shear-thickening polymer solutions, the apparent viscosity of some worm-like micellar solutions increases with the shear rate and/or the duration of shear. We present the first report of freeze-fracture experiments on worm-like micellar solutions which enables us to definitively describe the microscopic structure of unsheared and sheared micellar solutions. When unsheared, two different solutions appear as an entangled network containing polydisperse water cells of diameter ≤ 3 μm. When these solutions were sheared and formed a gel-like phase, they exhibited two distinct structures as recently predicted[1]. The first shear-induced structure consisted of a background network of entangled micelles whose water cells were more homogenous than in the unsheared sample. This background was riddled with the second structure, fractures containing aligned micelles. Regions of aligned micelles probably have low viscosity, suggesting that for the sheared system to flow it broke into islands of entangled networks which flowed with respect to each other. The fractures are separated by a length scale of ~5μm.

1. C.H. Liu and D.J. Pine,*Phys. Rev. Lett.* **77**, 2121-2124 (1996).

Tu-Pos429

IMAGING THE ELECTROCYTE OF *TORPEDO MARMORATA* BY SCANNING FORCE MICROSCOPY ((**L.I. Pietrasanta**†*, A. Schaper†, G.Q. Fox§, F.J. Barrantes*, and T.M. Jovin†,‡)) †Department of Molecular Biology, § Electron Microscopy Group, Max Planck Institute for Biophysical Chemistry, P.O. Box 2841, 37018 Göttingen, Germany. *Instituto de Investigaciones Bioquimfcas, C. C. 857, 8000 Bahía Blanca, Argentina.

Scanning force microscopy (SFM) and scanning electron microscopy (SEM) were used to examine the tissue structure of the electric organ of *Torpedo marmorata* in air and in liquid after applying fracturing and cryosectioning techniques and chemical fixation. The electric organ is organized in columns of stacked electrocytes, arranged in a honeycomb pattern. The columns were cut along a plane normal to the cell stack and thin sections were transferred to polylysine coated glass cover slips. The polarity of the electrocytes was made apparent by immunofluorescence microscopy directed to different domains of the acetylcholine receptor (AChR), thus revealing the innervated face of the cell. The SFM was operated under ambient conditions (18-27 °C, relative humidity 15-40%) in the permanent contact mode (with and without feedback electronics i.e. in the isoforce mode for measurements of the topography or in the error mode), and in the tapping mode. SFM and SEM both showed cell surfaces to be overlaid by a network of collagen fibers by their characteristic banding pattern with ~64 nm periodicity and ~2.5 nm corrugation amplitude. In liquid, significantly lower structural resolution was achieved by SFM, probably due to sample elasticity.

Tu-Pos430

SCANNING PROBE MICROSCOPY OF SOFT SAMPLES: COMPARISON OF AFM WITH SICM. ((M. Milovanovic, Y.E. Korchev[1], M.J. Lab[1] and C.L. Bashford)) Div. Biochemistry, St. George's Hosp. Med. Sch., London SW17 0RE & Dept. of Physiology, Charing Cross and Westminster Med. Sch., London W6 8RP.

Currently there is a great interest in applying scanning probe microscopy to the imaging of soft biological samples such as cells, cellular organelles and macromolecules in liquids. The atomic force microscope (AFM) is already an established instrument which has been used to study the topography, micromechanical properties of biological material and binding forces between macromolecules. The scanning ion-conductance microscope (SICM), which utilises a glass micropipette as the sensitive probe, can image the topography of biological samples and may also be used for probing other properties of the surface at precise locations. The probe of the SICM registers ion current without having an intimate physical contact with the sample. We have compared atomic force microscopy and scanning ion-conductance microscopy using soft polymer films containing very small pores. SICM images this material as reliably as AFM.

We are grateful to Mr D Rogerson of Nanovision (Quesant UK) for the loan of the AFM stage and BBSRC and British Heart Foundation for financial support.

Tu-Pos431

DNA KINKS IN AQUEOUS BUFFERS AS IMAGED WITH A NOVEL HIGH-RESOLUTION AFM ((Wenhai Han,* Mensur Dlakic,† Rodney E. Harrington† and **Stuart M. Lindsay***)) *Department of Physics and Astronomy, Arizona State University, Tempe, AZ 85287-1504; †Department of Biochemistry, School of Medicine, University of Nevada at Reno, Reno, NV 89557-0014. (Sponsored by S. M. Lindsay)

A novel form of Atomic Force Microscope (AFM) with a magnetically-oscillated tip (MacMode) provides unprecedented resolution of small DNA fragments spontaneously adsorbed to mica in the presence of divalent cations and imaged *in situ*. Kinks (localized bends larger than 45°) were observed only in axially strained mini circles and their frequency was highly dependent on the ionic environment. The average kink angle was 78 ± 22°. In the presence of Zn ions the number of kinks increased four times on average compared to the buffer with Mg ions only. In the buffer containing both Zn and Mg ions at near-physiological concentrations, we observed approximately the same number of kinks as in Zn alone. This has important implications regarding the effects of axial strain and ionic conditions on the local DNA structure. The spectral analysis of measured intervals between kinks suggests that they bend DNA into both the major and minor grooves.

Tu-Pos432

DETECTION OF RECOGNITION EVENTS ON BIOLOGICAL SAMPLES WITH FORCE MICROSCOPY. ((**P. Hinterdorfer**, K. Schilcher, H.J. Gruber, W. Baumgartner, and H. Schindler)) Institute for Biophysics, University of Linz, A-4040 Linz, Austria.

Antibodies were covalently bound to tips of an atomic force microscope (AFM) via a spacer molecule for the localization of antigenic sites (PNAS (1996) 93, 3477). For applications of this method as a general tool in biology the biological sample has to be strongly attached to flat surfaces. Different strategies for the binding of proteins to atomically flat surfaces (mica, template-stripped gold) were tested using various short- and long-chain crosslinkers. Protein densities were measured and yielded values of $\approx$ 300 - 5000 proteins / μm^2. Cells were immobilized on silicon and mica surfaces via crosslinkers containing binding molecules. The surface concentration increased to $\approx$ 5000 / mm^2 for RBL-cells and $\approx$ 50 / mm^2 for heart cells when WGA or C_{18} were used as binding molecules. The adhesion strength of the cells was measured with a home-built flow apparatus. Topographic AFM-images show cell surfaces and singly resolved channel-proteins (ryanodine receptor) and globular proteins. First applications towards imaging of recognition sites using different AFM-modes are discussed.

This work was supported by the Austrian Research Funds Project S6607 MED.

Tu-Pos433

SUB-PICONEWTON INTERMOLECULAR FORCE MICROSCOPY. ((T. Aoki*, M. Hiroshima*, K. Kitamura*, **M. Tokunaga**+ and T. Yanagida*+)) *Dept. of Biophysical Engineering, Osaka Univ., Toyonaka, Osaka 560 and +Yanagida Biomotron Project, ERATO, JST, Senba-Higashi 2-4-14, Mino, Osaka 562 (Japan). (Spon. by S. Miyamoto)

We refined scanning probe force microscopy with the following distinct advantages: 1) measuring forces with subpiconewton resolution, which is 100 times more sensitive than AFM; 2) keeping the height position of a cantilever constant, which enables non-contact measurement. Handmade cantilevers with a stiffness of approximately 0.1 pN/nm were used. They are more than 1000-fold more flexible than those that are generally used. The thermal bending motion of the cantilever was reduced to less than 1 nm in rms amplitude by exerting laser radiation pressure modulated by a feedback system on it. In addition, the cantilever's position is kept constant even when forces are exerted. This system resolved electrostatic repulsive force of less than a piconewton that is produced in the nanometers gap between a positively charged probe and a positively charged glass surface. It was also clearly observed that the attractive force between a hydrophobic probe and a hydrophobic glass surface acts in a range of as long as 100nm. Thus, our unique system allows one to detect the intermolecular force of subpiconewton order by controlling the gap between the probe and the material surface with nanometer accuracy.

Tu-Pos434

A RECONSIDERATION OF THE EFFECT OF CALCIUM ION INFLUENCE ON THE STRUCTURE OF DPPC MULTILAMELLAR ARRAYS((**J.M. Collins**)) Physics Department, Marquette University, Milwaukee, WI. 53228-1881.

Numerous investigators have reported on studies of the interaction of divalent metal ions with lecithin vesicles(Bangham and Dawson, BBA59, 1962; Hauser, et al., Eur.J.Biochem.58, 1975; Inoko, et al., BBA413, 1975; and Lis, et al., Biochem.20, 1981). These investigators found a definite correlation between divalent metal cation concentration and structure/swelling properties of various lipid compositions. Parsegian and Rand (Biochem.20, 1981) worked out the electrostatic potential function and the surface charge density distribution for Dipalmitoyl-phosphatidylcholine(DPPC) multilamellar arrays using measured osmotic stress versus bilayer separation data from x-ray diffraction studies. Among others, Ohshima et al. (J.Coll.Inter.Sci., 86, 1981) worked out the binding constants of Ca^{2+} and Mg^{2+} in DPPC aqueous mixtures. The take home message is that over a limited range of Ca^{2+} aqueous concentration, Ca^{2+} associates with the head groups of DPPC in aqueous suspension leading to structure/swelling function changes observable by several experimental techniques including XRD, DSC, neutron diffraction, and electrophoresis. We will report on a temperature study of DPPC suspensions in aqueous $CaCl_2$ suspensions involving both small angle x-ray diffraction and polarized light microscopy. The x-ray diffraction data yields the liquid crystalline parameters associated with the multilamellar array which is consistent with previously reported studies. The light microscopy demonstrates some curious domain changes in the gross structure of the arrays following heat treatment.

Tu-Pos435

FAST SPATIALLY RESOLVED FLUORESCENT MEASUREMENTS WITH MULTIPOINT IMAGING PHOTOMETER. ((**A.A. Dromaretsky**[1], S.I. Kabanchenko[1], A.F. Fomina[2])) [1]Bogomoletz Inst. Physiol., Kiev, Ukraine & [2]Allegheny Univ. of Health Sci., Philadelphia, PA 19129. (Spon. by I. Levitan)

Here we describe a Multipoint Imaging Photometer (MIP) system based on an Imaging Dissector Tube (IDT). This system has the advantages of a common photometer combined with imaging capabilities. The image spatial resolution of the MIP system is set to 50 X 50 pixels to compromise between image quality and speed of scanning. The system permits selection of different pixels within the image (up to eight in present modification) for fast photometric measurements. In some respects the MIP system can exceed both an imaging system and a photometer. The system has broader dynamic range (20 bit) and better time resolution (up to 1 ms) than common imaging systems. It has a lower level of dark noise (~5 photons/s) than common PMT-based photometers and allows fast photometric measurements from different areas within the image. The MIP system is connected to an IBM-PC parallel port and can be synchronized with electrophysiological and/or other experimental equipment. We have used the MIP system for intracellular Ca^{2+} measurements in cultured bovine chromaffin cells loaded with Fura Red or Oregon Green. Particularly we studied Ca^{2+} oscillations recorded simultaneously from different cells before and after stimulation by nicotine. We conclude that the MIP system would be ideally suited for fast fluorescent measurements of spatially distinct signals such as, for example, presynaptic and postsynaptic Ca^{2+} changes during synaptic transmission.

Tu-Pos436

MAPPING FLUOROPHORE DISTRIBUTIONS IN 3 DIMENSIONS BY QUANTITATIVE MULTI-ANGLE TOTAL INTERNAL REFLECTION FLUORESCENCE MICROSCOPY (MA-TIRFM). ((**B.P. Ölveczky**, N. Periasamy and A.S. Verkman)) U.C.S.F. San Francisco, CA

The exponential decay of evanescent field intensity beyond a dielectric interface depends upon beam incident angle. In principle, the 3-D distribution of fluorophores in an evanescent field can be deduced from TIRFM images obtained at multiple incident angles. Instrumentation was constructed for computer-automated MA-TIRFM using a right angle F2 glass prism (n=1.62) to create the dielectric interface. A laser beam (488 nm) was attenuated by an acousto-optic modulator, and directed to a selected spot in the focal plane on the glass surface. Incident angle was set using 3 micro-stepper motors controlling 2 mirrors and an optical flat. TIRFM images were acquired by a cooled CCD camera for ~0.5 degree steps in incident angle (between the critical angle and 89°). For cell studies, cells were grown directly on the glass prisms (without refractive index-matching fluids) and positioned in the optical path. Images of the samples were acquired at multiple angles, and corrected for beam intensity using "reference" images (at each incident angle) acquired after addition of an aqueous-phase fluorophore which distributed uniformly in the evanescent field. Instrument performance was validated using monolayers of fluorescein-phosphatidylethanolamine on optical surfaces at specified distances from the dielectric interface. Fluorophore z-distribution was determined by inverse Laplace transform of angle-resolved intensity functions. MA-TIRFM was used to resolve with nanometer z-resolution the 3-D geometry of cell-substrate contact for calcein-labeled 3T3 fibroblasts and MDCK cells.

Tu-Pos437

PHOTOLYSIS OF CAGED CALCIUM IN NERVE TERMINALS USING AN ARC LAMP DRIVEN BY A PULSE POWER SUPPLY. ((**Shyue-fang Hsu** and Meyer B. Jackson)) Department of Physiology, University of Wisconsin.

To develop a convenient source of high intensity light in experiments with caged compounds we used a power supply modified by Optiquip (Highland Mills, NY) to drive an arc lamp at approximately 10-times the rated power of the bulb for brief periods of time. When this system was used with a 100 W Hg arc lamp, a one msec pulse of high intensity illumination photolyzed enough caged calcium in a single nerve terminal to elicit large secretion responses. We used this illumination system in the squid giant synapse to photolyze nitrophenyl-EGTA and induce responses qualitatively similar to those induced by illumination with a flash lamp (Hsu, Augustine, and Jackson, Neuron 17, 501-512, 1996). However, the pulse-power system produced larger responses than the flash lamp due to stronger illumination. Postsynaptic currents in the squid synapse, recorded by voltage clamping the postsynaptic cell, decayed with a time constant of 20 msec, which was slightly faster than the decay of the postsynaptic potential recorded under current clamp. We used the same illumination system in nerve terminals of the posterior pituitary, and saw rapid exocytosis and endocytosis. The kinetics of these membrane trafficking processes were qualitatively similar to, but faster than, those elicited by calcium entry through calcium channels (Hsu and Jackson, J. Physiol. 494, 539-553, 1996).

Tu-Pos438

STUDY OF MOLECULAR AGGREGATION BY ANALYSIS OF PHOTON HISTOGRAMS OF SINGLE MOLECULES. ((Yan Chen, Peter T. So and Enrico Gratton)) Laboratory for Fluorescence Dynamics, Dept. of Physics, University of Illinois at Urbana Champaign, Urbana, IL 61801

Molecular aggregation is a crucial regulatory mechanism in biological systems. However, most experimental techniques require relatively high concentrations (from mM to μM). Since many interesting physiological events happen at concentrations below micromolar, we have explored the possibility to detect molecular aggregation in the low concentration range (from μM to pM) using two-photon fluorescence microscopy. Two-photon fluorescence microscopy has an inherent 3-D resolution and using high numerical aperture objectives the excitation volume can be made as small as 0.1 fL, which only contains 0.06 molecules at 1 nM concentration. A small excitation volume is essential for detecting fluorescence fluctuations among molecules. By analyzing the histogram of photons bursts, one can obtain the degrees of aggregation from their distribution (H. Qian and E. Elson, 1990, PNAS, 87, 5479). We model our photon histograms with a simple two species system and compare experimental results to the theoretical predictions. This method of analysis is intrinsically simpler than the technique of fluctuation correlation spectroscopy, which requires the calculation of higher order correlation functions for the multiple species system. (This work was supported by NIH RR03155.)

Tu-Pos439

SINGLE MOLECULE KINETICS USING TOTAL INTERNAL REFLECTION FLUORESCENCE MICROSCOPY AND DIGITAL IMAGING ((**Andrew W. Drake** and Nancy L. Thompson)) Department of Chemistry, University of North Carolina, Chapel Hill, NC, 27599-3290

The heterogeneity of the individual binding and dissociating behavior of proteins on planar membranes is masked by the average off-rates measured with total internal reflection-fluorescence photobleaching recovery. Detecting these reactions at the single molecular level will provide new information about the previously observed heterogeneous protein-membrane binding. In this work we utilize total internal reflection of an argon-ion laser to illuminate surface-bound fluorescent particles in equilibrium between a planar surface and an adjacent solution. The evanescently excited fluorescence emitted by the surface-bound particles is detected by a cooled slow-scan charge coupled device camera. By analyzing consecutive images, a distribution of surface residency times is generated. With this method we have studied avidin-coated fluorescent latex beads binding to biotinylated rabbit IgG applied to a fused silica surface coated with protein A. The model system provides information which will be used to develop future analysis of more biologically pertinent single protein-membrane interactions.

Tu-Pos440

TWO-PHOTON 3-D PARTICLE TRACKING IN CELLS. ((**Timothy Ragan**[1], Peter T.C. So [2] and Enrico Gratton [1])) [1] Laboratory for Fluorescence Dyamics, Dept. of Physics, Universtity of Illinois at Urbana-Champaign, 1110 W. Green St., Urbana, IL, 61801. [2] Dept. of Mechanical Engineering, Massachusetts Institute of Technology, 77 Mass. Ave., Cambridge, MA 02139.

Particle tracking is a powerful method to explore various problems in cell biology. It can be used to study membrane protein and lipid diffusion, cytoplasm compartmentalization, endocytosis of extracelullar proteins and phagocytosis of antigens. In particular, particle tracking experiments have led to a better understanding of the motion and behavior of proteins in the plasma membrane. Unfortunately, most of the particle tracking techniques developed to date have used area detectors and have thus been limited to two-dimensional systems. To address this limitation, we have developed a 3-D particle tracking system that uses the inherent localization of two-photon excitation. We use a feedback system to position the sub-femtoliter two-photon excitation volume to maximize the fluorescence and obtain a series of images from which we construct the 3-D trajectory of the particle. In addition, the images provide information about the local environment of the particle. The axial range of our system is over 30 μm and has a frequency response of approximately 50 Hz. It is capable of tracking particles across the length of most cells and with a frequency response sufficient to follow many cellular processes. To illustrate the capability of our instrument, we present data on the endocytotic pathway of macrophage cells. [This work was supported by NIH RR03155.]

Tu-Pos441

MULTI-PHOTON EXCITATION FLUORESCENCE MICROSCOPY AND SPECTROSCOPY OF *IN VIVO* HUMAN SKIN. ((**Barry R. Masters**[1], Peter T. C. So[2,3], and Enrico Gratton[2])) [1]Department of Anatomy and Cell Biology, Uniformed Services University of the Health Sciences, Bethesda, MD 20814 USA [2] Laboratory of Fluorescence Dynamics, Department of Physics, University of Illinois at Urbana, Illinois 61801 USA [3]Present address: Department of Mechanical Engineering, Massachusetts Institute of Technology, Cambridge, MA 02139 USA

Multi-photon excitation microscopy at 730 nm and 960 nm was used to image the autofluorescence of *in vivo* human skin from the surface to a depth of about 200 microns. The emission spectra and fluorescence lifetimes were determined. We have imaged the fluorescent cytoplasm of individual skin cells at depths of between 25 to 75 μm below the skin surface for both excitation wavelengths. Fluorescence emission spectra and fluorescent lifetimes of the tissue were obtained at single points, relative to the surface (0-50 microns) and at deeper depths (100-150 microns). The source of the fluorescence emission spectra and fluorescence lifetimes are consistent with reduced pyridine nucleotides, NAD(P)H, as the primary source of the skin autofluorescence using 730 nm excitation. With 960 nm excitation, fluorescence emission at 520 nm indicates the presence of flavoprotein contribution. A second, discrete fluorescence emission component, which starts at 425 nm is observed with 960 nm excitation. This presence of fluorescence emission at wavelengths less than half the excitation wavelength suggests three or more photon excitation processes. This conjecture is further confirmed by the observation that fluorescence intensity increases with excitation intensity at a power of 2.5. Further work is required to identify these emitting species. This study demonstrates the use of multi-photon excitation microscopy for functional imaging of the metabolic states of *in vivo* human skin cells. (This work was supported by NIH RR03155.)

Tu-Pos442

IMPROVING DIC MICROSCOPY WITH POLARIZATION MODULATION.

((**G. Holzwarth**[1], S.C. Webb[1], D.J. Kubinski[2] , and N. S. Allen[2]))
[1]Department of Physics, Wake Forest University, Winston-Salem, NC 27109;
[2]Department of Botany, North Carolina State University, Raleigh, NC 27695

Differential interference contrast(DIC) light microscopy, particularly when coupled with digital image processing, is a powerful tool for the high-resolution microscopy of unstained, transparent biological specimens. We will show analytically, as well as with images of diatoms, that switching the polarization of the incident light by 90° changes image highlights into shadows and *vice versa*. Using a ferroelectric liquid-crystal modulator, this switching can be done at frame rates, synchronized to the camera. By subtracting alternate frames, a stream of difference DIC images is created in which contrast is doubled, compared to conventional video-enhanced DIC, while image defects and noise tend to cancel. Subtraction of alternate images is carried out efficiently by frame buffer operations and amounts to massively parallel synchronous detection. The new method affords images with greater contrast without the problems inherent in obtaining a separate background image as in current VE-DIC practice.

Supported by NSF facilities grants DIR 87-22684(to WFU) and BIR-9418205 and North Carolina Biotechnology Center grant 9410-DG-1012(both to NCSU).

Tu-Pos443

LANTHANIDE PROBES FOR SOFT X-RAY MICROSCOPY

((**M. M. Moronne**, J. Nagy, and D. Hamamoto)) Lawrence Berkeley National Laboratory, University of California, Berkeley, CA 94720, USA.

Synchrotron based scanning x-ray microscopes are capable of Rayleigh resolutions approaching 50 nm, with improvements expected to reach 20 nm in the near future. To take advantage of the high resolution offered by x-ray instruments for biological studies, specific labels for subcellular targets are needed. We previously reported (Moronne et al, 1995, Biophysical J. 68(2):A139) that lanthanide based fluors are sufficiently bright and radiation stable to be the basis of a family of x-ray excitable probes. In this context, we have developed a biotinylated lanthanide-polychelate (bioLPC) that can deliver 80-240 lanthanide atoms to a targeted molecule. Using a rhodamine tracer coupled to the polychelate probe and confocal microscopy, we have shown that bioLPC binds with a specificity fully equivalent to conventional avidin-biotin labels for actin microfilaments, microtubules, and FISH DNA probes. Using the scanning x-ray microscope at the National Synchrotron Light Source modified for luminescence detection (SLXM), we have demonstrated effective labeling of *in vitro* preparations of microtubule assemblies and actin filaments in 3T3 mouse fibroblasts. At present, the NSLS flux limits the rate of image acquisition to hours; however, third generation synchrotron sources such as the Advanced Light Source in Berkeley should reduce imaging times to a few minutes making x-ray excited luminescent imaging practical. (Supported under DOE contract DE-AC03-76SF00098)

Tu-Pos444

SOFT X-RAY CONTACT MICROSCOPE AND IMAGING OF LIVE SPECIMENS.

((**Toshikazu Majima**, Hideaki Shimizu, Yuko Nakaishi,* Shin-ichi Abe* Toshihisa Tomie, Eisuke Miura, Toshihiko Kanayama, Masahiro Yamada)) Electrotechnical Laboratory, Umezono, Tsukuba, Ibaraki 305, Japan, *Faculty of Science, Kumamoto University, Kumamoto 860, Japan.

One of expectations of x-ray microscope has been observations of subcellular structure in living organisms. By using soft x-ray microscope, one can obtain x-ray images of living specimens in water. Among various types of x-ray microscopes, advantage of a x-ray contact microscope using a laser produced plasma as x-ray source is its simple and compact compositions. It is inevitable to develop a simple x-ray microscope system for improvement of the x-ray microscope as a popular instrumentation in biological research. Results of application of the system on living specimens such as bacteria, chlamydomonas and newt spermatozoa are showing that the soft x-ray contact microscope is useful to clarify subcellular structure of live specimens with resolution superior to light microscope.

Tu-Pos445

SYNCHROTRON INFRARED MICROSPECTROSCOPY AS A MEANS OF STUDYING CHEMICAL COMPOSITION AT A CELLULAR LEVEL.

((**Lisa M. Miller**, G. Lawrence Carr, Gwyn P. Williams and Mark R. Chance))
Department of Physiology and Biophysics, Albert Einstein College of Medicine of Yeshiva University, Bronx, NY 10461 and The National Synchrotron Light Source, Brookhaven National Laboratory, Upton, NY 11973.

Infrared microspectroscopy is the union of microscopy and spectroscopy for the purpose of microanalysis. Light microscopy provides a way to generate magnified images, resolve microstructural detail, and record images to facilitate their interpretation. Infrared spectroscopy provides a means for analyzing the chemical makeup of materials. Because of its longer wavelengths, infrared radiation limits the spatial resolution that can be achieved, but its ability to resolve chemical components through infrared absorption is of great importance. Combining light microscopy and infrared spectroscopy permits the correlation of microstructure with molecular chemistry. The performance of an infrared microspectrometer is significantly improved with the use of synchrotron radiation. Synchrotron infrared radiation is 1000-times brighter than a standard thermal-emission source, produces less Boltzmann source noise, and is also highly collimated. All of these features improve the spectral and spatial resolution of the spectrometer such that data can be obtained with high signal-to-noise at the diffraction limit, which is 3-5 μm in the mid-infrared region. Since cellular components such as proteins, lipids, and nucleic acids all have characteristic infrared signatures, we will demonstrate the use of infrared microspectroscopy as a means of chemically mapping tissue samples and even single cells. This work is supported by the NIH Grant RR-01633.

Tu-Pos446

HIGH-SPEED DIGITAL-IMAGING-MICROSCOPY-WITH CONTINUOUS FOCUS SCANNING. ((R.A. Tuft, D.S. Bowman, W.A. Carrington, K.E. Fogarty and F.S. Fay)) Dept. of Physiology, UMMC, Worcester MA.

In order to acquire images of fast dynamic changes in molecular distributionin live cells, we have developed a new operating mode for the acquisition of wide field 3-dimensional microscope images at high temporal and spatial resolution utilizing a high-speed digital imaging microscope. At the heart of the new system is an experimental CCD camera which captures 128x128 x 12 bit pixel images at a maximum of 540 frames per second. Quantum Efficiency is 68% at $\lambda = 550$ ηm and noise is 6.5 e^- rms per pixel. Previous studies used a stepped focus protocol, with rapid objective translations at rates of 1 μm/msec, followed by a cover-slip settling time of several msec to allow flow of immersion oil from the changing objective/cover-slip gap, and subsequent image exposure of several msec. Recent studies, involving high speed intracellular signalling events, such as Ca^{2+} sparks, have required higher temporal and spatial resolutions than possible with such protocols. High speed 3D images are now acquired using water immersion lenses at rates of up to 1 image/2 msec while continuously scanning focus in a sawtooth waveform at rates as fast as .5 μm/msec. Images acquired in this fashion are then processed by a modified image restoration algorithm which reverses the focus blurring in addition to the customary deconvolution of the image blurring arising from the optics. Applications to the imaging of Ca^{2+} sparks as well as GFP labeled organelles in living cells will be presented.

Tu-Pos447

CONFOCAL THETA MICROSCOPY OF BIOLOGICAL SPECIMENS. ((Ernst H.K. Stelzer and Steffen Lindek)) Light Microscopy Group, Cell Biophysics Programme, European Molecular Biology Laboratory (EMBL), Heidelberg, Germany. (Spon. by E.-L. Florin)

Confocal theta microscopy is a novel method by which the resolution in confocal fluorescence microscopy is substantially enhanced [1]. The basic idea is to use a second objective lens to detect the fluorescence light at an angle ϑ to the illumination axis. Since in fluorescence microscopy the confocal point spread function (PSF) is the product of the illumination and the detection PSFs, the overlap of the PSFs determines the extent of the confocal PSF and thus the resolution. The extent of the PSF is considerably decreased when the detection axis is rotated by $\vartheta = 90°$ relative to the illumination axis. This leads to an observation volume which is almost spherical and which is three times smaller than in confocal microscopy. In confocal theta microscopy water-immersion objective lenses with a moderate numerical aperture are used [2]. Therefore the confocal theta microscope has several advantages for biological applications [3]: (a) Since it uses water immersion, no aberrations are introduced by a mismatch of the refractive indices of mounting and immersion media. (b) Use of aqueous immersion and mounting media allow the observation of biological samples in their natural environment. (c) The working distance of the lenses used in the theta microscope is very large, which makes the microscope ideal for the observation of large biological samples of up to about 1 mm in diameter such as whole embryos or tissue sections.

1. E. H. K. Stelzer and S. Lindek (1994), Opt. Commun. **111**, 536-547.
2. S. Lindek et al. (1994), Rev. Sci. Instr. **65**, 3367-3372.
3. E. H. K. Stelzer et al. (1995), J. Microsc. **179**, 1-10.

Tu-Pos448

TOTAL INTERNAL RELECTION FLUORESCENCE MICROSCOPY (TIRFM) VISUALIZES DYNAMICS OF SECRETORY VESICLES BETWEEN DISTINCT POOLS IN BOVINE ADRENAL CHROMAFFIN CELLS.
((**Martin Oheim***†, Robert H. Chow † and Walter Stühmer*)) *MPI für Exp. Medizin, D-37075 Göttingen; †Univ. of Edinburgh Medical School, Dept. Physiol., EH8 9AG, Scotland, U.K. (Spon. R. Schneggenburger)

We have monitored single chromaffin granules (vesicles) in bovine adrenal chromaffin cells using a non-invasive optical sectioning technique, total internal reflection microscopy (TIRFM). Using TIR, fluorescence excitation is limited to an optical slice near a glass/water interface. In cells located at the interface, granules loaded with fluorescent dye such as Lysotracker Green (Molec. Probes) can be visualized near to or docked at the plasma membrane. This approach has been reported to detect fusion of vesicles (Steyer & Almers, Biophys.J. 70 A86, 1996). Here we give evidence that (1) TIRFM resolves single vesicles and (2) the fluorescence signal originates from one class of vesicles, presumably large, dense core vesicles (LDCVs). (3) Given a distribution of vesicle diameters centered around the average diameter of LDCVs and a known average dye concentration, the depth of origin of fluorescence can be estimated, which reveals (4) that distinct pools of vesicles can be visualized. With K^+ depolarization, (5) the time course of secretion monitored with TIRFM parallels that from amperometric or capacitance measurements, giving an independent assay for pool depletion. (6) TIRFM reports depletion of the pool closest to the plasma membrane within 20 ms of stimulation, consistent with the idea of a release-ready pool, as well as vesicles being translocated between different pools. (Supported partly by a British Council ARC grant to RHC &WS).

PHYSICAL CHEMISTRY OF PROTEINS

Tu-Pos449

EFFECTS OF MUTATIONS ON THE CHANGE IN HYDRATION ASSOCIATED WITH THE ALLOSTERIC CONFORMATIONAL EQUILIBRIUM OF ASPARTATE TRANSCARBAMYLASE
((V.J. LiCata, N.J. Moerke, D.S. Burz and N.M. Allewell)) Dept. of Biochemistry, University of Minnesota, 1479 Gortner Avenue, St. Paul, MN 55108.

Aspartate transcarbamylase (ATCase) is a highly regulated, multi-subunit enzyme that catalyses the first committed step in pyrimidine biosynthesis. Upon ligation, ATCase undergoes a conformational transition from a low activity T-state to a high activity R-state. This transition involves major changes in the molecular architecture, including structural rearrangements of several intersubunit interfaces and a 12 A expansion of the molecule along its three-fold axis. We have used osmotic stress (Parsegian, et al., 1996, *Meth. Enzymol. 259*, 43) to examine the changes in hydration associated with the T to R transition in several mutants of ATCase in which residues involved in the T to R switch have been altered.

Residues Y240 and D271 form a salt-bridge in the ATCase T-state which is disrupted in the R-state. Mutations in either residue (Y240F, D271N, D271S) do not alter the change in hydration that accompanies the conformational expansion.

Residue R130 forms a salt bridge across the c:r subunit interface to E204 in the T-state, which switches to a bond with D200 in the R-state. Elimination of this salt-bridge switch by the mutation R130G results in more than a twofold increase in the uptake of water during the T to R transition. This mutant takes up ~300 waters during the conformational expansion at pH 8.3. The magnitude of the hydration change is pH dependent. At high osmotic stress the mutant retains full regulatory response to the effectors ATP and CTP. Gel permeation chromatography of ligated and unligated R130G at pH 7 reports that the difference in Stokes radii between T and R forms is greater for R130G than the wild type. These results suggest that the salt-bridge switch involving residue R130 is important in regulating the structural magnitude of the T to R conformational transition. Supported by NIH grant DK-17335.

Tu-Pos450

ON THE ORIGINS OF THE ENTHALPY-ENTROPY COMPENSATION: RESULTS FROM THROMBIN AND INHIBITOR INTERACTION AT THE FRE
Yudu Cheng, Jing Wang, Jacek Slon-Usakiewicz, Enrico O. Purisma and Yasuo Konishi
NRCC, Biotechnology Research Institute, Montreal, Quebec, Canada

The residues of Phe^{H56} and Ile^{H59} in the fibrinogen recognition exosite(FRE) binding segment of two different thrombin inhibitors are mutated into glycine or alanine, and the thermodynamic and conformational effects of the mutation are analyzed. The overall relative enthalpy ($\Delta\Delta H°_{exp}$) and entropy($\Delta\Delta S°_{exp}$) changes are linearly correlated with a slope of 300 K and an intercept of 3.6 kcal/mol. The enthalpy-entropy compensation has been observed for many small and macromolecular systems but remains not well understood on the molecular basis. By decomposing the overall enthalpy and entropy changes into their solute($\Delta\Delta H°_{solute}$, $\Delta\Delta S°_{config}$) and solvent($\Delta\Delta H°_{solva}$, $\Delta\Delta S°_{solvent}$) components, it is found that the solute enthalpy and entropy are linearly correlated with a slope of 160 K and an intercept of 5.8 kcal/mol. No linear correlation is observed for the solvent enthalpy and entropy. Therefore, the overall enthalpy-entropy compensation is an intrinsic property of the solute-solute interaction. Meanwhile, the overall enthalpy or entropy is found to be predominated by the solute enthalpy or entropy. The smaller slope and larger intercept in the linear correlation of the $\Delta\Delta H°_{solute}$ and $\Delta\Delta S°_{config}$ indicate that the solute enthalpy and entropy is weakly compensated without the solvent participation. Therefore, the solvent plays a role in enhancing the enthalpy-entropy compensation. Furthermore, either the $\Delta\Delta H°_{solute}$ or $\Delta\Delta S°_{config}$ derived from the experimental data is comparable to the solute enthalpy and entropy estimated from the molecular modelling. This enables the visualization of the structural features of the enthalpy-entropy compensation. For example, a large shift towards thrombin of the backbone and the side chain of the inhibitor is predicted for the mutants of F56G or F56A. Theoretically, this conformational change is featured by a small decrease in the $\Delta\Delta H°_{solute}$ accompanied by a large decrease in the $\Delta\Delta S°_{config}$. Experimentally, this conformation change is featured a very small $\Delta\Delta H°_{exp}$ accompanied by a large negative $\Delta\Delta S°_{exp}$.

Tu-Pos451

DIELECTRIC BEHAVIOR IN THE INTERIOR OF PROTEINS: RESULTS FROM A LARGE-SCALE MOLECULAR DYNAMICS SIMULATION OF SOLVATED LYSOZYME.
((**Francisco Figueirido**, Gabriela S. Del Buono and Ronald M. Levy)) Department of Chemistry, Wright-Rieman Laboratories, Rutgers, The State University of New Jersey, Piscataway, NJ 08855-0939.

The dielectric behavior of the interior of a protein is an area of much current interest. Although a simplistic behavior is assumed in the so-called 'continuum models,' molecular dynamics (MD) simulations can, in principle, provide more detailed information. We discuss how to obtain an estimate of the interior dielectric from a single (long) simulation of the solvated protein. We also present the preliminary analysis of a 900 picosecond MD simulation of solvated lysozyme in a cubic box of 76 Å linear dimension surrounded by more than 14,000 SPC water molecules. From this analysis an estimate of the dielectric constant in the interior of the protein is obtained.

Tu-Pos452

DYNAMIC LIGHT SCATTERING AND PRECRYSTALLIZATION OF HUMAN APOPROTEIN A-I
((**V. M. Bolaños-García,**[†]* **J. Mas-Oliva,**[†] **M. Soriano-García,*** **and A. Moreno*,[‡]**)) *Inst. de Química; [†] Inst. de Fisiol. Celular, UNAM. AP 70-243, 04510 México, D.F. MEXICO. (Spons. by A. Ortega).

Since human apolipoprotein A-I, a protein involved in lipid transfer between lipoproteins, has not been yet crystallized, in the present study we describe how dynamic light scattering experiments were useful to determine the precrystallization conditions under which a crystal nucleus can be obtained. The hydrodynamic radius, diffusion coefficient, estimated molecular weight and polidispersity at different pH values were evaluated based on DLS. A quick protein aggregation is observed when the pH is closer to the isoelectric point of apoA-I, in agreement with the protein solubility theory. For apoAI at 2 mg/ml and pH= 8.0, the calculated geometrical factor H value is 4.80 $x10^{-9}$ mol g^{-2} cm^2 $molecule^{-1}$. The turbidity of apoA-I solution changes following an asymptothic line when Li_2SO_4 is the precipitant agent. When Li_2SO_4 reaches 0.37 M, apoA-I starts to aggregate and the hydrodynamic radius increases from 12 $x10^{-8}$ cm to 145 $x10^{-8}$ cm. Under these conditions, crystalline nucleus are formed when apoAI concentration is between 2 and 4 mg/ml and Li_2SO4 kept between 0.5-1.0 M. Our next goal will be focused to growth these nucleus until they reach a suitable size for X-ray diffraction analysis.

Tu-Pos453

DISSOCIATION/UNFOLDING OF β-LACTOGLOBULIN INDUCED BY HYDROSTATIC PRESSURE.
((V.L.V. Mesquita, M.M. Botelho and S.T. Ferreira)) Depto. Bioquímica Médica, Universidade Federal do Rio de Janeiro, RJ 21941-950, Brazil

β-lactoglobulin (β-LG) is a homodimer of 18 kDa subunits found in milk. We have investigated subunit dissociation/unfolding of β-LG induced by hydrostatic pressure, pH and temperature. Application of pressure ranging from 1 to 3500 atm promoted a fast (< 10 min.), significant (10-12 nm) red-shift in the intrinsic fluorescence emission of β-LG, indicating dissociation/unfolding of the protein. Refolding upon decompression occurred with considerable hysteresis, indicating loss of free energy of folding/association upon application of pressure. Low temperatures (3 °C) favored unfolding, suggesting entropic stabilization of β-LG structure. Alkaline pH promoted protein conformational changes favoring unfolding. Interestingly, subunit dissociation/unfolding was not affected by a 10-fold change in concentration of β-LG, indicating anomalous behavior in pressure-induced dissociation of this protein. In order to investigate the incomplete renaturation after decompression, gel-filtration FPLC, SDS-PAGE and non-denaturating electrophoretic analysis were carried out, revealing formation of a covalent partially folded dimer. This appeared related to disulfide cross-linking of monomers. Studies are under way to further characterize the unfolding of β-LG by pressure.
Supported by: FINEP, FAPERJ and CNPq.

Tu-Pos454

K-CARRAGEENAN-CASEIN INTERACTION IN DEUTERATED MIXTURES OF BOVINE AND CAPRINE WHOLE CASEINS: AN OXYGEN-17 NUCLEAR MAGNETIC RESONANCE STUDY.
((A. Mora-Gutierrez[1], T.F. Kumosinski[2], and H.M. Farrell[2], Jr.)). [1]Prairie View A&M University, CARC, Prairie View, TX 77446 and [2]USDA, ARS, ERRC, Philadelphia, PA 19118.

Carrageenan is a family of water soluble galactans extracted from marine red algae. Their ability to form aqueous gels has given them substantial commercial importance. The ^{17}O NMR results show that the mechanism of κ-carrageenan interaction with milk caseins is electrostatic in nature. The κ-carrageenan-casein interaction appears to depend largely on the ratios of κ- to α_{s1}-casein. A structural dependence upon protein components in salt containing κ-carrageenan-casein sol-gels from bovine and caprine milk has been clearly demonstrated. Stronger salt containing κ-carrageenan-casein sol-gels were formed from bovine casein and caprine casein of high α_{s1}-casein content, while salt containing κ-carrageenan-casein sol-gels from caprine casein of low α_{s1}-casein content were weaker. K-carrageenan-casein structures from bovine and caprine milk consist of a network of aggregated caseins which contains trapped water. In casein from bovine milk, κ-carrageenan addition resulted in a more porous, hydrated network structure.

Tu-Pos455

PRELIMINARY THERMODYNAMIC CHARACTERIZATION OF THE SELF-ASSOCIATION OF THE CYANOBACTERIAL REPRESSOR SMTB.
((S. R. Kar, J. Lebowitz, A. C. Adams, K. B. Taylor and L. M. Hall)) Biophysical Sciences Graduate Program, The Department of Microbiology and The Department of Biochemistry and Molecular Genetics, University of Alabama at Birmingham, Birmingham, AL 35294-2041.

The *Synechococcus* PCC7942 metallothionein repressor gene *smtB* has been cloned into the high expression pET29a(+) vector and purified to homogeneity. It has been established by analytical ultracentrifugation that the self-association of SmtB (M_r =13410) is a function of temperature, pH and salt. At pH7.4, 4°C, physiological salt and no heavy metal ions, the self-association is best described by monomer⇌dimer⇌tetramer model, with $K_{a(1,2)}$=9.3x10^7 M^{-1} for monomer-dimer equilibrium and $K_{a(2,4)}$=2.7x10^3 M^{-1} for dimer-tetramer equilibrium. At 22°C, $K_{a(1,2)}$ decreases to 2.7x10^5 M^{-1} while $K_{a(2,4)}$ remains at 1.2x10^3 M^{-1}. This observation indicates that ionic and/or hydrogen bond interactions are relatively predominant in the monomer-dimer association at pH7.5. At pH6.0, 4°C, physiological salt and no heavy metal ions, the protein exhibits monomer⇌dimer equilibrium, with $K_{a(1,2)}$=1.1x10^6 M^{-1}. At 22°C, $K_{a(1,2)}$ increases only slightly to 8.6x10^6 M^{-1}. In the presence of 150μM Zn^{2+}, the monomer-dimer interactions increases 100-fold at pH7.4, 22°C and physiological salt, with $K_{a(1,2)}$= 1.3x10^7 M^{-1} while $K_{a(2,4)}$ decreases to 1.5x10^2 M^{-1}. The weight-average sedimentation coefficient of SmtB increases 11% from 2.0S to 2.22S in the presence of 150μM Zn^{2+} at 22°C, physiological salt and pH7.4. The functional relevance of the self-associated forms of SmtB with regard to DNA-binding and repressor activity *in vivo* are currently under investigation. Single crystals of SmtB have been grown and preliminary diffraction data obtained in an effort to solve its structure.

Tu-Pos456

NON-ISODESMIC INDEFINITE ASSOCIATION OF ANTHRAX TRUNCATED PROTECTIVE ANTIGEN
((**E. K. Dimitriadis**)) BEIP, NCRR, NIH, Bethesda, MD 20892. (Spon. by M. S. Lewis)

The 63-kDa truncated protective antigen (PA63) is known to be one of the two components of the *Bacillus anthracis* toxin. Its oligomerization while bound to membrane receptors is thought to be critical for the introduction of the lethal factor (LF) into the cytosol. Here we study the self-association of PA63 in solution using analytical ultracentrifugation. Mathematical modeling of the data indicates that PA63 exhibits indefinite association which can be analyzed both as an isodesmic association for which ΔG^0 remains constant for the binding of each additional monomer or as an association exhibiting exponentially decreasing values of ΔG^0. The decay rate of the values of ΔG^0 for the addition of another monomer was determined by the analysis and therefore the effective range of possible models examined includes the isodesmic association as a special case. Thermodynamically the two systems exhibit opposite trends with respect to the values of ΔH^0 and $T\Delta S^0$ with temperature. Entropic considerations and the quality of the mathematical fit, however, favor the model with decreasing ΔG^0 values. ΔH^0 and $T\Delta S^0$ decrease with increasing temperature with the entropic term being dominant in the value of ΔG^0 at all temperatures and both are negative at 37°C. The chemical bond energy, as reflected in the temperature invariant enthalpy, $\Delta H^0(0)$, also decreases as the oligomer grows. The association also exhibits negative, slowly increasing values of ΔC_p^0 suggesting the burial of active sites with the growth of the PA63 oligomer.

Tu-Pos457

ASSOCIATION OF ANTHRAX PROTECTIVE ANTIGEN AND LETHAL FACTOR: A THERMODYNAMIC ANALYSIS (([*]Y. Singh, [*]S. H. Leppla, [+]E. K. Dimitriadis and [+]M. S. Lewis)) [*]LME, NIDR, [+]BEIP, NCRR, NIH, Bethesda, MD 20892. (Spon. by S. H. Yoo)

The *Bacillus anthracis* toxin consists of two distinct proteins, the 63-kDa truncated protective antigen (PA63) and the 90-kDa lethal factor (LF). Membrane receptor bound PA63 oligomer is known to associate with LF and result in the internalization of the latter into the cytosol. The sequence of events from the PA63 oligomerization to the LF internalization remains as yet unknown. Using analytical ultracentrifugation, we have studied the separate self-association of PA63 and of LF in solution and then studied their heterogeneous association. LF was found to exhibit a monomer-dimer association. The values of ΔH^0 and of $T\Delta S^0$ decrease with increasing temperature and are both negative at 37°C. PA63 exhibited an indefinite association which could be analyzed either as an isodesmic association or as an association exhibiting decreasing values of ΔG^0 with the addition of successive monomers (see accompanying abstract). For the isodesmic case, both ΔH^0 and $T\Delta S^0$ increased with temperature with the entropic contribution to ΔG^0 being dominant. In contrast, for the non-isodesmic case, both ΔH^0 and $T\Delta S^0$ decreased with temperature. The heterogeneous association of PA63 and LF was best fit as a monomer-decamer association of the PA63-LF complex. This association also exhibited decreasing values of ΔH^0 and $T\Delta S^0$ with increasing temperature with the entropic term being the dominant contribution to ΔG^0.

Tu-Pos458

KINETICS OF THE REACTIONS BETWEEN THE MOLECULAR CHAPERONE DNAK AND PEPTIDES. ((C. D. Farr & S. N. Witt)) Department of Biochemistry and Molecular Biology, Louisiana State University Medical Center, Shreveport, LA 71130.

We are investigating the pre-steady-state kinetics of the binding of the dansyl-VSV13 peptide (KLIGVLSSLFRPK) to DnaK over a range of temperatures using stopped-flow fluorescence. The values of the apparent second-order on-rate constant at 25, 37 and 42 °C are ~2 x 10^4, 7 x 10^4 and 2 x 10^5 $M^{-1}s^{-1}$, respectively; the off-rate constants at 25 and 37 °C are ~0.05 and 0.06 s^{-1}, respectively. These rate constants are much larger than the reported rate constants for the binding and dissociation of the dansyl-Cro peptide (MQERITLKDYAM) to DnaK. For example, the values of the apparent second-order on-rate constant for the DnaK-Cro complex formation are 18 and 200 $M^{-1}s^{-1}$ at 25 and 37 °C, respectively; the dissociation rate constants are 1.3 x 10^{-4} and 3.4 x 10^{-3} s^{-1}, at 25 and 37 °C, respectively. These results demonstrate that the sequence of the peptide strongly influences the rates of DnaK-peptide complex formation and dissociation.

Tu-Pos459

ELECTROSTATICALLY CONTROLLED BINDING OF PHOSPHOLIPASE A_2 (APPD49) TO SUPPORTED LIPID BILAYERS. ((S. A. Tatulian* and R. L. Biltonen§)) Departments of Molecular Physiology and Biological Physics* and Pharmacology§, University of Virginia School of Medicine, VA 22906-0011

Binding of phospholipase A_2 (PLA_2) to phospholipid assemblies is a prerequisite for enzyme activation. Therefore, determination of binding parameters, such as the binding constant, binding site density and binding cooperativity, is critical for understanding the mechanism of interfacial activation of PLA_2. We employed attenuated total reflection Fourier transform infrared spectroscopy to study the binding of PLA_2 purified from the venom of *A. p. piscivorus* (APPD49) to supported lipid bilayers of varying surface charge density and at different ionic strengths (pH = 8.2). The protein-to-lipid ratio (P/L) was deduced from the ratio of absorption band areas due to the protein amide I and lipid methylene stretching vibrations, corrected for corresponding molar absorption coefficients, and the surface density of bound protein was determined as 2(P/L)/A (A is the cross-sectional area per lipid molecule). Scatchard plots indicated positive cooperativity of PLA_2 binding to negatively charged membranes. A decrease in the mole fraction of the acidic lipids in the membranes from 0.4 to 0, as well as an increase in the ionic strength from 0.008 to 1 M (by adding NaCl), decreased the Hill constant from ~2 to ~1. For DPPC/DPPG (3:2) bilayers, a similar increase in the ionic strength caused a decrease in the binding site density (N) from 0.22 to 0.14 nm^{-2} and a lowering of the apparent binding constant (K) from $5*10^5$ to $3*10^4$ M^{-1}. In the presence of 2 mM Ca^{2+}, both N and K decreased 3-4 times, indicating the dual effect of Ca^{2+}, which while supporting the catalysis as a cofactor, suppresses the binding of PLA_2 to bilayers. The effects of Na^+ and Ca^{2+} can be explained by competition between these cations and the basic protein for acidic lipids. N increased from 0.075 to 0.36 nm^{-2} and K from $2*10^5$ to $6*10^5$ M^{-1} when the mole fraction of POPG in POPC/POPG bilayers increased from 0 to 0.2. Our results indicate an important role of electrostatic effects in PLA_2-membrane interactions.

Tu-Pos460

A NEW EQUATION FOR THERMODYNAMIC EVALUATION OF LIGAND-PROTEIN BINDING BY USING ISOTHERMAL TITRATION CALORIMETRY.
((A.A. Saboury and **A.A. Moosavi-Movahedi**)) Institute of Biochemistry and Biophysics, University of Tehran, Tehran, Iran.

The reversible combination of a ligand with a specific site on the surface of a protein or other biopolymer is one of the most familar and important processes in biochemistry. If the multiple binding sites on a macromolecule, M_n, are equivalent and independent, the ligand binding sites can be reproduced by a model system of monovalent molecules: $M_n \longrightarrow nM$, which "n" is the number of binding sites. By titration of a solution containing "M" with a solution of ligand "L", the equilibrium reaction

$$M + L \rightleftharpoons ML \qquad K = [M][L] / [ML]$$

progresses to increase the concentration of the "ML" complex. The heat of reaction depends on the concentration of ML complex: $Q \propto [ML]$. The maximal value of heat is obtained when all the M is present as ML: $Q_{max} \propto [M]_{total}$. It can be shown that $Q/Q_{max} = [L] / (K + [L])$, which it is very similar to the Michaelis equation, or in terms of Lineweaver-Burk form

$$\frac{1}{Q} = \frac{1}{Q_{max}} + \frac{K}{Q_{max}} \frac{1}{[L]}$$

Thus, the plot of 1/Q versus 1/[L] gives dissociation equilibrium constant (K) and molar enthalpy of binding ($\Delta H = Q_{max}$). If $[L]_{total} >> [M]_{total}$ it can be assumed that $[L] \cong [L]_{total}$.

This method was applied to the binding of fluoride ion with active sites of jack bean urease at pH = 7.0 (Tris 30 mM) and T = 300 K. For this reaction, it can be deduced that n = 12. From the foregoing equation, . = 0.94 mM and ΔH = – 11.885 kJ mol^{-1}. The dissociation equilibrium constant measured by this method is a markedly consistent with inhibition constant obtained from assay of enzyme activity in the presence of fluoride ion.

NOVEL TECHNIQUES

Tu-Pos461

Mg-ATP ENHANCES THE FLUORESCENT LABELING OF *E. COLI* O157:H7 BY DAPI. ((S-I. Tu, D. Patterson, and J. Uknalis)) USDA, ARS, NAA, Eastern Regional Research Center, 600 E. Mermaid Lane, Wyndmoor, PA 19038

In an effort to develop new methods for detecting pathogenic bacteria in foods, we have labeled freshly isolated cells of *E coli* O157:H7 at the stationary phase with nucleic acid indicator, DAPI. The treated cells were then immobilized with antibody coated on magnetic beads and fixed with 1% glutaraldehyde before fluorescence intensity determined either spectroscopically or microscopically. The addition of Mg-ATP during the labeling stage could significantly increase detected fluorescent intensity. Neither Mg^{2+} nor ATP alone could enhance the labeling intensity. The extent of enhancement appeared to increase with the pH of the medium (maximum ~ 9.0). The addition of Mg-ATP to DAPI-labeled the bacteria also increased, but to a lesser extent, the intensity of the fluorescence. These results suggested that both the uptake and the in-vivo quantum yield of DAPI labeled nucleic acids could be increased by Mg-ATP.

Tu-Pos462

Multiphoton Fluorescence spectroscopy through optical fibers
S. Maiti, J. K. Ranka, A. L. Gaeta and Watt W. Webb, School of Applied and Engineering Physics, Cornell University, Ithaca, NY 14853

Multiphoton excitation in biological fluorescence microscopy provides inherent three-dimensional resolution, minimizes out of focus background and photodamage and provides for easy separation of the fluorescence signal from the Rayleigh and Raman scattered excitation light. The extension of this tool to internal *in vivo* studies requires the replacement of the optical microscope by a compact insertable probe. We investigate the possibility of using single-mode optical fibers for both excitation and collection of multiphoton fluorescence, which should make it possible to attain a lateral resolution of ~ 5 μm and a longitudinal resolution of < 25 μm with a probe that may be as thin as 125 μm. We have studied the propagation of 100-fs, transform limited pulses at 800 nm through a 25-cm-long single-mode fiber (short pulses are required for efficient multiphoton excitation). Pulses are observed to broaden both temporally and spectrally in a peak-power-dependent manner due to dispersion and self-phase modulation. As a result of the highly nonlinear chirp, pulsewidth at the output can be shortened only slightly by introducing a negative chirp at the input. However, even with pulse broadening and the comparatively poor collection efficiency of the fiber, it is demonstrated that at a 100MHz repetition rate with 100 mW of average power, two-photon-excited fluorescence from 20 nM rhodamine-6G in ethanol can be detected above background with <50 ms of data averaging. Application of this technique in tissue preparations is underway.

Supported by NIH and NSF grants to the Developmental Resource for Biophysical Imaging and Optoelectronics and USARO grants to JKR and ALG

Tu-Pos463

TWO-PHOTON CONTINUOUS SCANNING MICROPHOTOLYSIS FOR LATERAL TRANSPORT MEASUREMENTS AT HIGH SPATIAL AND TEMPORAL RESOLUTION.

((U. Kubitscheck, O. Heinrich, **Peter Wedekind** and R. Peters)) Institut für Med. Physik und Biophysik, Westfälische Wilhelms-Universität Münster, D-48149 Münster, Germany

A comparatively simple laser scanning microscopic method for the determination of lateral diffusion coefficients at high temporal and spatial resolution is described. Combining two previously developed methods, Continuous Fluorescence Microphotolysis and Scanning Microphotolysis, the new method is referred to as Continuous Scanning Microphotolysis. The principle of the method is simply to operate a commercial laser scanning microscope in the line scanning mode while monitoring the fluorescence emitted from the continuously scanned line as an x-t "image". Fluorescence excitation can be effected by either single- or two-photon absorption. In the former case a standard, low power ion laser is sufficient while for two-photon excitation a femtosecond-pulsed titan sapphire laser can be employed. In both cases the laser beam power is adjusted such that a substantial but not excessive degree of photobleaching is induced. X-t images are evaluated for the intensity of the scanned line in dependence on scanning time.The fluorescence decay curves obtained in this manner are evaluated in terms of diffusion coefficients and photobleaching rate constants by numerical simulation of appropriate diffusion-reaction systems. The validity of the experimental and theoretical procedures was tested by measurements on a simple well-defined model system. (Support by the German Research Foundation, grant Pe 138/15-4, is gratefully acknowledged)

Tu-Pos464

Two-Photon 3-D Particle Manipulation: An Application of Brownian Ratchet

((Peter T. C. So)) Department of Mechanical Engineering, Massachusetts Institute of Technology, Cambridge, MA 02139.

Typical fluorescence microscopy is a tool for passive observation. Two-photon microscopy has a localized excitation volume of 0.1 femtoliter. The ability to selectively initiate photochemical reaction inside this small region will provide many new opportunities for interactive experimentation. A particular promising application is in the area of two-photon 3-D particle manipulation. Objects larger than 0.5 micrometer can be successfully manipulated using optical tweezers or micro-pipettes. Atomic force microscopy and scanning tunneling microscopy has been used to move individual atoms. However, there are no reliable methods to manipulate objects, such as small bacteria or virus particles, of sizes below 0.1 micrometer but larger than the atomic dimension. The ability to manipulate these objects will facilitate studies such as bacterial cell invasion or virus membrane docking. Combining the concept of Brownian ratchet and two-photon localized excitation, nanomanipulation of small object may become possible. Consider the diffusion of an object in a photopolymerizable medium. The spatial symmetry of the diffusion can be broken by locally polymerizing the medium adjacent to the object. By active feedback control of the polymerization position, the object trajectory can be directed. This work is supported by the Sloan Foundation.

Tu-Pos465

TWO-PHOTON FCS USING A DUAL CHANNEL SINGLE PHOTON COUNTING SYSTEM. (S. **McClendon**, W.M. Yu and E. Gratton) Laboratory for Fluorescence Dynamics, University of Illinois at Urbana-Champaign, Urbana, IL 61801

Fluorescence Correlation Spectroscopy (FCS) measures the intensity fluctuation from a sample to obtain dynamic information about the system (such as diffusion rates, protein aggregation, etc). In a number of systems, we are interested in studying the dynamic behavior of two aspects of the system simultaneously. To achieve this, we have constructed a dual channel, single photon counting detection system, and implemented it in a two-photon microscope. The signal detected at two separate photomultiplier tubes can be treated as separate signals and individually autocorrelated (as in normal FCS) or cross correlated to study the relation between the two signals. Our experimental setup consists of an inverted two-photon fluorescence microscope, and a custom made dual-channel photon-counting data acquisition PC card. The sample rate (typically between 100 Hz and 100 kHz) depends upon the system being investigated. An advantage of this system over normal FCS (when it is used in the cross-correlation mode) is the ability to ignore information other than fluctuations between the two quantities of interest. We present data on live cells labelled with various fluorescent probes, studied using our dual channel FCS system. Supported by NIH grant RR03155.

Tu-Pos466

PUMP-PROBE STIMULATED-EMISSION MICROSCOPY. ((C. **Buehler**, C. Y. Dong, P. T. C. So, and E. Gratton)) Laboratory for Fluorescence Dynamics, Department of Physics, University of Illinois at Urbana-Champaign, 1110 West Green Street, Urbana, IL 61801.

Pump-probe stimulated-emission microscopy involves a multi photon process that enables fluorescence lifetime imaging with confocal-like spatial resolution and sub-nanosecond time resolution. In this novel technique, two lasers running at different amplitude modulation frequencies and different colors are focused onto a common volume in the specimen. One laser excites the biochemical system and the other causes stimulated emission. The offset in the lasers' repetition frequencies, typically a few KHz, results in a heterodyning of the high frequency fluorescence decay to the frequency difference of the two lasers. Because the stimulated emission process occurs primarily at the overlapping volume of the pump and the probe beams, a 3-D sectioning effect comparable to confocal or two-photon microscopy can be obtained by observing the fluorescence at the lasers' difference frequency. Furthermore, as an inherent feature of pump-probe method, this instrument has ultrafast time resolution without using fast photodetectors. In the case of pulsed laser sources, the achievable time resolution is ultimately determined by the pulse widths of the two lasers. We will present data characterizing the performance of the instrument and applications of identification of cellular structures using fluorescence lifetime imaging.(This work is supported by NIH grant #RR03155)

Tu-Pos467

QUANTITATIVE DETERMINATION OF LOCAL ASSOCIATION PHENOMENA BY SINGLE MOLECULE MICROSCOPY *.

((G.J. Schütz, W. Trabesinger, H.J. Gruber, H. Schindler and Th. Schmidt)) Institute for Biophysics, University of Linz, Altenberger Str. 69, 4040 Linz, Austria.

We have studied the photophysical parameters of various fluorophores with respect to their usage in quantitative analysis of local stoichiometries. In particular, the variation of the fluorescence quantum yield due to interaction with the environment was studied for Rhodamines and Cyanines bound to lipids, antibodies, toxins and nucleotides. By the development of a statistical methodology for interpretation of fluorescence intensities we were able to determine the number of ligands bound to an individual molecule. This methodology was applied to the study of avidin aggregation on a phospholipid membrane, of labelling stoichiometry of individual antibodies, and of oligo-nucleotide reactions.

(* Supported by the Austrian Research Funds, project S06607-MED)

Tu-Pos468

AFM MEASUREMENTS OF VISCOELASTIC PROPERTIES OF CELLS.

((Torge Kuhn, Markus Schmidt and **Vincent T. Moy**)) Department of Physiology & Biophysics, University of Miami School of Medicine, Miami, FL 33101.

The dynamic network of the cell cytoskeleton underlies a variety of cellular function such as cell adhesion and locomotion. To shed light on the architecture of the cytoskeleton, we have developed an AFM specifically designed to investigate the micromechanical properties of cells. Two novel techniques are introduced to characterize the viscoelastic properties of cells: (i) the constant force measurement and (ii) the force relaxation measurement. These methods measure the cell's creep and relaxation functions. In the constant force experiments, the indentation of the cell under a constant force exerted by the AFM tip is measured over time. In the force relaxation experiments, the restoring force of the sample is measured at a constant indentation. Experiments on L929 cells revealed viscoelastic properties consistent with the standard linear solid (Kelvin) model. The elastic component of these cells varies around 3,000 Pa and the mean viscous component over 20 second scans is about a factor of 3 larger (10,000 Pa s). Comparison between adherent and loosely attached L929 cells showed that the adherent cells are stiffer by a factor of 2. Treatment with the anti-cytoskeletal drugs, cytochalasin D and nocodazole, resulted in a 50% decrease in cell elasticity. Together, these results demonstrate that the AFM can be applied to obtained precise viscoelastic measurements of the cell. (Supported by Whitaker Foundation).

Tu-Pos469

WAVELENGTH-DEPENDENT TURBIDIMETRIC ANALYSIS OF GELATION. ((**J.M. Messer** ,T.M. Laue and T.P. Moody)) Dept. of Biochemistry and Molecular Biology, Univ. of New Hampshire, Durham NH 03824.

Turbidity can be used to monitor gel formation using an ordinary spectrophotometer. The wavelength dependence of the turbidity contains information pertaining to the size, shape and concentration of the scattering species present in the gel. The composition of a gel solution has been modeled as a mixture of small particles, which are not considered to be part of the gel, plus three other species: long rods, long random coils and reflecting material, which are considered to make up the gel. A computer program has been written to aid in the analysis of experimental data. The program is used in two ways: 1) turbidity data are synthesized using estimates for structural parameters that describe each species and 2) these estimates are then used to obtain the weight fraction of each scattering species in a gel solution by linear least squares fitting. The mass concentration of gel estimated from the fit is compared to that determined by pelleting. Grant acknowledgments: NSF BIR-9314040, USDA NE123.

Tu-Pos470

PATTERED ADSORPTION OF IN VITRO CENTROSOMES. ((**J.F. Mooney**, A.J. Hunt, J.R. McIntosh, C.T. Rogers)) University of Colorado, Boulder, CO 80309

Self-assemble monolayers (SAMs) can be a useful substrate for the patterning of proteins on a glass surface. Through the use of biotin/streptavidin interactions and antibody specificity, the SAM, n-octadecyltrimethoxysilane (OTMS), has been used to adhere a variety of proteins to the substrate. Biotinylated BSA, which adsorbs to OTMS, can adsorb a layer of streptavidin which in turn can be used to adsorb an arbitrary biotinylated protein or biotinylated antibody to a protein of interest.* This procedure has now been used to adsorb centrosomes for in vitro studies. An advantage of the OTMS procedure is that the adsorption can be confined to certain regions of a coverslip by patterning the OTMS coverage on the glass. Using conventional photolithography, a chromium coated glass mask can be used to create a pattern of photoresist on top of a OTMS coated substrate. This photoresist layer can be used to protect the underlying OTMS from removal by an ion mill (a collimated beam of argon ions accelerated across a potential to bombard the surface). The areas not coated in photoresist are milled so that the OTMS is removed, leaving behind the bare glass substrate. After removal of the photoresist with acetone, there are now regions of OTMS surrounded by bare glass. This can be used to confine adsorption of the centrosomes to the OTMS areas and securely attach them for *in vitro* study. (Supported by ONR grant N00014-94-1-0621)

* J.F.Mooney, A.J.Hunt, J.R.Mcintosh, C.A.Liberko, D.M.Walba, C.T.Rogers, "Patterning of Functional Antibodies and Other Proteins by Photolithography of Silane Monolayers", **Proc.Nat.Acad.Science** *in press*

Tu-Pos471

LIFETIME-RESOLVED FLOW CYTOMETRY FOR CELL SORTING AND POPULATION HETEROGENEITY USING A HETERODYNING FREQUENCY-DOMAIN APPROACH (**W.M. Yu**, G. Durack†, W.W. Mantulin and E. Gratton) Laboratory for Fluorescence Dynamics, and †Plant and Animal Biotechnology Laboratory, University of Illinois at Urbana-Champaign, Urbana, IL 61801.

Flow cytometry is a widely used technique in many branches of biological science. The added capability of measuring fluorescence lifetimes in a conventional flow cytometer allows us to study lifetime distributions among cell populations very efficiently. Cell sorting based on lifetime differences improves accuracy. We have developed a time-resolved flow cytometer using a fast, frequency domain, heterodyning technique. In our experimental setup, an Argon ion laser is sinusoidally modulated through a Pockels-cell at about 100 Mhz. The cross-correlation frequency is determined by the speed which a cell passes through the laser beam. For example, a flow of 1 m/s, the cell is under the laser beam for approximately 10μs. Typical cross-correlation frequencies applied at the detectors in our instrument are on the order of 400 kHz to 800 kHz, so that several periods of the cross correlation frequency can be acquired per cell. By referencing the phase signal from a second photomultiplier tube, the phase shift of the cell's fluorescence, relative to the light source, is obtained directly. There is no need to analyze nonfluorescence particles and to change filters for obtaining null phase information as performed in existing phase sensitive flow cytometers (Sailer et al., 1996, Cytometry 25:164-172). In our instrument, cell scattering, fluorescence intensity and lifetime information are obtained simultaneously. Data for fluorescent latex spheres and live cells labeled with fluorescence probes demonstrating various heterogeneities are presented. Supported by NIH RR03155 and UIUC/CRI Flow Cytometry grant.

Tu-Pos472

IMPROVEMENT IN PROTEIN FOOTPRINTING TECHNIQUE; USE OF DIFFERENT CHEMICAL PROTEASES IN DETECTION OF LIGAND-INDUCED PROTEIN CONFORMATIONAL CHANGES ((**Noel Baichoo** and Tomasz Heyduk))Department of Biochemistry and Molecular Biology, St. Louis University Medical School,1402 S. Grand Blvd., St. Louis, MO 63104, USA.

High resolution protein footprinting has recently been described [1] and applied to mapping contact domains of proteins involved in protein-protein [2] and protein-DNA[1]interactions. Using this technique any process that results in a change in solvent accessibility of the protein backbone to chemical protease can be monitored. In all these studies domains of affected proteins have been identified by protection against or hypersensitivity to iron-EDTA mediated proteolysis. To extend the utility of this technique, a range of chemical proteases differing in charge and hydrophobicity have been used. This allows correlations between protein properties and frequency of cleavage. Also, the applicability of the technique to detect and map ligand-induced conformational change in the protein was tested.

The cAMP receptor protein (CRP) was used as a model system. The binding of cAMP to CRP dramatically increases the specific DNA binding activity of the protein and was shown to involve conformational change in the protein. Binding of cAMP produced measurable differences in the susceptibility to cleavage by Fe-EDTA and almost all of these changes were detected in C-terminal domain (DNA binding domain) of the protein. Additional changes were observed at the ends of the C-helix which provides the intersubunit contacts in CRP dimer. The boundaries of the regions in the C-terminal domain which exhibited changes in susceptibility to Fe-EDTA cleavage almost exactly corresponded to boundaries of D, E and F alpha helices which are involved directly in the recognition of DNA. Most notably, the F-helix, which provides all base specific contacts in CRP-DNA complex, became hypersensitive to Fe-EDTA cleavage upon binding of cAMP. Protein footprinting technique appears to be sensitive enough for detection and mapping ligand induced conformational changes in proteins.

1. Heyduk, E. And Heyduk T. (1994) *Biochemistry* **33**, 9643-9650
2. Heyduk, T., Heyduk, E., Severinov, K., Tang, H., and Ebright, R.H.(1996) *Proc. Natl. Acad. Sci. USA* **93**, 10162-10166

Tu-Pos473

EFFECTS OF SOLVENT FLOW ON ANALYTICAL ELECTROPHORESIS. ((**T.J. Wilson**[1], T.P. Moody[1], H.K. Shepard[2], J. Heirtzler[1] and T.M. Laue[1])) [1]Department of Biochemistry and Molecular Biology, [2]Department of Physics, University of New Hampshire, Durham, NH 03824.

We have constructed an electrophoresis apparatus in which macroion electrophoretic mobility, steady-state concentration gradients and diffusion may be studied. The apparatus consists of a fused-silica cuvette sealed top and bottom by semi-permeable membranes. This arrangement permits the establishment of an electric field along the cuvette's length while retaining macromolecules in the field of view. We consider the extent to which hydrostatic and electrokinetic flows may effect various experiments. Computer simulations demonstrate that such flows may significantly perturb steady-state electrophoresis and diffusion measurements. Solvent flow has been characterized under a variety of experimental conditions using the macromolecule rhodamine-dextran, which carries zero net charge. These measurements enable experimental data to be corrected for the effect of solvent flow and will lead to improved methods as insight into these processes is developed. (This work was supported by NSF grant BIR-931404.)

Tu-Pos474

DETERMINATION OF MACROION DIFFUSION COEFFICIENTS USING AN ANALYTICAL ELECTROPHORESIS APPARATUS **((H.K.Shepard[1], T.J. Wilson[2], T.P.Moody[2], J.O.Wooll[2], & T.M.Laue[2])) University of New Hampshire, [1]Department of Physics, [2]Department of Biochemistry and Molecular Biology, Durham, NH 03824-3544**

Using a unique analytical electrophoresis apparatus in which both electrophoretic mobility (μ) and steady-state concentration gradients may be studied, we present methods to determine the effective macroion diffusion coefficient in the presence or absence of an electric field (E). These methods are based on deriving approximate analytical solutions for the simple one-dimensional diffusion equation $\partial c/\partial t = D\partial^2 c/\partial x^2 - \mu E \partial c/\partial x$, which assumes that macroion motion can be usefully described with coupled flow effects being summarized in effective diffusion and frictional coefficients. The approximate analytic solutions are shown to be good approximations to numerical simulations of the differential equations and provide a good phenomenological description of experimental data for the oligonucleotide $pd(A)_{20}pd(T)_{20}$ in 100 mM KCl, 20 mM Tris-HCl, ph 8.0 buffer. (This work was supported by NSF grant BIR-9314040 and by the Office of the Vice President for Research and Public Service of the University of New Hampshire.)

Tu-Pos475

TWO DIMENSIONAL FINITE ELEMENT SIMULATION OF ELECTROPHORESIS AND SEDIMENTATION. ((**T.P. Moody**[1], H.K. Shepard[2] and T.M. Laue[1])) [1]Dept. of Biochemistry and Molecular Biology, [2]Dept. Of Physics, Univ. of New Hampshire, Durham NH 03824.

In a typical electrophoresis experiment, the electric field is assumed to be invariant with position in the device. Near walls that are parallel to the direction of the field, however, the strength of the field may vary. If the distance between such walls is sufficiently small, such edge effects may substantially affect transport. Similarly, in sedimentation, walls that are parallel to the gravitational field may interact with solution components and, in so doing, affect transport. Edge effects due to interactions between walls and components can also occur in electrophoresis. Again, the smaller the volume of the system, the more such edge effects will affect transport. A two dimensional version of the Claverie method is used to simulate transport in a system that exhibits edge effects. Transport in one dimension includes a flux due to the field and a flux due to diffusion, while that in the other, orthogonal dimension involves a flux due to diffusion alone. This latter flux is zero in the absence of edge effects. Simulation results are shown that may be relevant to novel analytical electrophoresis and analytical ultracentrifugation methods under development in our laboratory. Grant acknowledgments: NSF BIR-9314040, NSF DIR-9002027.

Tu-Pos476-Tu-Pos506

Reserved for High School Student Posters.

LOCAL Ca^{2+} SIGNALING IN MUSCLE AND NERVE

W-AM-SymI-1 **C. Franzini-Armstrong, University of Pennsylvania**
Clustering of Ryanodine Receptors and Dihydropyridine Receptors

W-AM-SymI-2 **I. Parker, University of California, Irvine**
Elementary Ca^{2+} Release from IP_3 Receptors

W-AM-SymI-3 **J. A. Connor, Lovelace Institutes**
Ca^{2+} Signaling in Neural Dendritic Spines

W-AM-SymI-4 **W. J. Lederer, University of Maryland, Baltimore**
Ca^{2+} Sparks in Muscle

MYOSIN I

W-AM-A1

SH1 AND SH2-MODIFIED MYOSIN HEADS ACTIVATE THE REGULATED ACTIN. ((**Andrey A. Bobkov***, Elena A. Bobkova[†], Earl Homsher[†] and Emil Reisler*)) *Dept. of Chem. & Biochem. and Molecular Biology Inst., UCLA, Los Angeles, CA 90095. [†]Dept. of Physiol., School of Medicine, UCLA, Los Angeles, CA 90025.

The reactive SH1 (Cys-707) and SH2 (Cys-697) groups of the myosin head (S1) can be selectively labeled and have been used as an attachment sites for either fluorescent or spin probes in solution and fiber experiments. It was shown in the *in vitro* motility assays with unregulated actin, that selective modification of SH1 or SH2 groups disrupts the motor function of myosin [Root & Reisler (1992) *Biophys. J.* **63**, 730-740]. In this study we examined the effect of SH1 and SH2-modified S1 on the motility of the regulated actin. N-ethylmaleimide (NEM), (N-1[1-oxyl-2,26,6-tetramethyl-4-piperidinyl]iodacetamide (IASL), (iodoacetamidoethyl)aminonaphthalene-1-sulfonic acid (IAEDANS) and iodoacetamide (IAA) were used to selectively modify SH1 group on S1. 4-[N-[(iodoacetoxy)ethyl]-N methylamino]-7-nitrobenz-2-oxa-1,3-diazole (IANBD) was used to selectively modify SH2 group on S1. Addition of S1 modified with any of these reagents to the *in vitro* motility assay solutions increased the percentage of regulated actin filaments moving over unmodified HMM and their sliding velocity at pCa 5, 7, and 8. Addition of unmodified S1 had no effect on actin sliding under the same conditions. Acto-S1 ATPase measurements showed that IASL-SH1-S1, IAEDANS-SH1-S1 and IANBD-SH2-S1 had significantly lower K_m than unmodified S1. This indicates that SH1 and SH2-modified S1 have higher than unmodified S1 affinity to actin in the presence of ATP. Overall, these results demonstrate that SH1 and SH2 modified S1 can activate the regulated actin. Such activation improves the efficiency of unmodified heads, increasing the percentage of moving actin filaments and their velocity in the *in vitro* motility assay.

W-AM-A2

Glu124-Arg149 OF THE REGULATORY LIGHT CHAIN IS LOCATED ON THE PHOSPHORYLATION SIGNALLING PATHWAY IN SMOOTH MUSCLE MYOSIN. ((Guanming Wu, A. Wong, & R.C. Lu)) Muscle Research Group, Boston Biomed. Res. Inst., Boston, MA 02114

Regulatory light chain mutants, RLC-C18 and RLC-C165, containing Cys at 18 and 165, respectively, labeled with benzophenone-4-iodoacetamide, were exchanged into myosin in their phosphorylated (P) or unphosphorylated (unP) forms. Previously we showed by SDS-PAGE that intrachain photocrosslinking in RLC-C18 occurs only in the unP state. In the case of RLC-C165, the yield of one of two crosslinked bands decreased significantly whereas the other was unaffected by phosphorylation (Qian et al., Biophys.J. 70, A3, 1996). Peptide mapping in conjunction with mass spectrometry showed that C165 crosslinks to a tryptic peptide A17-K34 which includes the phosphorylation site S19 and this crosslinking is unaffected by phosphorylation. We also found that two adjacent tryptic peptides in the C-terminal domain, E124-R132 and F133-R149, are crosslinkable to C165 as well to C18; however, crosslinking to these two peptides, whether from C18 or C165, is inhibited in the phosphorylated state. The results clearly showed that the proximity between C165 and the region containing the phosphorylation site is not affected by phosphorylation. On the other hand, phosphorylation changes the spatial relationship between the region of E124-R149 and the region containing both C165 and C18. In scallop myosin the region corresponding to E124-R149 is located at the interfaces between RLC and the essential light chain as well as the heavy chain (Xie et al., Nature, 368, 306, 1994). In light of this work our results indicate that the region containing E124-R149 is involved in the transmission of the phosphorylation signal to the rest of molecule via its contacts with the essential light chain and the heavy chain. Supported by NIH AR41637 & AR28401.